The Use of Auditory Evoked Potentials to Assess Encoding of the Peripheral Auditory System in Hearing-Impaired Listeners

Dissertation

Presented in Partial Fulfillment of the Requirements for the Degree Doctor of Philosophy in the Graduate School of The Ohio State University

By

William Jason Riggs, Au.D.
Graduate Program in Speech and Hearing Sciences

The Ohio State University

2021

Dissertation Committee:

Eric C. Bielefeld, Advisor

Aaron C. Moberly

Christina Roup

Shuman He

Abstract

The three manuscripts presented here examine the role of acoustic and electrically evoked potentials to assess sensory and neural encoding processes by the peripheral auditory system in hearing-impaired listeners. The first manuscript defined how spectral and temporal properties of the phonemes /da/ and /ba/ were encoded in the peripheral auditory system using electrocochleography (ECochG) in normal and hearing-impaired listeners. Results suggest that the fundamental frequency of each phoneme is the dominant spectral content encoded by the peripheral auditory system. Additionally, spectral encoding by the sensory cells of the cochlea, as measured by the cochlear microphonic response, is strongly correlated with word recognition performance. In the second manuscript, acoustic click train stimulation was employed to study the impact of Ménière's disease on two temporal response properties of the auditory nerve: adaptation and recovery from adaptation. The findings of this study suggest little evidence of neural damage in Ménière's disease that exceeds that of other forms of sensorineural hearing loss. Finally, in the third manuscript, electrical stimulation of the auditory nerve was utilized to investigate the effect of aging on the response properties of the auditory nerve. The sensitivity of the auditory nerve to steady state pulse trains was not found to be significantly different between older and younger adult cochlear implant users, although trends of poorer function in older adults did exist, especially at higher pulse rates. Results suggest potential negative effects of aging on temporal response properties to electrical pulse train stimulation at high pulse rates.

Overall, evoked potentials provide a robust technique to objectively study processing of the auditory system in normal and hearing-impaired listeners.

Dedication

Dedicated to my mother and father as well as my wife and family for all their never-ending encouragement and support over the years.

Acknowledgments

I would like to extend my sincere appreciation to my advisor Dr. Eric Bielefeld for his support, and guidance throughout my Ph.D. program. I would also like to thank all my committee members Drs. Aaron Moberly, Shuman He, and Christina Roup for their insightful feedback and expertise, as well as their time. Finally, I would like to thank Dr. Oliver Adunka for his flexibility, mentorship, and encouragement throughout my Ph.D. program.

Vita

2006-2009……B.S. Business Management
Wright State University
Dayton, Ohio

2009-2013……Au.D. Doctor of Audiology
University of Akron
Akron, Ohio

2015-2017……Research Audiologist
The Ohio State University
Columbus, Ohio

2017- present……..Research Scientist
The Ohio State University
Columbus, Ohio

Publications

Riggs, W. J., Vaughan, C., Skidmore, J., Conroy, S., Pellittieri, A., Carter, B., Stegman, C., He, S. (2021). The sensitivity of the electrically-stimulated auditory nerve to amplitude modulation cues declines with advancing age. *Ear Hear*. In press.

He, S., Xu L, Skidmore, J., Chao, X., Riggs, W. J., Wang, R., Vaughan, C., Luo, J., Shannon, M., Warner, C.. (2020). Effect of increasing pulse phase duration on neural responsiveness of the electrically stimulated cochlear nerve. *Ear Hear*. 41(6):1606-1618.

Riggs, W. J., Fitzpatrick, D. C., Mattingly, J. K., Harris, M. S., Hiss, M. M., Rajkumar, S., Zhan, K. Y., Brown, K.D., Moberly, A. C., Dodson E. E., Adunka O. F. (2020). Electrocochleography during translabyrinthine approach for vestibular schwannoma removal. *Otol Neurotol*. 41(3):e369-e377.

Riggs, W. J., Hiss, M. M., Skidmore, J., Varadarajan, V., Mattingly, J. K., Moberly, A.C., Adunka, O. F. (2020). Utilizing electrocochleography as a microphone for fully implantable cochlear implants. *Sci Rep*. 10 (1), 3714.

Mattingly, J. K., Zhan, K. Y., Hiss, M. M., Harris, M. S., Dodson, E. E., Moberly, A. C., Adunka, O. F., Riggs W. J. (2019). Intraoperative electrocochleography in patients with Ménière's disease undergoing endolymphatic sac decompression and shunt surgery. *Otol Neurotol*. 40 (9):1208-1216

Field of Study

Major Field: Speech and Hearing Science

Table of Contents

List of Tables

List of Figures

CHAPTER 1: INTRODUCTION

Since their advent, auditory evoked potentials have provided a robust approach to objectively study how sound is detected by the ear and transmitted to the auditory cortex. The aim of the current work was to utilize auditory evoked potentials and various types of stimuli to study how the impaired peripheral auditory system processes sound.

The first manuscript describes a study evaluating temporal and spectral encoding of speech-like stimuli (e.g., syllables) by the peripheral auditory system using electrocochleography (ECochG). ECochG response patterns, including waveform morphology, were identified and correlated with word recognition capabilities in normal and hearing-impaired listeners.

The second manuscript investigated temporal response properties of the auditory nerve in ears with Ménière's disease using ECochG. In this study, broadband clicks, spaced together to form a train, were used to induce adaptation of the auditory nerve and to measure the auditory nerve's recovery from the adaptation.

In the third manuscript, an electrical stimulation testing paradigm was used to investigate the effects of advancing age on adaptation of the auditory nerve in post-lingually deafened adult cochlear implant (CI) users.

CHAPTER 2: REVIEW OF LITERATURE

Sensory and Neural Structures of the Peripheral Auditory System

The human ear processes sound through delicate sensory cells in the organ of Corti. This group of cells is divided into two main types, known as outer hair cells (OHCs) and inner hair cells (IHCs) that span the entire length of the tonotopically-tuned basilar membrane. There are three rows of OHCs, which total approximately 12,000 cells. In contrast, there is one row of IHCs, comprised of about 3,500 cells (Möller, 2000). At the top of each hair cell are stereocilia, which move in response to sound, resulting in opening and closing of ion channels, leading to depolarization and hyperpolarization of the hair cell. This region is of significant importance in signaling neural activation, as this is the beginning stage of the transduction process, whereby mechanical energy from the basilar membrane is transformed into electro-chemical energy that is critical for auditory nerve activation (Salvi et al. 2007).

The auditory nerve, a division of the eighth cranial nerve that begins at the cochlea, is comprised of approximately 30,000 bipolar neurons, termed spiral ganglion cells (SGCs). It is composed of approximately 90-95% Type I fibers, which synapse on the IHCs and about 5-10% Type II fibers, which synapse on the OHCs (Musiek, 2007). The primary role of the auditory nerve is to transmit signals from the cochlea to the cochlear nucleus of the brainstem. For complex signals, this transmission requires precise neural synchrony in order to preserve the

important frequency and temporal cues required for the brain to decode the complex sound accurately.

Acoustically-Evoked Potentials of the Peripheral Auditory System

Acoustically-evoked potentials recorded within the vicinity of the inner ear are grouped together under the term ‘electrocochleography’ (ECochG). The ECochG response is the electrical output of multiple physiological processes of the peripheral auditory system. These physiological processes consist of activity of OHCs, IHCs, and SGCs. The activity from the OHCs is considered an alternating current potential, whereby it mimics the incoming sound’s acoustic properties. This response is called the cochlear microphonic (CM) (Wever et al., 1930). The CM represents the summation of changes in voltage that occur during displacement of stereocilia, during which time ions move in and out of the OHCs (Hudspeth 1982). The activity from the IHCs also minimally contributes to the CM response, however their main contribution is to the summation potential (SP). This waveform represents the direct current shift from baseline in the ECochG response. While it is not entirely understood, the SP is thought to represent changes in hair cell voltage due to asymmetries in the cochlear transduction process (Durrant et al., 1998; Whitfield et al., 1965). The activation of the SGCs are responsible for the last component of the ECochG response, the compound action potential (CAP). This response is generated from the change in voltage that occurs when many SGCs are depolarized and activated following neurotransmitter release from the IHCs (Goldstein et al., 1958). The CAP’s presence in the ECochG response occurs

at the on-set of the stimulus, although occasionally, it can be evoked at the off-set as well.

Electrically-Evoked Potentials of the Peripheral Auditory System

Electrically-evoked potentials generated by the auditory nerve and obtained through a CI are termed electrically-evoked compound action potentials (eCAPs) (Brown, 1990). The eCAP response represents synchronized neural activity of the auditory nerve that is generated by several auditory nerve fibers in response to electric charges delivered by an electrode contact of the CI. The response morphology is typically composed of a biphasic response with a negative deflection (N1) followed by a positive peak (P2) that all occur within 0.8 ms of electrical stimulation (Brown & Abbas, 1990; Brown, Abbas, et al., 1990; Brown et al., 1998). This technique allows for direct measurement of auditory nerve function without influence of the function of the hair cells.

Role of Peripheral Auditory Evoked Potentials

Since their conception, peripheral auditory evoked potentials have previously been utilized in numerous fashions in both animal and human studies. These have ranged from basic investigations of understanding the processing of sound by the cochlea and auditory nerve to clinical applications to identify response patterns that are reflective of pathologic conditions. The following discussion will focus on their human clinical applications.

Electrocochleography

A primary role of ECochG has focused on identification of auditory disorders. Specifically, ECochG measurements have been used to help identify endolymphatic hydrops and Auditory Neuropathy Spectrum Disorder (ANSD). Endolymphatic hydrops is a known pathological condition of the inner ear that, when present in conjunction with symptoms of episodic vertigo and fluctuating low-frequency sensorineural hearing loss (SNHL), is consistent with Ménière's disease (Monsell et al., 1995). MD's evoked potential phenotype characteristics have classically been identified as an SP/AP amplitude ratio to broadband clicks that exceeds 0.30 μV (Gibson et al., 1983), or an absolute SP amplitude evoked by a 1000 Hz tone burst that is more negative than -3 μV (Gibson, 1991). ANSD is a disorder often found in children that results from dys-sychronous response activity of the peripheral and sometimes central auditory system, leading to abnormal sound perception (Berlin et al., 2003; Starr et al., 1996). ANSD's ECochG characteristics have been identified as the presence of a prominent CM response without a subsequent CAP response. Further investigations in ANSD have concluded that, aside from identification of the disorder, subcategories (e.g., pre-synaptic, post-synaptic site-of-lesion) of the disorder can be identified using ECochG (McMahon et al., 2008; Santarelli et al., 2008).

A second and more recent area of clinical ECochG application has involved CIs. Adunka et al. (2006) described using ECochG intraoperatively at the time of cochlear implantation surgery to monitor cochlear function during the CI electrode

insertion process. This study demonstrated the feasibility of using ECochG during CI surgery and has since been followed by further and more sophisticated investigations. Specifically, these investigations have included recording the ECochG response through the CI electrode, allowing for intracochlear measurements during insertion surgery (Campbell et al., 2015; Harris, Riggs, Koka, et al., 2017; Haumann et al., 2019). Through this approach, ECochG measurements of CM amplitude are made continuously from any designated electrode contact of the CI during the insertion of the electrode into regions of the cochlea where intact OHCs are still present. The results are quickly analyzed and are characterized by an audible tone that is played aloud for the surgeon to hear. Depending on the changes that occur to the CM response, the surgeon can utilize this information to decide whether or not to make adjustments to the insertion process in attempts to avoid or minimize intracochlear trauma caused by the electrode, with the overall goal of preserving residual hearing (Harris, Riggs, Giardina, et al., 2017; Saoji et al., 2019).

Similarly, ECochG measurements recorded from the round window immediately prior to electrode insertion have been carried out to estimate the overall “cochlear health.” This ECochG approach consists of measurements made using tone burst stimulation across several clinically relevant frequencies to evoke supra-threshold CM responses (Choudhury et al., 2012). The resulting composite metric from measuring CM responses to different frequencies reflects the presence of remaining hair cells in the inner ear and has been used to estimate post-

operative speech perception capabilities in CI recipients with compelling accuracy (Canfarotta et al., 2020; Fitzpatrick et al., 2014; Fontenot et al., 2019). Additionally, ECochG recording through the CI can predict residual hearing (e.g., audiometric thresholds) with high accuracy (Koka et al., 2017; O'Connell et al., 2017).

Electrically-Evoked Compound Action Potential

Measurements of eCAP amplitudes have been used to help set initial (MAP) stimulation levels of the CI following surgical implantation. Investigations in both adults (Brown et al., 2000; Franck et al., 2001; Potts et al., 2007) and children (Gordon et al., 2002; Gordon et al., 2004; Hughes et al., 2000; Thai-Van et al., 2004) found that eCAP amplitudes can be used in a limited fashion when necessary to estimate behavioral threshold and comfortable levels of CI MAPs. However, the use of eCAPs in estimation of appropriate stimulation levels has somewhat faded out of practice, as there is often substantial individual variability between objective eCAP measurements and corresponding stimulation loudness levels.

As the use of eCAPs to estimate MAP stimulation levels has slowed, focus shifted toward understanding how eCAP responses to features of speech, such as temporal cues, as well as the eCAP's relationship to other individual factors (e.g., age), are related to outcome performance with a CI. In this regard, results have shown that the auditory nerve's response to amplitude modulated electrical stimulation is important for encoding speech envelope cues in CI users (Tejani et al., 2017). Other studies evaluating temporal responsiveness of the auditory nerve

have implemented eCAP measurements to investigate the effects of age on auditory encoding. These findings have indicated that the auditory nerve's ability to follow the envelope of modulated electrical pulse train stimulation (Riggs et al., 2021), as well as the auditory nerve's ability to recover from constant amplitude pulse train stimulation, declines with advancing age (Mussoi et al., 2020).

More recently, there has been growing trend in the use of eCAPs to understand how auditory nerve function is impacted by various causes of hearing loss (e.g., genetic-linked). For example, using amplitudes of the eCAP response, Luo et al. (2020) found that the Gap Junction Beta-2 (GJB2) mutation does not lead to auditory nerve degradation compared to idiopathic SNHL. Similarly, these authors showed that the Solute Carrier family 26 member 4 (SLC26A4) gene results in auditory function similar to idiopathic SNHL. In disorders that result in deficiency of the auditory nerve, He et al. (2018) showed that auditory fibers arising from the apical regions of the cochlear spiral are largely compromised. Altering different stimulation parameters of the CI could lead to better activation of the auditory nerve in this patient population (He et al., 2020).

Overall, ECochG and eCAPs are robust electrophysiological techniques that allow for evaluation of functional properties of the cochlea and auditory nerve, and continue to hold promise as objective tools for aiding clinical management of hearing impaired listeners.

REFERENCES

Adunka, O., Roush, P., Grose, J., et al. (2006). Monitoring of cochlear function during cochlear implantation. *Laryngoscope, 116*, 1017-1020.

Berlin, C. I., Morlet, T., Hood, L. J. (2003). Auditory neuropathy/dyssynchrony: its diagnosis and management. *Pediatr Clin North Am, 50*, 331-340, vii-viii.

Brown, C. J., Abbas, P. J. (1990). Electrically evoked whole-nerve action potentials: parametric data from the cat. *J Acoust Soc Am, 88*, 2205-2210.

Brown, C. J., Abbas, P. J., Gantz, B. (1990). Electrically evoked whole-nerve action potentials: data from human cochlear implant users. *J Acoust Soc Am, 88*, 1385-1391.

Brown, C. J., Abbas, P. J., Gantz, B. J. (1998). Preliminary experience with neural response telemetry in the nucleus CI24M cochlear implant. *Am J Otol, 19*, 320-327.

Brown, C. J., Hughes, M. L., Luk, B., et al. (2000). The relationship between EAP and EABR thresholds and levels used to program the nucleus 24 speech processor: data from adults. *Ear Hear, 21*, 151-163.

Campbell, L., Kaicer, A., Briggs, R., et al. (2015). Cochlear response telemetry: intracochlear electrocochleography via cochlear implant neural response telemetry pilot study results. *Otol Neurotol, 36*, 399-405.

Canfarotta, M. W., O'Connell, B. P., Giardina, C. K., et al. (2020). Relationship between electrocochleography, angular insertion depth, and cochlear implant speech perception outcomes. *Ear Hear, Publish Ahead of Print*.

Choudhury, B., Fitzpatrick, D. C., Buchman, C. A., et al. (2012). Intraoperative round window recordings to acoustic stimuli from cochlear implant patients. *Otol Neurotol, 33*, 1507-1515.

Durrant, J. D., Wang, J., Ding, D. L., et al. (1998). Are inner or outer hair cells the source of summating potentials recorded from the round window? *J Acoust Soc Am, 104*, 370-377.

Fitzpatrick, D. C., Campbell, A. T., Choudhury, B., et al. (2014). Round window electrocochleography just before cochlear implantation: relationship to word recognition outcomes in adults. *Otol Neurotol, 35*, 64-71.

Fontenot, T. E., Giardina, C. K., Dillon, M., et al. (2019). Residual cochlear function in adults and children receiving cochlear implants: correlations with speech perception outcomes. *Ear Hear, 40*, 577-591.

Franck, K. H., Norton, S. J. (2001). Estimation of psychophysical levels using the electrically evoked compound action potential measured with the neural response telemetry capabilities of Cochlear Corporation's CI24M device. *Ear Hear, 22*, 289-299.

Gibson, W. P. (1991). The use of electrocochleography in the diagnosis of Ménière's disease. *Acta Otolaryngol Suppl, 485*, 46-52.

Gibson, W. P., Prasher, D. K., Kilkenny, G. P. (1983). Diagnostic significance of transtympanic electrocochleography in Ménière's disease. *Ann Otol Rhinol Laryngol, 92*, 155-159.

Goldstein, M. H., Kiang, N. Y. S. (1958). Synchrony of neural activity in electric responses evoked by transient acoustic stimuli. *J. Acoust. Soc. Am., 30*, 107–114.

Gordon, K. A., Ebinger, K. A., Gilden, J. E., et al. (2002). Neural response telemetry in 12- to 24-month-old children. *Ann Otol Rhinol Laryngol Suppl, 189*, 42-48.

Gordon, K. A., Papsin, B. C., Harrison, R. V. (2004). Toward a battery of behavioral and objective measures to achieve optimal cochlear implant stimulation levels in children. *Ear Hear, 25*, 447-463.

Harris, M. S., Riggs, W. J., Giardina, C. K., et al. (2017). Patterns seen during electrode insertion using intracochlear electrocochleography obtained directly through a cochlear implant. *Otol Neurotol, 38*, 1415-1420.

Harris, M. S., Riggs, W. J., Koka, K., et al. (2017). Real-time intracochlear electrocochleography obtained directly through a cochlear implant. *Otol Neurotol, 38*, e107-e113.

Haumann, S., Imsiecke, M., Bauernfeind, G., et al. (2019). Monitoring of the inner ear function during and after cochlear implant insertion using electrocochleography. *Trends in Hearing, 23*.

He, S., Chao, X., Wang, R., et al. (2020). Recommendations for measuring the electrically evoked compound action potential in children with cochlear nerve deficiency. *Ear Hear, 41*, 465-475.

He, S., Shahsavarani, B. S., McFayden, T. C., et al. (2018). Responsiveness of the electrically stimulated cochlear nerve in children with cochlear nerve deficiency. *Ear Hear, 39*, 238-250.

Hudspeth, A. J. (1982). Extracellular current flow and the site of transduction by vertebrate hair cells. *J Neurosci, 2*, 1-10.

Hughes, M. L., Brown, C. J., Abbas, P. J., et al. (2000). Comparison of EAP thresholds with MAP levels in the nucleus 24 cochlear implant: data from children. *Ear Hear, 21*, 164-174.

Koka, K., Saoji, A. A., Litvak, L. M. (2017). Electrocochleography in Cochlear implant recipients with residual hearing: comparison with audiometric thresholds. *Ear Hear, 38*, e161-e167.

Luo, J., Xu, L., Chao, X., et al. (2020). The effects of GJB2 or SLC26A4 gene mutations on neural response of the electrically stimulated auditory nerve in children. *Ear Hear, 41*, 194-207.

McMahon, C. M., Patuzzi, R. B., Gibson, W. P., et al. (2008). Frequency-specific electrocochleography indicates that presynaptic and postsynaptic mechanisms of auditory neuropathy exist. *Ear Hear, 29*, 314-325.

Moller, A. R. (2000). *Hearing: Its Physiology and Pathophysiology*. New York: Academic Press.

Monsell, E., Balkany, T. A., Gates, G. A., et al. (1995). Committee on Hearing and Equilibrium guidelines for the diagnosis and evaluation of therapy in Ménière's disease. American Academy of Otolaryngology-Head and Neck Foundation, Inc. *Otolaryngol Head Neck Surg, 113*, 181-185.

Musiek, F. E. (2007). Structure and Function of the Auditory Nerve. In F. E. Musiek, J. A. Baran (Eds.), *The Auditory System*. Boston, MA: Pearson.

Mussoi, B. S., Brown, C. J. (2020). The effect of aging on the electrically evoked compound action potential. *Otol Neurotol, 41*, e804-e811.

O'Connell, B. P., Holder, J. T., Dwyer, R. T., et al. (2017). Intra- and postoperative electrocochleography may be predictive of final electrode position and postoperative hearing preservation. *Front Neurosci, 11*, 291.

Potts, L. G., Skinner, M. W., Gotter, B. D., et al. (2007). Relation between neural response telemetry thresholds, T- and C-levels, and loudness judgments in 12 adult nucleus 24 cochlear implant recipients. *Ear and Hearing, 28*, 495-511.

Riggs, W. J., Vaughan, C., Skidmore, J., et al. (2021). The sensitivity of the electrically-stimulated auditory nerve to amplitude modulation cues declines with adavancing age. *Ear and Hearing*.

Salvi, R. J., Eddins, A. C., Wang, J. (2007). Cochlear Physiology II: Mostly Electrophysiology. In F. E. Musiek, J. A. Baran (Eds.), *The Auditory System*. Boston, MA: Pearson.

Santarelli, R., Starr, A., Michalewski, H. J., et al. (2008). Neural and receptor cochlear potentials obtained by transtympanic electrocochleography in auditory neuropathy. *Clin Neurophysiol, 119*, 1028-1041.

Saoji, A. A., Patel, N. S., Carlson, M. L., et al. (2019). Multi-frequency electrocochleography measurements can be used to monitor and optimize electrode placement during cochlear implant surgery. *Otol Neurotol, 40*, 1287-1291.

Starr, A., Picton, T. W., Sininger, Y., et al. (1996). Auditory neuropathy. *Brain, 119 (Pt 3)*, 741-753.

Tejani, V. D., Abbas, P. J., Brown, C. J. (2017). Relationship between peripheral and psychophysical measures of amplitude modulation detection in cochlear implant users. *Ear Hear, 38*, e268-e284.

Thai-Van, H., Truy, E., Charasse, B., et al. (2004). Modeling the relationship between psychophysical perception and electrically evoked compound action potential threshold in young cochlear implant recipients: clinical implications for implant fitting. *Clin Neurophysiol, 115*, 2811-2824.

Wever, E. G., Bray, C. (1930). Action currents in the auditory nerve in response to acoustic stimulation. *Proc. Nat. Acad. Sci., U.S. A., 16*, 344-350.

Whitfield, I. C., Ross, H. F. (1965). Cochlear-microphonic and summating potentials and the outputs of individual hair-cell generators. *J Acoust Soc Am, 38*, 126-131.

CHAPTER 3: MANUSCRIPT 1

Characterizing Electrophysiological Response Properties of the Peripheral Auditory System Evoked by Phonemes in Normal and Hearing-Impaired Ears

William J. Riggs, Meghan M. Hiss, Oliver F. Adunka

Department of Otolaryngology-Head and Neck Surgery

The Ohio State University Columbus, 43210

ABSTRACT

Objective: This study aimed to identify temporal and spectral domain characteristics of the phoneme/syllable evoked electrocochleography (ECochG) response. It also explored potential associations between the ECochG spectral content and hearing sensitivity and word recognition scores (WRS) in normal and hearing impaired listeners.

Design: This was a prospective study with 25 adult participants. All participants underwent intraoperative ECochG testing, and responses were recorded from the round window niche. Participants were divided into two groups based on their preoperative pure tone averages: participants with normal/mild sensorineural hearing loss (SNHL) and participants with moderate/moderately-severe SNHL. Target stimuli included a 40 ms /da/ and an 80 ms /ba/ presented in alternating polarity (rarefaction/condensation). Waveform response amplitude, latency, and spectra were analyzed and compared between groups using Nonparametric Kruskal-Wallis tests. Structural similarity index measure (SSIM) was used to determine similarity between the stimulus spectrum and that of the ECochG differential waveform.

Results: ECochG alternating waveform morphology evoked by the /da/ stimulus consisted of five prominent peaks labeled N_1-N_5 and its spectrum was dominated by the fundamental (F_0) frequency. The ECochG alternating response evoked by /ba/ consisted of nine prominent peaks labeled N_1-N_9 and was also dominated by

F_0. Amplitudes and latencies were not statistically different between groups for either stimulus. Significant positive correlations were found between SSIM and WRS for responses evoked by both /da/ (r= 0.56, p=0.004) and /ba/ (r= 0.67, p=0.006).

Conclusions: Auditory nerve encoding of F_0 amplitude of the phoneme-evoked ECochG response at suprathreshold stimulation levels is not significantly impacted by hearing loss among those losses ranging from normal to moderately-severe SNHL. Additionally, suprathreshold encoding of phonemes by sensory hair cells, as measured by the CM response, predicted listener word recognition performance on NU-6 word lists.

INTRODUCTION

The auditory brainstem response (ABR) has been used extensively in the field of audiology over the last several decades to evaluate function of the peripheral and central auditory pathways (e.g., Hall et al., 1997; Jewett et al., 1970; Picton et al., 1976). The ABR can be used as an objective method to estimate audiometric thresholds (Stapells et al., 1997), to evaluate the presence of a retrocochlear disorder, such as a vestibular schwannoma (Eggermont et al., 1980), and to help identify various disorders, such as endolymphatic hydrops (Don et al., 2005) or auditory neuropathy spectrum disorder (Starr et al., 1996). Historically, the choice of stimuli has been limited to either a 100 μs broadband click for neurodiagnostic evaluation of retrocochlear pathology, or narrowband tone bursts to estimate audiometric thresholds. More recently, the potential utility of more complex stimuli, such as phonemes/syllables, has been explored to probe auditory function. Phoneme stimuli are thought to represent more real-world aspects of communication and carry greater acoustic features than traditional tone burst or click stimuli (Skoe & Kraus, 2010).

Initially termed complex ABR (cABR), the now more commonly-known frequency following response (FFR), refers to the sustained scalp recorded response generated by the auditory brainstem following the delivery of an acoustic phoneme (Bidelman 2018; Johnson et al., 2008). While various phonemes have been traditionally employed, the most common stimulus to evoke the FFR has been a 40 ms /da/ (e.g., Anderson et al., 2013; Cunningham et al., 2001; Kraus et

al., 2016; Russo et al., 2004; Skoe & Kraus 2010). The /da/ is a consonant-vowel syllable that is primarily composed of a brief stop-burst followed by a sustained vowel that dominates the majority of the signal (Skoe & Kraus 2010). The scalp-recorded FFR response elicited by the /da/ has been found to produce an onset and offset response (labeled V and O) as well as three dominant FFR peaks in between (labeled D, E, F). While other smaller peaks often exist in the response, V, O, D, E, and F are the most reliable peaks commonly identified (Kraus et al., 2016; Skoe & Kraus, 2010; Skoe et al., 2015).

With the development of the FFR response, several studies have investigated how the auditory system encodes phonemes in different clinical populations, and many of these study paradigms have reported compelling findings. For example, Cunningham and colleagues (2009) found that children with learning disabilities exhibited smaller FFR amplitudes of the fundamental frequency (F_0) than children without a learning disability, suggesting underdeveloped auditory pathways as a contributing factor. When considering background noise, Anderson et al. (2010) found that children who perform poorly on speech-in-noise tasks also exhibit delayed FFR peak amplitudes, indicative of poor temporal resolution processing. Kraus et al. (2016) used the FFR to study children athletes with and without a history of mild traumatic brain injury (e.g., concussion). Here, they found the F_0 of the FFR to be smaller in amplitude in the concussion group compared to the control group (no concussion). Additionally, after the concussion resolved, the FFRs were found to be similar between groups.

Therefore, the authors suggested the FFR's potential clinical application in diagnosing mild traumatic brain injury.

With the establishment and investigational uses of the FFR, the acceptance of this approach has not been without its challenges. Specifically, speculation has existed on the exact underlying generators responsible for the phoneme-evoked scalp response. Kraus and White-Schwoch (2015) describe a conceptual framework that characterizes the FFR response as being predominately generated by central auditory brainstem pathways, but which are influenced by active top-down processes such as attention and cognitive-sensory coupling. For example, musicians with previous musical training have more finely tuned auditory circuits. Additionally, other work has suggested that the FFR includes a component/contribution from the auditory nerve (Bidelman 2018). However, all FFR approaches use a far-field technique to infer site generators. Furthermore, Nuttall and colleagues (2015) suggested that amplitudes and latencies of the phoneme ABR also reflect individual differences in cochlear spectral processing (e.g., auditory filters). As nearly all of the previous studies investigating speech ABR have been far-field-recordings, meaning the recordings were made from electrodes located at a significant distance from the source generators, it remains unclear how the auditory nerve responds when evoked by phoneme stimuli. As the peripheral auditory system is the initial stage of processing acoustic sounds, it is highly relevant to understand how the cochlea and auditory nerve are activated by a phoneme, using an electrophysiological measurement prior to its arrival at the

central auditory pathway. This could have implications for interpreting the FFR as traditionally measured, especially if applying this approach in patients with sensorineural hearing loss (SNHL). One approach to accomplish this could be through the use of electrocochleography (ECochG).

ECochG is the near-field measurement of the peripheral auditory system activation in response to an acoustic stimulus. The ECochG response reflects the electrical activity of both the cochlea and auditory nerve (e.g., see Eggermont, 2017 for review). The primary components of the ECochG response include the cochlear microphonic (CM) and summating potential, both thought to arise from cochlear hair cells, and the compound action potential (CAP) generated by the auditory nerve.

The importance of understanding response properties of the auditory nerve in humans to phoneme stimulation could facilitate interpretation of far-field FFR recordings. For example, Song and colleagues (2011) found that the F_0 amplitude of the FFR response varies with a person's ability to understand speech in background noise despite normal audiometric thresholds. While the FFR is thought to be a subcortical-dominated response that can be influenced by top-down processes (Kraus & White-Schwoch, 2015), Song and colleagues (2011) were unable to measure the auditory nerve's processing of the phoneme stimuli. Thus, any deficits of auditory nerve encoding likely would have been undetected by the authors' technique. It is important to note that recent animal work has shown that extensive damage to the hair cell/auditory nerve synapse can exist in the presence

of normal audiometric thresholds (Kujawa & Liberman, 2009). This type of phenomenon, commonly termed “hidden hearing loss” (Schaette & McAlpine, 2011), underscores the importance of capturing peripheral encoding processes of phoneme stimuli when making interpretations of subcortical auditory processing deficits, as the FFR response could be impacted by encoding deficits of the peripheral auditory system. Thus, establishing a framework to objectively evaluate peripheral auditory encoding of phonemes would have significant importance for interpreting the FFR clinically. The aim of the present study was to investigate response properties of the healthy and impaired peripheral auditory system using an intraoperative ECochG paradigm. Specifically, we aimed to 1) define the morphological and spectral components of the speech-evoked ECochG for different levels of hearing sensitivity (normal/mild and moderate/moderately-severe) and 2) investigate how spectral encoding by the cochlear-dominated portion of the ECochG response (the CM) related to word recognition performance. Our overall hypothesis was that the normal/mild SNHL hearing group would exhibit larger time and spectral domain amplitudes than the moderate/moderately-severe SNHL group.

MATERIALS AND METHODS

Participants

Study participants consisted of 25 adults (16 females, 9 males) aged 21 – 81 years (mean: 51.7 yrs, standard deviation [SD]: 15.7 yrs). Participants were recruited from The Ohio State University Otolaryngology/ Head & Neck surgery Clinic, where they were scheduled to undergo various surgical procedures (see Table 3.1). Participants were divided into two groups based on their pre-operative air conduction pure tone average (PTA) at 500, 1000, 2000 Hz: 1) participants with normal/mild SNHL (PTA between -10 dB HL and 40 dB HL), 2) participants with moderate/moderately-severe SNHL (PTA between 41 dB HL and 70 dB HL) (Clark 1981). The study was approved by The Ohio State University's Biomedical Institutional Review Board (protocols: 2015H0045 and 2015H0087). Written informed consents were obtained from study participants prior to participation.

ID	Age	Sex	Ear Tested	Surgical Procedure	PTA (HL)	WRS (%)	Group	Stimulus	
								/Da/	*/Ba/*
B1	42	M	L	ELS	63	76	2	X	X
B2	61	M	L	ELS	45	60	2	X	X
B3	30	F	L	ELS	50	96	2	X	X
B4	66	F	L	Lab	58	36	2	X	X
B5	58	F	L	VS	15	100	1	X	-
B6	47	F	L	VS	18	100	1	X	X
B7	65	F	L	ELS	45	40	2	X	X
B8	68	M	L	Lab	47	88	2	X	-
B9	51	M	R	ELS	42	92	2	X	X
B10	56	F	L	ELS	47	4	2	X	X
B11	44	F	L	ELS	52	100	2	X	-
B12	75	M	R	PCO	43	40	2	X	X
B13	28	F	L	CI	58	36	2	X	X
B14	54	M	R	CI	70	32	2	X	X
B15	36	M	L	VS	70	16	2	X	X
B16	62	F	R	Lab	43	76	2	X	X
B17	40	M	R	SCD	18	100	1	X	-
B18	81	F	R	ELS	50	92	1	X	-
B19	21	F	R	VS	13	100	1	X	-
B20	48	F	L	VS	52	60	2	X	-
B21	38	F	L	SCD	10	100	1	X	X
B22	35	F	L	VS	15	100	1	X	-
B23	74	F	R	PCO	12	100	1	X	X
B24	60	F	L	ELS	70	64	2	X	-
B25	54	M	R	ELS	23	100	1	X	X

Table 3.1. Demographic, audiometric, and study information for all participants. M: male, F: female, L: left, R: right, ELS: endolymphatic sac, VS: vestibular schwannoma, hearing level: HL, labyrinthectomy: Lab, posterior canal occlusion: PCO, superior canal dehiscence: SCD, Did not test: -, Did test: X, pure tone average (0.5, 1.0, 2.0 kHz): PTA, word recognition score: WRS.

Stimulus

Stimuli consisted of two consonant-vowel-stop-burst tokens, /da/ and /ba/, which were synthesized using Klatt software (SenSyn, Sensimetrics Corporation, Malden, MA) at a sampling rate of 48 kHz. The /da/ was 40 ms in duration, and its spectrum consisted of a rising fundamental (F_0 [103–125 Hz]) with three formants (F_1, F_2 and F_3) that varied from 220 to 720 Hz (F_1), 1700 to 1240 Hz (F_2), and 2580 to 2500 (F_3) over the last 30 ms of the signal. The /ba/ was 80 ms in duration, and its spectrum was comprised of an F_0 at 120 Hz and three formants varying over time: F_1 (400 Hz-760 Hz), F_2 (1000 Hz-1200 Hz), and F_3 (2000–2500 Hz). Stimulation level was stimulus-dependent, with /da/ being delivered at 108 dB peak sound pressure level (pSPL) and the /ba/ being delivered at 89 dB pSPL. The difference in stimulation levels was due to our interest in assessing ECochG representation of multiple phonemes at different intensity levels. However, due to the recording time required per phoneme, we were limited in data-acquisition time. Thus, we chose two phonemes with different peak levels as the stimuli. Peak stimulation levels were calibrated using a 2 cc coupler and 1 inch condenser microphone routed to a sound level meter (System 825, Larson Davis, Depew, NY) set to “peak hold” mode.

Electrophysiological Measurements

A Biologic Navigator Pro Auditory Evoked Potential apparatus (Natus Medical Inc, San Carlos, CA) was used to deliver stimuli and record electrophysiological activity. Stimuli were delivered through a transducer (ER-3,

Etymotic Research, Elk Grove Village, IL) connected to an insert earphone placed in the external auditory canal. ECochG responses were differentially recorded using a horizontal montage with the active electrode placed at the round window of the cochlea, the reference electrode placed at the contralateral pre-auricular point (Ac), and the ground electrode placed at the high forehead (Fz). Impedances were always less than 10 kΩ and balanced between electrodes. Recordings were comprised of 1024 sampling points with an epoch of 64 ms for /da/ and 85 ms for /ba/. Recording filters were set at 70 Hz for the high pass and 3000 Hz for the low pass. Repetition rate was 13.1/s for 500 stimulus trials presented in alternating polarity (250 per phase) with the artifact rejection threshold set at 47 μV.

Electrophysiological Analysis

Peak Measurements

To define the auditory nerve portion of the phoneme-evoked ECochG response, an alternating waveform was created (sum of the ECochG response to rarefaction and condensation phases of the stimulus [$ECochG_{alt}$]) and used to measure peak latencies and amplitudes. As employed in traditional ABR measurements, identifiable regions of maximal amplitude displacement (i.e., manual peak picking) were identified by two experienced ECochG researchers (WJR and MMH) separately, blinded from the other's results. In the event the two researchers were not in agreement on the presence of a peak, a third researcher (OFA) was consulted. Peak identification was initially conducted on the normal/mild SNHL group, as it was expected that this group would provide the

better template to establish the primary neural peaks of the response due to a lesser degree of hearing loss. This allowed for establishing an expected latency for identifying peaks in the ECochG responses of the group with moderate/moderately-severe SNHL, as it was expected that this group would have poorer waveform morphology due to greater severity of hearing loss. Following peak identification, amplitude was measured as the peak-to-peak displacement (μV). As with conventional ECochG labeling, each peak was labeled at the negative region of maximal displacement starting with N_1 for the first negative peak followed by P_1 at the corresponding positive peak for the first identifiable response. This labeling continued for each consecutive response, where each additional peak was labeled in a consecutive fashion (e.g., N_1, N_2, N_3…). The amplitude of the peak was considered significant if it was three standard deviations (SDs) above the pre-stimulus region's maximal peak-to-peak displacement. The latency of each peak was recorded at the negative region of maximal displacement for each peak.

Spectral Analysis

A fast Fourier transform (FFT) using zero padding was applied to the $ECochG_{alt}$ response to calculate spectral coding of F_0 amplitude. Total amplitude of the spectrum from 100–130 Hz was calculated, and a response was considered significant if it was greater than three SDs above the noise floor calculated from three bins below the spectrum region.

The structural similarity index measure (SSIM) was implemented to evaluate spectral morphology of the hair cell-dominated (i.e., CM) portion of the

ECochG response (calculated difference of the responses obtained to rarefaction and condensation phases of the stimulus [$ECochG_{diff}$]). While not perfect at eliminating the neural portion, this calculated waveform helped emphasize the CM response and stimulus formant structure while minimizing neural contributions from the onset CAP (Koka et al., 2017; Skoe & Kraus, 2010; Aiken et al., 2008). Riggs et al. (2020) described this approach in a preliminary study, and here we have expanded upon this approach with the addition of more participants. The SSIM is a mathematical model designed to compare two images and determine their overall similarity based on three components: structure (contour), luminance (intensity), and contrast (Wang et al., 2002; Wang et al., 2004). Our implementation held the weighting factor equal for each of the three components (e.g., 1, 1, 1) as these are the default weighting factors. Our interest was in finding a single value that could account for the entire spectrum of the $ECochG_{diff}$ response over time. Thus, spectrograms were created from the $ECochG_{diff}$ response, and its spectral structure (i.e., formant energy over time) was compared with the spectral structure of the stimulus. The SSIM ranges from 0 to 1, where 1 is an exact replication and 0 indicates a lack of any structural similarity between the two images.

Prior to spectrogram analysis, the $ECochG_{diff}$ response was normalized to its maximal amplitude and was aligned in its time domain to the time point (ms) of where the maximal value was achieved when using a cross correlation between the stimulus time domain waveform and the $ECochG_{diff}$ time domain waveform.

This approach slid the ECochG$_{diff}$ response along the x-axis of the stimulus until maximal correlation was reached, which yielded a lag time (ms), such that the ECochG$_{diff}$ response needed to be shifted to ensure best alignment. As the stimulus and ECochG recording window are of different lengths, it was necessary to align the two prior to performing spectral analysis. This helped ensure that the spectral structure would not be affected by time differences in the spectrograms when evaluated using the SSIM. Spectrograms were broadband with a window length of 0.005 seconds and contained time segments comprised of 240 points per segment that were shaped by a Hamming window. Frequency content for each portion of the spectrogram was calculated using FFTs with zero padding on each windowed time segment. Spectrograms were displayed with a view range of 70 Hz- 3000 Hz (same as ECochG filter settings) and were then gray-scaled (intensity range of 0–1). All ECochG$_{diff}$ responses used in the analyses were required to have at least one significant spectral response to be included in the SSIM model. Significance was determined by estimating the noise floor three bins above and below the boundary of each formant (F_1-F_3) for three points along the entire length of each formant (beginning, middle, end), which were 18, 25, and 35 ms and 12, 40, and 68 ms for the /da/ and /ba/, respectively.

Hearing Sensitivity

Audiometric thresholds and word recognition scores (WRS) were obtained from each participant's pre-operative hearing evaluation via chart review. All participants were required to have testing completed within six months of the

participant's surgery. The audiometric testing included a NU-6 word list for WRS. To evaluate any potential associations that residual hearing may have with the SSIM, we calculated measures of hearing sensitivity using various PTAs to use in correlation analyses. These PTA variations included the traditional three frequency PTA (average audiometric threshold at 0.5, 1.0, and 2.0 kHz) (Fletcher, 1929), a low-frequency PTA (average audiometric threshold at 0.25, 0.5, and 1.0 kHz), a high-frequency PTA (average audiometric threshold at 4.0, 6.0, and 8.0 kHz) and finally a PTA that encompassed every test frequency (average audiometric threshold at 0.25, 0.5, 1.0, 2.0, 4.0, 6.0. and 8.0 kHz).

Statistical Analysis

Statistical analysis was performed using IBM SPSS (version 26) and MATLAB (R2019) software. To quantify auditory nerve peak-to-peak amplitudes and latencies, measures of central tendency were characterized by calculating arithmetic means, while measures of dispersion were characterized by calculating SD. Amplitudes, latencies, and SSIM indices were assessed for normality using the Kolmogorov-Smirnov test. Nonparametric Kruskal-Wallis tests were carried out to assess amplitude and latency differences between groups for both stimuli, while Pearson product-moment correlation tests were used to assess relationships among the SSIM, PTA and WRS. Additionally, Welch independent samples t-tests were used to assess group differences in F_0 amplitudes. Note, the Welch test was chosen due to the unequal group sizes used in these comparisons. All tests were two-tailed, and significance was determined at the 95% confidence level.

RESULTS

Due to time constraints of testing in the operating room, of the 25 participants included, all underwent testing with the /da/ stimulus but only 16 had /ba/ testing completed. The average audiometric air conduction thresholds for each group can be found in Figure 3.1. There were nine participants in the normal/mild SNHL group and 16 in the moderate/moderately-severe SNHL group. The difference in group sizes was not unexpected, as the current ECochG approach is invasive and only attainable during a surgical procedure. Few participants with normal/mild SNHL require otologic surgery, as compared to those with typically greater SNHL secondary to a disease process (e.g., Ménière's disease, vestibular schwannoma, etc.). The age range of participants in each group can be seen in Figure 3.2. The median age for the normal/mild SNHL group was 43.5 years (range: 21.0-74.0), which was lower than the median age of the moderate/moderately-severe group of 56.0 years (range 28.0-81.0 years).

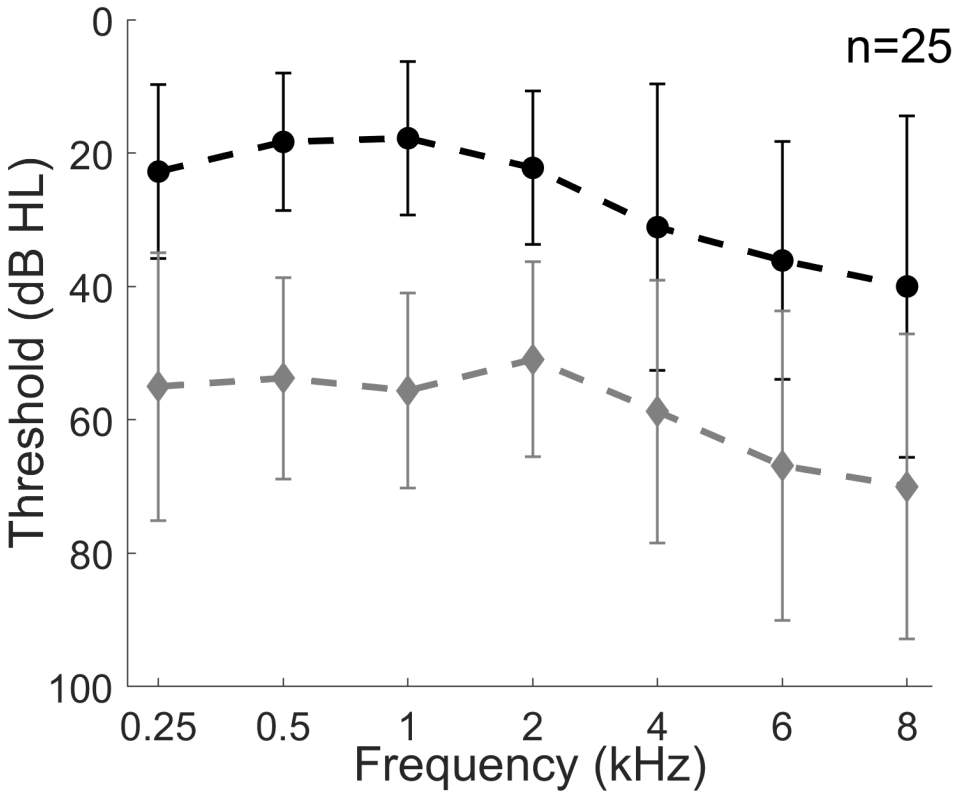

Figure 3.1. Average audiometric air conduction thresholds for the two groups of participants. Error bars represent 1 standard deviation. Black dots represent Group 1 (normal/mild SNHL) and grey diamonds represent Group 2 (moderate/moderately-severe SNHL).

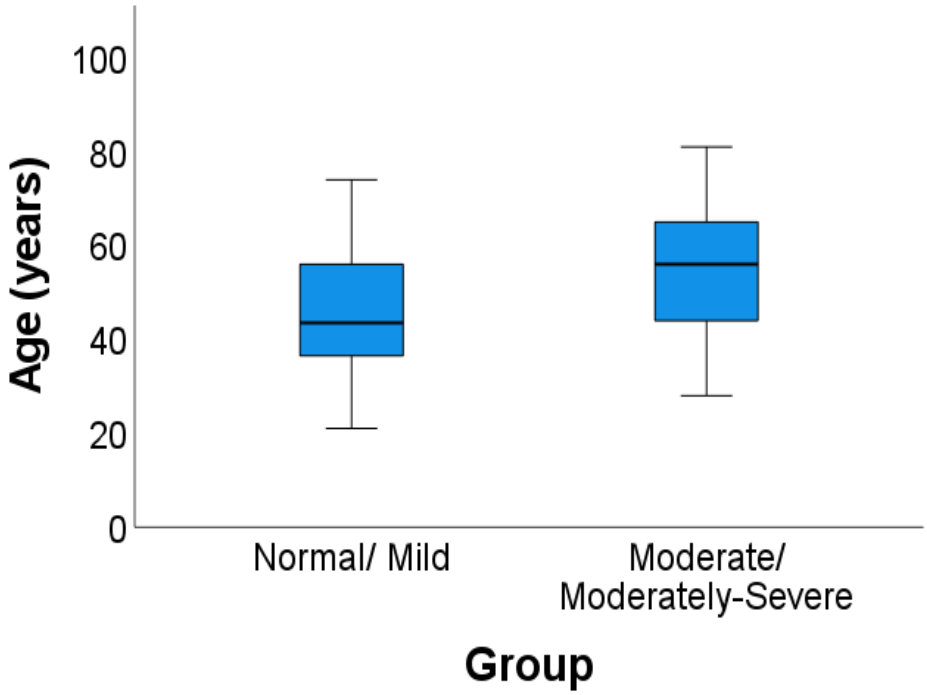

Figure 3.2. Box and whisker plots show the distribution of participant age in the two study groups, normal/mild and moderate/moderately-severe SNHL. Boxes represent the 25th and 75th percentiles while the solid black line represents the median.

/Da/- Auditory Nerve (ECochG$_{alt}$) Morphology

Table 2 displays the mean peak-to-peak amplitudes and absolute and inter-peak latencies for all identifiable peaks of the response. All participants from both groups had a significant response at each peak and were included in all analyses. In Group 1 (normal/mild SNHL), the morphology of ECochG$_{alt}$ consisted of five prominent peaks occurring at mean latencies of 2 ms (N_1), 16.2 ms (N_2), 25 ms (N_3), 33.6 ms (N_4), and 40.6 ms (N_5) (Figure 3.3-A). As visualized in Figure 3.3, Group 2 had similar latencies for each peak (see Table 3.2 for values). A grand average was calculated for each group and overlaid to show the similarity in morphology between groups. Two additional negative peaks were noticed between P_1 and N_2 at the region of the transition from *b*-*a*, though small in amplitude and not consistently present across subjects. Thus, we chose not to label these two peaks. Wave N_4P_4 was found to yield the largest amplitude, followed by N_3P_3, N_1P_1, N_2P_2, and finally N_5P_5, respectively, for both groups. Unexpectedly, Group 2 had a similar overall waveform morphology with the same trend in amplitudes as Group 1, and the groups were not significantly different in response amplitude (see Table 3.22 for results of Kruskal Wallis procedures). Similarly, when considering peak latency measured at the negative peak, no significant differences were found between groups for any peak (see Table 3.2).

	Group			
	1		*2*	
Peak	**Latency (ms)**	**Amplitude (μV)**	**Latency (ms)**	**Amplitude (μV)**
N_1P_1	2.01 (sd: 0.5)	6.81 (6.8)	2.343 (0.6)	6.64 (8.6)
N_2P_2	16.19 (0.4)	5.20 (4.1)	16.25 (0.6)	5.76 (7.1)
N_3P_3	24.97 (0.4)	6.90 (6.0)	25.0 (0.9)	7.57 (8.1)
N_4P_4	33.65 (0.3)	7.97 (7.3)	33.7 (0.6)	8.03 (8.1)
N_5P_5	40.63 (0.7)	2.91 (2.6)	41.1 (1.6)	3.86 (4.8)
N_1-N_2	14.19 (0.2)	-	13.91 (0.6)	-
N_2-N_3	8.77 (0.4)	-	8.76 (1.0)	-
N_3-N_4	8.68 (0.3)	-	8.73 (0.6)	-
N_4-N_5	7.0 (0.8)	-	7.4 (1.6)	-

/da/- Group Peak-to-Peak Amplitudes and Latencies Kruskal Wallis Results

Amplitude	X^2	df	P-value	Latency	X^2	df	P-value
N_1P_1	0.01	1	0.91	N_1	2.40	1	0.12
N_2P_2	0.09	1	0.77	N_2	0.07	1	0.79
N_3P_3	0.49	1	0.49	N_3	0.00	1	0.98
N_4P_4	0.41	1	0.52	N_4	0.42	1	0.84
N_5P_5	0.03	1	0.86	N_5	0.05	1	0.82

Table 3.2. Arithmetic means and standard deviations for each identifiable peak of the electrocochleography response (alternating waveform) evoked by the /da/ stimulus for two groups of adults (n=25) *(Top panel)*. Results of the Kruskal Wallis test for amplitude and latency between groups *(Bottom panel)*. Group 1 represents the normal/mild sensorineural hearing loss (SNHL) group while 2 represents the moderate/moderately-severe SNHL group. Millisecond: ms, microvolt (μV), standard deviation: sd, chi-square: X^2, degrees of freedom: df.

The F_0 energy was evaluated across groups, and its spectral content for $ECochG_{alt}$ can be found in Figure 3.3-B (left panel). Here, it can be seen that F_0 comprised the largest spectral component for both groups. Overall, there was a similar trend in spectral peaks. Figure 3.3-B (right panel) shows the F_0 amplitude distributions by group, with the black bar indicating group means. Visually, there is considerable variability in F_0 amplitude for both groups; however, amplitudes between groups were not statistically different ($t = 0.16$, $p = 0.87$).

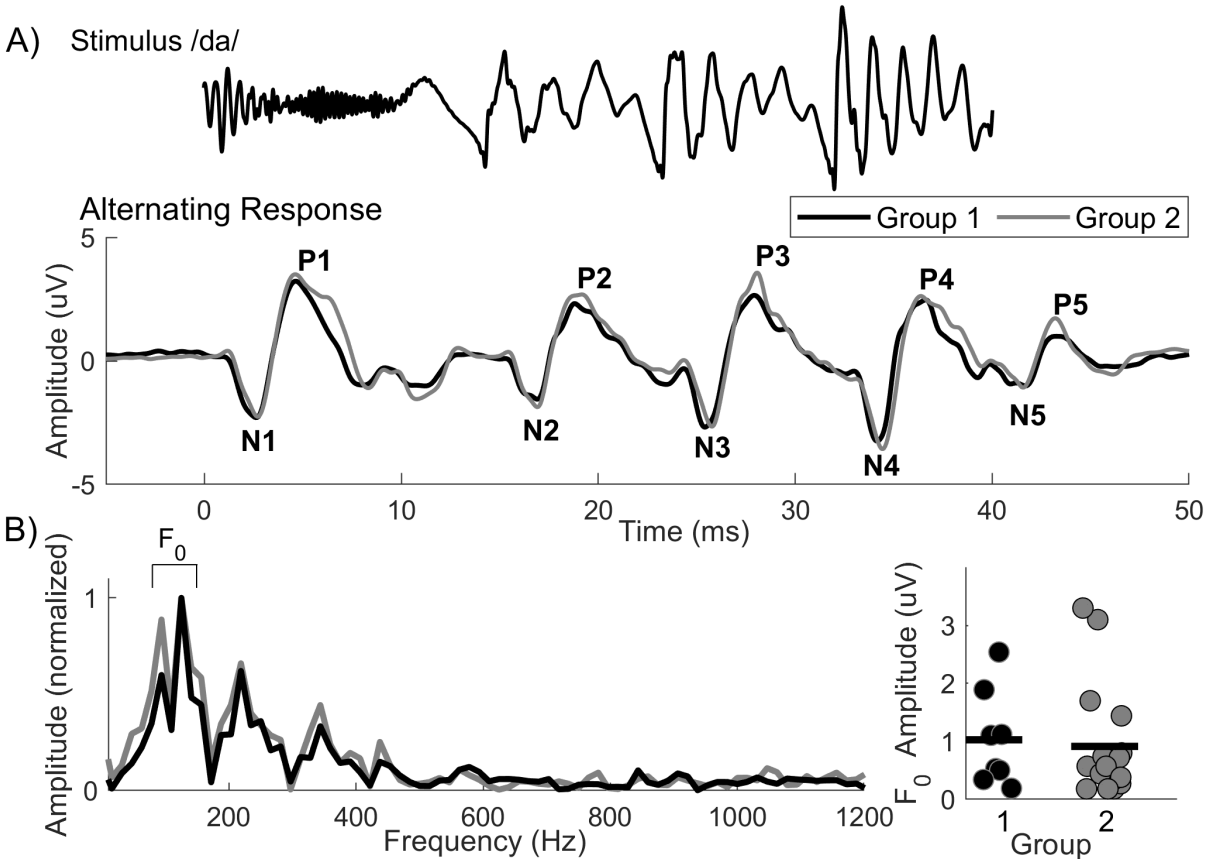

Figure 3.3. The top waveform displays the time domain representation of the 40 ms /da/ stimulus. The two bottom traces depict the grand average alternating electrocochleography response ($ECochG_{alt}$) evoked by the /da/ stimulus for each group: Normal hearing/mild sensorineural hearing loss (SNHL) (black; n=8) and moderate/moderate-severe SNHL (gray; n=17). B) Left panel shows the spectral content of $ECochG_{alt}$ and the right panel displays each participant's F_0 amplitude (filled circles) and group means (black bar).

/Da/- ECochG$_{diff}$: SSIM, PTA, and WRS

When considering CM activity, all participants were found to have at least one significant ECochG$_{diff}$ response. Thus, SSIM calculation was carried out for all 25 participants. The SSIM values were compared between groups, and the mean SSIM value for the /da/ was 0.43 (0.09 SD) for Group 1 and 0.37 (0.10 SD) for Group 2. They were not significantly different ($t = 1.72$; $p = 0.10$). Correlation analyses were conducted to explore the association between PTA and SSIM value (Figure 3.4-A). Here it can be observed that there is a slight negative trend of lower SSIM value associated with increasing PTA, however, none of these techniques were found to be significant (see Figure 3.4-A for p-values). The SSIM was then evaluated in a correlation analysis with WRS, and a significant positive correlation was found between SSIM value and WRS ($r = 0.56$; $p = <0.01$) whereby an increase in SSIM value resulted in a higher WRS (Figure 3.4-B). Finally, to evaluate the association of residual hearing and WRS, results of each PTA metric was used in correlation analysis with WRS. Significant negative correlations for all PTA measurement techniques with WRS were observed whereby WRS decreased with an increase in PTA (Figure 3.4-C).

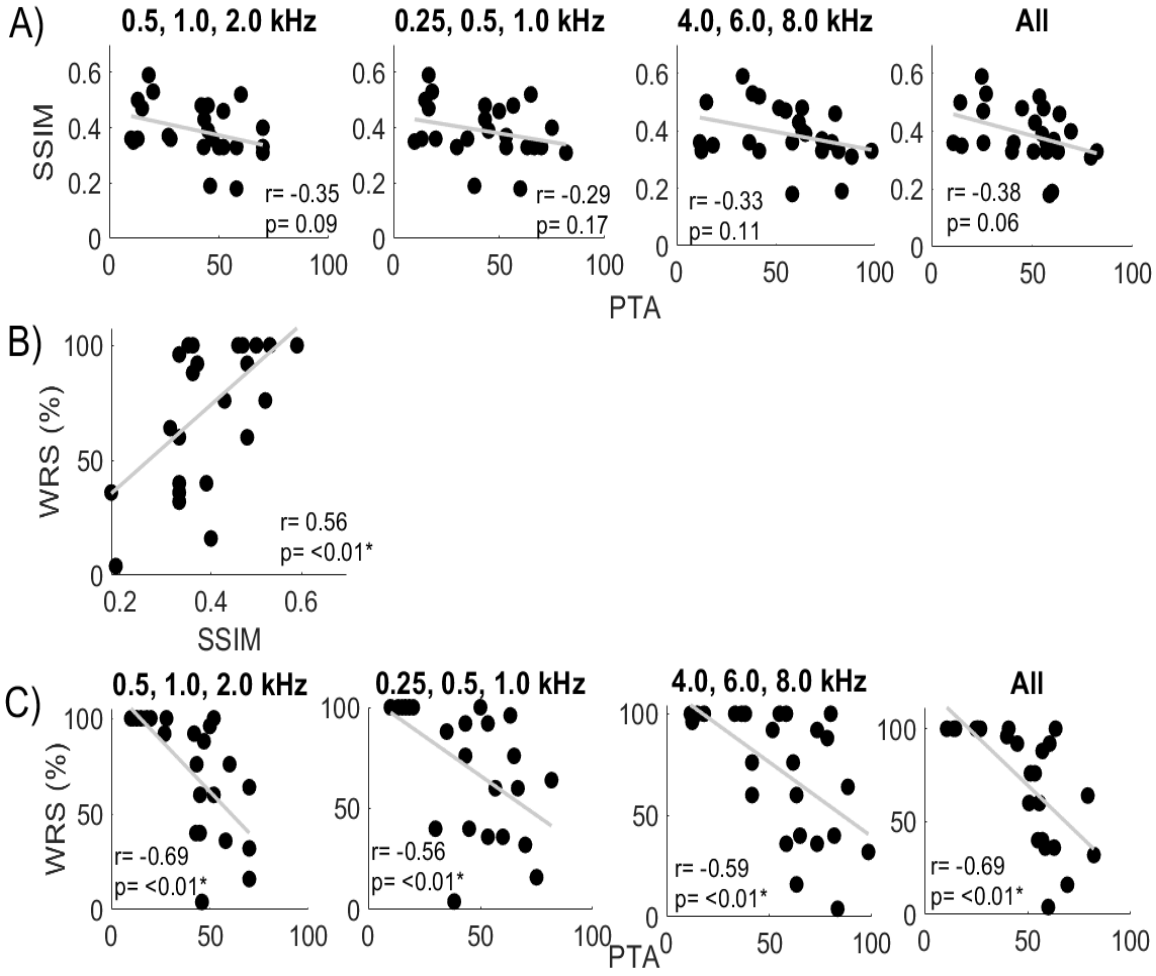

Figure 3.4. Results of Pearson product-moment correlations between A) the structure similarity index measure (SSIM) for the /da/ stimulus and each participant's pre-operative pure tone average (PTA), B) SSIM for the /da/ stimulus and word recognition score (WRS), C) PTA and WRS. A line of best fit is depicted in gray. Significant correlations are indicated by *.

/Ba/- Auditory Nerve (ECochG$_{alt}$) Morphology

Sixteen participants had /ba/ trials available for analysis (due to time constraints). Nine participants did not have a /ba/ trial completed - see Table 1 for included participants. ECochG$_{alt}$ response morphology can be seen in Figure 3.5-A. As observed with the /da/, responses were similar between groups, with nine reliable and identifiable peaks which were labeled (N_1...N_9). For the ease of visualization, the positive peaks (e.g., P_1) were not labeled. Note, participant B14 did not have significant peaks at the N_1P_1 and N_2P_2 regions, and their data were excluded from those individual peak analyses. Peak-to-peak amplitudes (e.g., N_1-P_1) and absolute and inter-peak latencies by Group can be found in Table 3.3. The /ba/ stimulus contains nine peak amplitude regions, and, upon close examination, each of those nine peaks appear to precede each of the nine peaks found in the ECochG$_{alt}$ response. Amplitude of wave N_9P_9 was found to yield the largest value, followed by N_7P_7, N_6P_6, N_8P_8, N_5P_5, N_4P_4, N_3P_3, N_1P_1, and finally N_2P_2, respectively, for both groups. Amplitudes did not differ between groups (see Table 3.3 for statistical results) with similar overall waveform morphology. Similarly, when considering peak latency measured at the negative peak, no significant differences were found between groups for any peak (see Table 3.3).

	Group			
	1		*2*	
Peak	**Latency (ms)**	**Amplitude (μV)**	**Latency (ms)**	**Amplitude (μV)**
N_1P_1	2.82 (sd: 0.9)	2.59 (2.6)	2.22 (0.7)	1.80 (3.3)
N_2P_2	10.95 (0.9)	2.58 (3.3)	10.38 (1.7)	1.81 (3.2)
N_3P_3	18.85 (0.7)	2.67 (2.3)	18.85 (1.4)	3.03 (5.8)
N_4P_4	27.35 (0.9)	3.9 (4.4)	27.72 (0.6)	3.36 (6.7)
N_5P_5	37.10 (0.5)	3.06 (1.1)	37.14 (0.5)	4.30 (7.7)
N_6P_6	45.88 (1.28)	4.33 (3.4)	46.09 (0.6)	4.98 (7.9)
N_7P_7	56.18 (0.5)	5.30 (3.7)	56.14 (0.5)	5.39 (8.7)
N_8P_8	66.82 (1.6)	3.35 (2.1)	66.03 (0.7)	4.78 (8.7)
N_9P_9	76.76 (0.5)	6.45 (5.23)	76.79 (0.5)	5.51 (8.5)
N_1-N_2	8.13 (0.4)	-	8.15 (0.4)	-
N_2-N_3	7.90 (0.3)	-	8.67 (1.7)	-
N_3-N_4	8.50 (1.2)	-	8.87 (1.3)	-
N_4-N_5	0.75 (0.8)	-	9.42 (0.4)	-
N_5-N_6	8.79 (0.9)	-	8.96 (0.6)	-
N_6-N_7	10.29 (1.0)	-	10.05 (0.7)	-
N_7-N_8	10.65 (1.6)	-	9.89 (0.3)	-
N_8-N_9	9.94 (1.4)	-	10.76 (0.5)	-

/ba/- Group Peak-to-Peak Amplitudes and Latencies Kruskal Wallis Results

Amplitude	X^2	df	P-value	Latency	X^2	df	P-value
N_1P_1	1.38	1	0.24	N_1	1.39	1	0.24
N_2P_2	0.61	1	0.43	N_2	0.04	1	0.84
N_3P_3	0.72	1	0.40	N_3	0.09	1	0.76
N_4P_4	1.47	1	0.23	N_4	0.95	1	0.33
N_5P_5	0.94	1	0.33	N_5	0.06	1	0.81
N_6P_6	0.72	1	0.40	N_6	0.03	1	0.86
N_7P_7	0.94	1	0.33	N_7	0.004	1	0.95
N_8P_8	0.53	1	0.47	N_8	1.07	1	0.30
N_9P_9	1.20	1	0.28	N_9	0.02	1	0.90

Table 3.3. Arithmetic means and standard deviations for each identifiable peak of the electrocochleography response (alternating waveform) evoked by the /ba/ stimulus for two groups of adults (n=25) *(Top panel)*. Results of the Kruskal Wallis test for amplitude and latency between groups *(Bottom panel)*. Group 1 represents the normal/mild sensorineural hearing loss (SNHL) group while 2 represents the moderate/moderately-severe SNHL group. Millisecond: ms, microvolt (μV), standard deviation: sd, chi-square: X^2, degrees of freedom: df.

The spectral content of ECochG$_{alt}$ was evaluated across groups, and the FFT results can be found in Figure 3.5-B (left panel). Similar to what was observed for the /da/ response, F_0 comprised the largest spectral component for both groups, and overall, there was a similar trend in spectral peaks. Mean F_0 amplitudes for the two groups can be seen in Figure 3.5-B (black line). They were not statistically different ($t = 0.46$, $p = 0.65$).

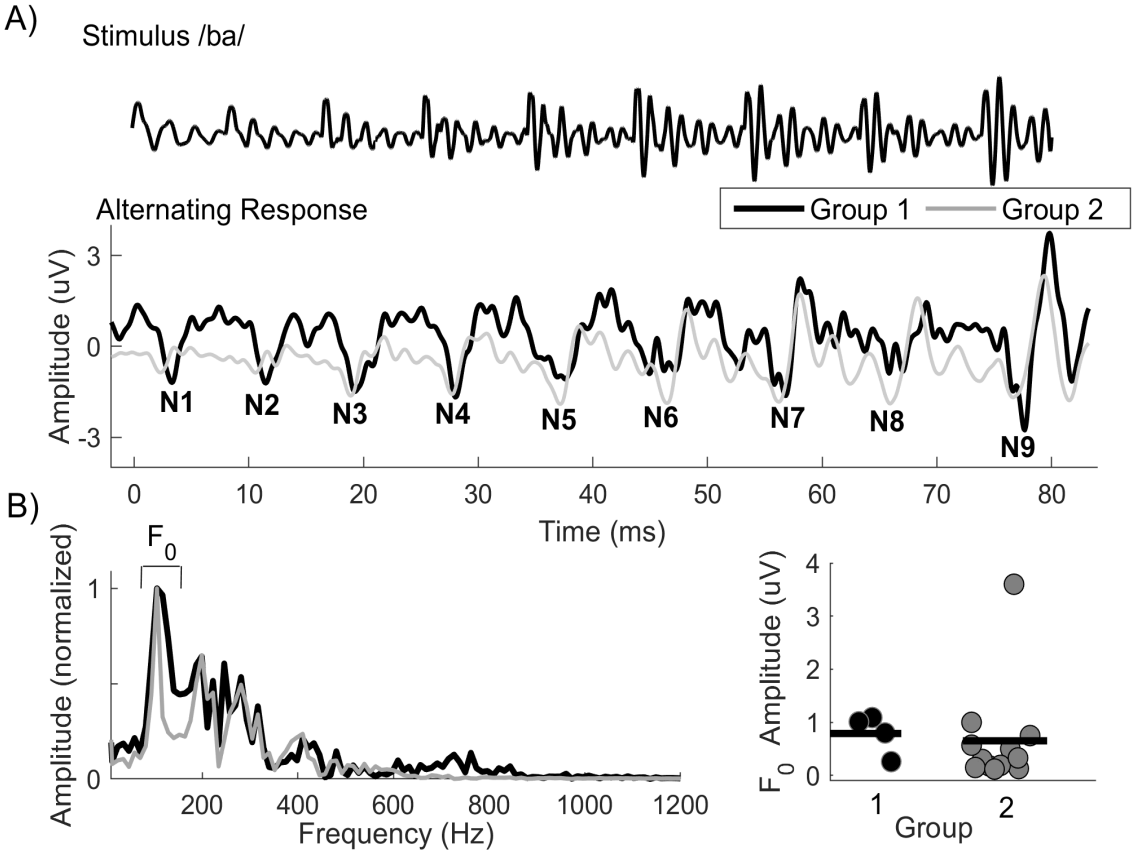

Figure 3.5. The top waveform displays the time domain representation of the 80 ms /ba/ stimulus. The two bottom traces depict the grand average alternating electrocochleography response evoked by the /ba/ stimulus for each group: Normal hearing/mild sensorineural hearing loss (SNHL) (black; n=4) and moderate/moderate-severe SNHL (gray; n=12). B) Left panel shows the spectral content of ECochG$_{alt}$ and the right panel displays each participant's F_0 amplitude (filled circles) and group means (black bar).

/Ba/- ECochG$_{diff}$: SSIM, PTA, and WRS

All 16 participants were found to have at least one significant formant response present in their ECochG$_{diff}$ response, thus, SSIM calculation was carried out for all participants The SSIM values were compared between groups, and the mean SSIM value for the /ba/ was 0.39 (0.15 SD) for Group 1 and 0.33 (0.15 SD) for Group 2. They were not found to be significantly different ($t = 0.59$; $p = 0.58$). The SSIM values were then correlated with the results of each PTA measurement metric to explore their association with each participant's level of residual hearing (Figure 3.6-A). Here, it can be observed that there is a slight negative trend of lower SSIM associated with increasing PTA, however, of these techniques only the high-frequency PTA measurement was found to be significantly correlated with the SSIM (see Figure 3.6-A for p-values). The SSIM was then used in a correlation analysis with WRS. A significant positive correlation was found between SSIM value and WRS ($r = 0.67$; $p < 0.01$), whereby an increase in SSIM value was associated with higher WRS (Figure 3.6-B). Finally, to evaluate the association of residual hearing and WRS, results of each PTA technique was used in a correlation analysis with WRS. Significant negative correlations for all PTA measurement techniques with WRS were observed whereby WRS decreased with an increase in PTA (Figure 3.6-C).

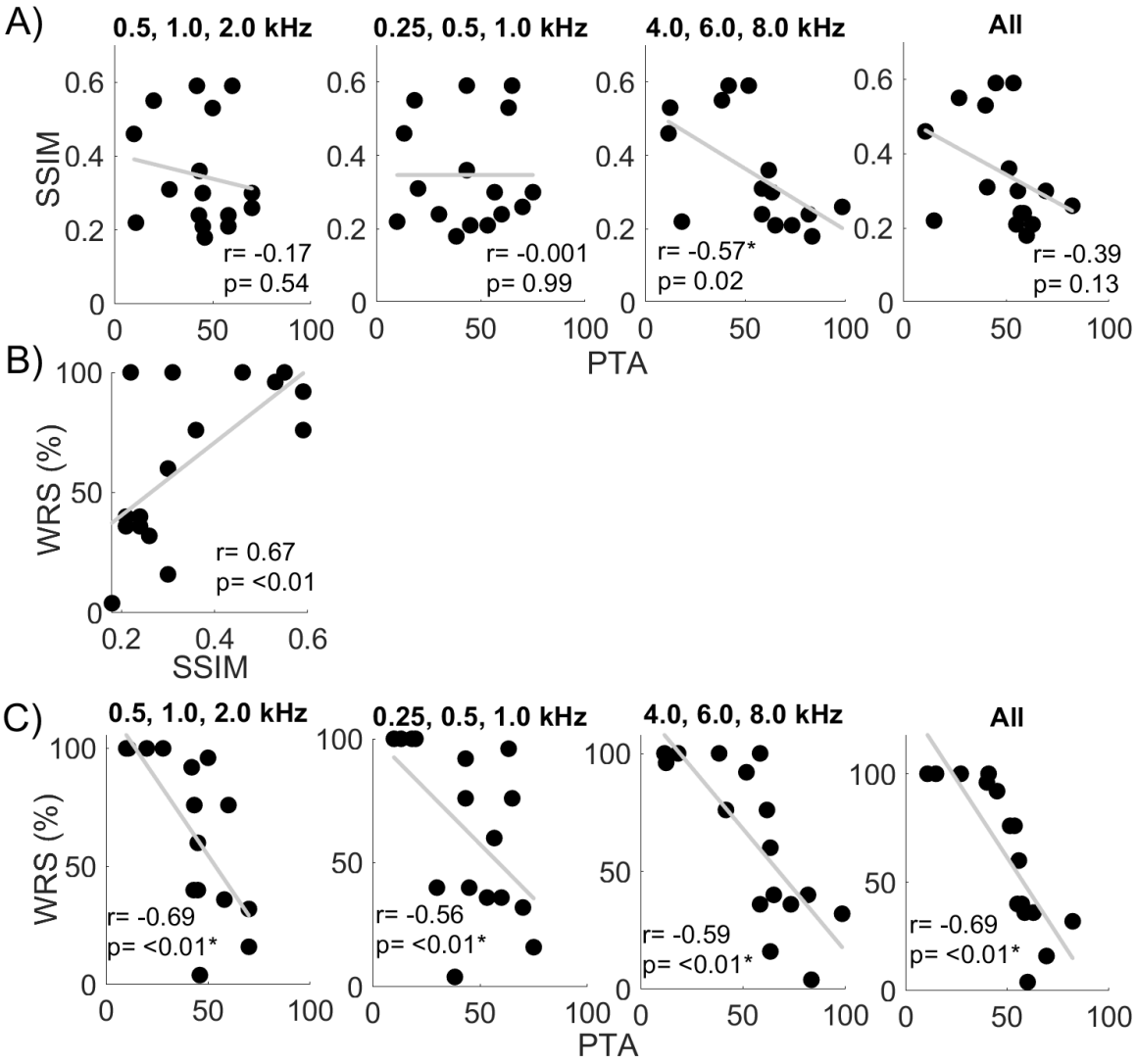

Figure 3.6 Results of Pearson product-moment correlations between A) the structure similarity index measure (SSIM) for the /ba/ stimulus and each participant's pre-operative pure tone average (PTA), B) SSIM for the /ba/ stimulus and word recognition score (WRS), C) PTA and WRS. A line of best fit is depicted in gray. Significant correlations are indicated by *.

DISCUSSION

In this study, we examined encoding of two phonemes by the peripheral auditory system with multiple goals. The first goal was to define waveform characteristics, including morphology and spectrum, in normal and hearing-impaired listeners. The second goal was to explore the relationship between hearing sensitivity and word understanding (i.e., WRS) to spectral encoding as measured by the CM activity of the ECochG response in normal and hearing-impaired listeners. Using suprathreshold stimulation levels, we identified waveform similarities between the two study groups (normal/mild hearing vs. moderate/moderately-severe hearing impairment) in peak amplitudes and latencies. Auditory nerve encoding of the F_0 was also found to be similar between groups. Additionally, we found evidence that speech understanding is directly correlated to the amount of spectral encoding by the inner ear of each phoneme (/da/, /ba/) as measured by the CM response. This is the first study known to the authors that defines the peripheral auditory system's response pattern to speech-like stimuli commonly used in auditory evoked potential studies that evaluate central auditory function in humans. Understanding how the peripheral auditory system encodes phonemes could provide a stronger basis for interpreting subsequent ABRs.

Temporal Processing

The auditory system's ability to distinguish between phonetic categories, such as stops, vowels, nasals, or fricatives, is heavily reliant on temporal envelope

features (Delgutte, 1997). With the use of both /da/ and /ba/, temporal response characteristics of auditory nerve function were observed in the ECochG$_{alt}$ response. Fluctuations in amplitude of the stimulus (i.e., amplitude modulations) appeared to elicit corresponding regions of peak amplitudes in each response waveform. That is, the auditory nerve responded to both the onset and the offset of the stimulus, but also responded to the periodicity portion of the vowel in both stimuli. This is a similar response pattern that has been well defined in FFR studies for /da/ (Russo et al., 2004; Skoe & Kraus 2010) and /ba/ (Akhoun et al., 2008), and while these studies measured brainstem responses, there is a similar overall pattern. Although not necessarily directly comparable due to stimulus level differences, it may be that the response patterns seen in FFR responses reflect much of the same activity that was coded by the auditory nerve, but at higher centers of the auditory system. Previous animal studies have shown that speech perception at the phoneme level is dependent upon adaptation properties of the auditory nerve (Delgutte, 1980) where rapid changes in amplitudes were represented in the discharge patterns of single auditory nerve fibers (Kiang, 1980; Kiang et al., 1979). It is likely that much of this information is retained in the central auditory system, thus yielding the similarities in our findings and those of far-field FFR.

A notable but unexpected finding was that, despite the two groups exhibiting different levels of hearing, the response properties were of similar morphology across groups for both phonemes. It should be noted that many participants within

Group 2 were undergoing endolymphatic sac decompression surgery, a treatment for Ménière's disease. The similarity in overall amplitudes could be interpreted to mean that the cochlea-auditory nerve communication was intact in these patients, although this could be somewhat misleading. Ménière's disease is known to result in fluctuating hearing acuity, potentially influencing our results as some participants in Group 2 who had Ménière's may have had changes in their hearing between the time of audiometric testing and electrophysiological testing. The stimuli were also presented at high presentation levels that were most likely substantially supra-threshold for participants in both groups, mitigating audibility effects due to differences in audiometric thresholds. Thus, it is likely that if lower levels were utilized differences between groups may have been observed.

Spectral Processing

In addition to temporal processing, another important aspect to speech perception is the auditory system's ability to process spectral fine structure characteristics of phoneme formants and their transitions, which allows one to distinguish between vowels and place of articulation for consonants (Delgutte, 1997). In particular, vowels are nearly entirely specified by their first two or three formants (Klein et al., 1970; Peterson et al., 1952). Our technique for assessing how these features were encoded at the periphery yielded interesting results. Here, we found that spectral characteristics of each phoneme were directly related to word recognition capabilities. The formant frequency structures were best preserved in the ECochG responses of those participants with the best WRS.

While this finding is not necessarily surprising, it underlies the importance of spectral encoding by the cochlea. It does have implications for possible future clinical applications, where a less invasive approach could be employed to evaluate auditory function in a clinical setting for diagnostic purposes.

Residual Hearing

To evaluate whether the SSIM provided useful information outside of what would be captured through audiometric testing, we investigated the relationship between audiogram thresholds, WRS, and SSIMs. As expected, PTA was strongly related to WRS. This is an expected finding, as this has been shown to strongly predictive of speech understanding in quiet (e.g., Fletcher, 1929). To determine if the relationship between SSIM and WRS was possibly due to residual hearing, we used multiple approaches to calculate PTA and explored correlations between the SSIM and each calculated PTA. The SSIM values for ECochG responses evoked by the /da/ stimulus were not significantly correlated with any PTA measure. This was similar for the ECochG responses evoked by the /ba/, with the exception of the high-frequency PTA, which was significant. It should be noted that while the majority of these correlations did not reach significance, there was a weak but consistent negative trend in which the SSIM decreased in value with an increase in PTA value. These findings could suggest a few possible explanations. First, the ECochG procedures and evoked responses were conducted at suprathreshold levels, while the PTA is a measure of auditory threshold. Thus, a weak association between the SSIM may be expected, as they were not evaluating hearing

sensitivity at the same or similar stimulation levels. Secondly, the SSIM only accounts for peripheral auditory function as measured by the CM. PTA, however, is not only dependent on peripheral function, such as the presence of sensory hair cells, but also higher-level auditory processing. Detection of pure tones requires the listener to respond/ indicate when a sound is heard. These differences in measurements of SSIM and PTA could be potential reasons for the lack of robust correlation between SSIM and PTA. Despite differences in the SSIM and PTA measurements, both were moderately correlated with WRS. These findings potentially suggest that the SSIM is partially impacted by residual hearing, but that each measurement appears to predominately evaluate different components of auditory encoding that are important for WRS.

Limitations

One important limitation of the current study is that we were unable to include concurrent far-field ABR in conjunction with ECochG. As typical far-field recordings to speech-like stimuli require upwards of 3000-6000 averages to obtain a reliable response, this was simply impractical to implement in an intraoperative paradigm. Additionally, much of the previous literature on speech-evoked potentials utilize a lower stimulus presentation level (e.g., 80 dB SPL) for the /da/ stimulus, thus likely limiting interpretation beyond the current study.

A second potential limitation of the current study is the variation in etiology of hearing loss for participants, especially between groups. Specifically, 13 participants were diagnosed with Ménière's disease. Eleven of them were in the

moderate to moderately-severe SNHL group. Ménière's disease is a disorder of the inner that often results in fluctuating SNHL and can have a greater effect on lower audiometric frequencies rather than higher frequencies (Merchant et al., 2005). Additionally, five participants had a vestibular schwannoma of the auditory nerve in the test ear. Vestibular scwhannomas can cause neural deficits that are not present in idiopathic or other forms of SNHL (Eggermont, 1980). The inclusion of these two patient populations with comparisons of patients with normal hearing or mild acquired SNHL somewhat limits the interpretability and generalization of the current results due to the extensive heterogeneity in causes of hearing loss across the participants.

Finally, a third limitation that is important to consider is the potential effect of aging on our results. The aging process is known to result in both functional and anatomical changes to the auditory system (e.g., Humes, 1983; Wu et al., 2019). The current sample age range spanned 60 years with the youngest participant age being 21 years old, and the oldest participant being 81 years old. While the two study groups were divided based on their hearing sensitivity, the group with moderate/moderately-severe SNHL had an older median participant age compared to the normal/mild SNHL group. As advancing age is known to result in deteriorations of the auditory system, any potential effects of age might have been masked due to both groups containing both younger and older adults.

CONCLUSION

Auditory nerve encoding of F_0 amplitude of the suprathreshold phoneme-evoked ECochG response is not significantly impacted by hearing loss among those losses ranging from normal to moderately-severe SNHL. Suprathreshold hair cell encoding of phonemes as measured by the CM response moderately predicts listener word recognition capability on NU-6 word lists.

REFERENCES

Akhoun, I., Gallego, S., Moulin, A., et al. (2008). The temporal relationship between speech auditory brainstem responses and the acoustic pattern of the phoneme /ba/ in normal-hearing adults. *Clin Neurophysiol, 119*, 922-933.

Anderson, S., Parbery-Clark, A., White-Schwoch, T., et al. (2013). Auditory brainstem response to complex sounds predicts self-reported speech-in-noise performance. *J Speech Lang Hear Res, 56*, 31-43.

Bidelman, G. M. (2018). Subcortical sources dominate the neuroelectric auditory frequency-following response to speech. *Neuroimage, 175*, 56-69.

Clark, J. G. (1981). Uses and abuses of hearing loss classification. *ASHA, 23*, 493-500.

Cunningham, J., Nicol, T., Zecker, S. G., et al. (2001). Neurobiologic responses to speech in noise in children with learning problems: deficits and strategies for improvement. *Clin Neurophysiol, 112*, 758-767.

Delgutte, B. (1980). Representation of speech-like sounds in the discharge patterns of auditory-nerve fibers. *J Acoust Soc Am, 68*, 843-857.

Delgutte, B. (1997). Auditory neural processing of speech. In W. Hardcastle, J. Laver (Eds.), *The handbook of phonetic science* (pp. 507-538). Oxford: Blackwell.

Don, M., Kwong, B., Tanaka, C. (2005). A diagnostic test for Ménière's Disease and Cochlear Hydrops: impaired high-pass noise masking of auditory brainstem responses. *Otol Neurotol, 26*, 711-722.

Eggermont, J. J. (2017). Ups and downs in 75 years of electrocochleography. *Front Syst Neurosci, 11*, 2.

Eggermont, J. J., Don, M., Brackmann, D. E. (1980). Electrocochleography and auditory brainstem electric responses in patients with pontine angle tumors. *Ann Otol Rhinol Laryngol Suppl, 89*, 1-19.

Fletcher, H. (1929). *Speech and hearing*. New York: Van Nostrand.

Hall, J. W., 3rd, Rupp, K. A. (1997). Auditory brainstem response: recent developments in recording and analysis. *Adv Otorhinolaryngol, 53*, 21-45.

Humes, L. E. (1983) . Spectral and temporal resolution by the hearing impaired. In: Studebaker GA, Bess FH, eds. *Monographs in Contemporary Audiology: The Vanderbilt Hearing Aid Report* . Upper Darby: 16-31.

Jewett, D. L., Romano, M. N., Williston, J. S. (1970). Human auditory evoked potentials: possible brain stem components detected on the scalp. *Science, 167*, 1517-1518.

Johnson, K. L., Nicol, T., Zecker, S. G., et al. (2008). Brainstem encoding of voiced consonant--vowel stop syllables. *Clin Neurophysiol, 119*, 2623-2635.

Kiang, N. Y. (1980). Processing of speech by the auditory nervous system. *J Acoust Soc Am, 68*, 830-835.

Kiang, N. Y., Eddington, D. K., Delgutte, B. (1979). Fundamental considerations in designing auditory implants. *Acta Otolaryngol, 87*, 204-218.

Klein, W., Plomp, R., Pols, L. C. (1970). Vowel spectra, vowel spaces, and vowel identification. *J Acoust Soc Am, 48*, 999-1009.

Kraus, N., Thompson, E. C., Krizman, J., et al. (2016). Auditory biological marker of concussion in children. *Sci Rep, 6*, 39009.

Kraus, N., White-Schwoch, T. (2015). Unraveling the biology of auditory learning: A cognitive-sensorimotor-reward framework. *Trends Cogn Sci, 19*, 642-654.

Kujawa, S. G., Liberman, M. C. (2009). Adding insult to injury: cochlear nerve degeneration after “temporary” noise-induced hearing loss. *J Neurosci* 29:14077–14085

Merchant, S. N., Adams, J. C., Nadol Jr., J. B. (2005). Pathophysiology of Ménière's syn- drome: are symptoms caused by endolymphatic hydrops. *Otol. Neurotol,* 26, 74–81.

Nuttall, H. E., Moore, D. R., Barry, J. G., et al. (2015). The influence of cochlear spectral processing on the timing and amplitude of the speech-evoked auditory brain stem response. *J Neurophysiol, 113*, 3683-3691.

Peterson, G. E., Barney, H. L. (1952). Control methods used in a study of the vowels. *Journal of the Acoustical Society of America, 24*, 175-184.

Picton, T. W., Woods, D. L., Baribeau-Braun, J., et al. (1976). Evoked potential audiometry. *J Otolaryngol, 6*, 90-119.

Riggs, W. J., Hiss, M. M., Skidmore, J., et al. (2020). Utilizing electrocochleography as a microphone for fully implantable cochlear implants. *Sci Rep, 10*, 3714.

Russo, N., Nicol, T., Musacchia, G., et al. (2004). Brainstem responses to speech syllables. *Clin Neurophysiol, 115*, 2021-2030.

Schaette R., McAlpine D. (2011). Tinnitus with a normal audiogram: physiological evidence for hidden hearing loss and computational model. *J Neurosci, 31*, (38):13452-7.

Skoe, E., Kraus, N. (2010). Auditory brain stem response to complex sounds: a tutorial. *Ear Hear, 31*, 302-324.

Skoe, E., Krizman, J., Anderson, S., et al. (2015). Stability and plasticity of auditory brainstem function across the lifespan. *Cereb Cortex, 25*, 1415-1426.

Song, J. H., Skoe, E., Banai, K., & Kraus, N. (2011). Perception of speech in noise: neural correlates. *J Cogn Neurosci*, *23,* (9), 2268–2279.

Stapells, D. R., Oates, P. (1997). Estimation of the pure-tone audiogram by the auditory brainstem response: a review. *Audiol Neurootol, 2*, 257-280.

Starr, A., Picton, T. W., Sininger, Y., et al. (1996). Auditory neuropathy. *Brain, 119 (Pt 3)*, 741-753.

Wang, Z., Bovik, A. C. (2002). A universal image quality index. *Ieee Signal Processing Letters, 9*, 81-84.

Wang, Z., Bovik, A. C., Sheikh, H. R., et al. (2004). Image quality assessment: From error visibility to structural similarity. *Ieee Transactions on Image Processing, 13*, 600-612.

Wu, P. Z., Liberman, L. D., Bennett, K., et al. (2019). Primary neural degeneration in the human cochlea: evidence for hidden hearing loss in the aging ear. *Neuroscience, 407*, 8-20

CHAPTER 4: MANUSCRIPT 2

Assessing Adaptation and Recovery of the Auditory Nerve in Ménière's Disease Using Electrocochleography

William J. Riggs, Meghan M. Hiss,
Edward. E. Dodson, Aaron C. Moberly,
Oliver F. Adunka
Department of Otolaryngology-Head
and Neck Surgery
The Ohio State University Columbus,
43210

ABSTRACT

Objective: Ménière's disease (MD) is a debilitating disorder of the inner ear that is known to cause extensive damage to the cochlea and vestibular system. Little is currently known about its effects on the auditory nerve. This study aimed to investigate temporal response properties, including neural adaptation and adaptation recovery, of the auditory nerve to acoustic stimulation in humans with MD.

Design: Study participants included individuals with sensorineural hearing loss (SNHL) undergoing various otologic surgical procedures who had a diagnosis of MD, vestibular schwannoma (VS), or SNHL of unknown origin. Electrocochleography (ECochG) was carried out intraoperatively from the round window. Stimuli included a train of 100 μs clicks used to induce adaptation and three click-train maskers followed by a single click (probe) spaced 5, 10, or 15 ms after the masker train ceased to assess adaptation recovery. Amplitude of the compound action potential (CAP) and summation potential (SP) evoked by each click train were measured. For adaptation, the CAP amplitude and SP-CAP ratio were calculated by comparing the amplitude of the CAP and SP-CAP ratio elicited by the last click of the train to the amplitude of the CAP and SP-CAP ratio to the control click (single click without prior stimulation). For recovery, the CAP amplitude and SP-CAP ratio to the probe click were compared to the CAP amplitude and SP-CAP ratio of the response evoked by the first click of the masker

train. Percent change in CAP amplitude and SP-CAP ratio were calculated. A one-way analysis of the variance (ANOVA) test and linear mixed models were conducted to assess group differences in the amount of adaptation and the rate of adaptation recovery exhibited by the auditory nerve.

Results: The VS group exhibited significantly greater change in the SP-CAP ratio than participants with MD, suggesting a greater amount of neural adaptation was induced. No differences were found between the MD and the SNHL group. The VS group showed a slower trend in the rate of recovery from adaptation than the MD and the SNHL group. However, no significant group difference was detected, and typically, full recovery was achieved by 10 ms.

Conclusions: Click train stimulation is a feasible approach to studying temporal response properties of the auditory nerve. Preliminary results suggest that MD does not impair auditory nerve function differently from what is observed in idiopathic SNHL. Furthermore, the current data suggest that the presence of a VS results in greater amounts of adaptation and a slower rate of recovery of the auditory nerve than what is observed in MD or idiopathic SNHL.

Key Words: electrocochleography, summating potential, neural adaptation, Ménière's disease; neural dysfunction; click train stimulation

INTRODUCTION

Ménière's disease (MD) is a debilitating disorder of the inner ear known to cause vertigo and hearing loss, and is typically accompanied by symptoms of tinnitus and aural fullness ("Committee on Hearing and Equilibrium guidelines for the diagnosis and evaluation of therapy in Ménière's disease. American Academy of Otolaryngology-Head and Neck Foundation, Inc," 1995; Paparella, 1984b). The pathophysiology of MD is not well understood. Temporal bone studies of patients who had MD confirmed that the disease results in extensive damage to both the vestibular and cochlear systems. This damage often results in reduction in the number of cochlear hair cells (outer and inner) and vestibular hair cells (type II cells), atrophy and degeneration of the stria vascularis, and hydrops of the endolymphatic space (Paparella, 1984b; Schuknecht, 1974; Tsuji et al., 2000).

Most authors describe cochlear and vestibular system degeneration with MD, however, few reports have evaluated the integrity of the neural tissues connecting to these two systems in patients with MD. A study by Tsuji et al. (2000) found a reduced number of Scarpa's ganglion cells in ears with a history of MD, compared to those without. The authors suggested this was due to a possible neuronal toxic effect subsequent to the pathophysiologic mechanism underlying MD or potentially retrograde degeneration caused by the loss of type II vestibular hair cells. Few reports exist describing the integrity of spiral ganglion neurons (SGCs) in patients with a history of the disease. Kariya et al. (2007) evaluated the contralateral ear in patients with unilateral MD and age-matched controls and

found a reduced number of SGCs in ears with MD and in the contralateral (unaffected) ear. This suggested likely injury to the SGCs secondary to MD; however, it is unclear why the unaffected ear also exhibited a reduction in the number of SGCs. Given the limited studies and findings on the impact the disease process has on the auditory nerve, it remains unclear as to whether the integrity of the auditory nerve in ears with MD is compromised. Understanding the functional integrity of the remaining SGCs would be of clinical relevance, as this may help expand our understanding of possible physiological abnormalities, potentially helping shed light on differentiating symptoms of clinical presentations and their site(s) of lesion and help explain variability in potential treatment outcomes such speech perception in those who go on to receive a cochlear implant.

Two temporal response properties that describe the function of the auditory nerve are: 1) adaptation, and 2) recovery from adaptation. Adaptation refers to the decrement in response amplitude of the auditory nerve that occurs during a constant stimulus condition, where amplitude gradually decays to a steady-state level (Harris et al., 1979; Kiang et al., 1965; Smith, 1977; Westerman et al., 1984; Young et al., 1973). When using acoustic stimulation, the underlying mechanisms of adaptation are thought to be localized to the inner hair cell/auditory nerve synapse and are believed to represent a decay in the firing rate of auditory nerve fibers (Eggermont et al., 1973b). In contrast, recovery from adaptation refers to the time it takes for the amplitude of the auditory nerve response to return to an un-adapted state following a period of masking (Smith, 1977; Young & Sachs, 1973).

In this scenario, the recovery time (i.e., rate) is thought to be primarily dependent on the recovery time constant of the post-synaptic membrane (i.e., synaptic mechanisms) (Eggermont & Spoor, 1973b).

Much of our understanding of the processes of adaptation and recovery have stemmed from single nerve fiber recordings in normal and hearing-impaired animals (e.g., Eggermont & Spoor, 1973b; Harris & Dallos, 1979; Kiang et al., 1965; Smith, 1977; Young & Sachs, 1973). These studies have provided insightful findings, such as identifying the desynchronizing factors responsible for adaptation, however, single fiber recording in humans is not feasible. Thus, authors have utilized the compound action potential (CAP) of the electrocochleography (ECochG) response, which represents the electrophysiological activity of many simultaneously excited nerve fibers (Eggermont, 1975), to study these processes in animals (Abbas et al., 1981; Gorga et al., 1981). These studies have found the response patterns of the CAP to be similar to those observed in single fiber recordings, suggesting the CAP's use as a potential tool to study adaptation and recovery properties of the auditory nerve in humans.

The main approach to study adaptation of the CAP in humans has employed transient stimuli, such as a train of 100 μs clicks (Santarelli et al., 2015; Santarelli et al., 2008). In this scenario, a single control click is presented followed by a "train" or series of clicks. The amplitude of the CAP response at the conclusion of the stimulus (i.e., the last click of the click train) is measured and compared to

the CAP amplitude evoked by the control click (i.e., a single click not part of a train of clicks) to quantify the amount of decrement (i.e., adaptation) in the CAP response. Furthermore, two main stimulation paradigms have previously been utilized to study recovery properties of the CAP. These stimulation paradigms have employed forward masking (i.e., tone bursts or white noise) techniques (Coats et al., 1972; Murnane et al., 1998; Relkin et al., 1995). In forward masking approaches, the CAP is measured in response to the probe that is preceded by a masker with various silent gap durations between the masker and probe (Coats & Dickey, 1972; Ohashi et al., 2013; Ohashi et al., 2012; Ohashi et al., 2014; Ohashi et al., 2005).

The motivation for the current study stems from the investigation by Ohashi and colleagues (2013). These authors found that, when using a paired click ECochG paradigm (i.e., a single click followed by a second click with the inter-click-interval varied) in patients with MD and those with idiopathic sensorineural hearing loss (SNHL), the CAP amplitude was often found to recover to the baseline amplitude at an increased rate (i.e., shorter time constant to fully recover) for the MD group when compared to those with idiopathic SNHL (Ohashi et al., 2013). These authors suggested that this finding likely reflected a pathological condition of the inner ear (e.g., increased calcium [Ca^{2+}]) that could have stemmed from the presence of endolymphatic hydrops, a condition often observed in patients with MD. The result was abnormally fast recovery from a forward masker that induced adaptation of the auditory nerve.

The possibility of potential alterations in auditory nerve function due the presence of endolymphatic hydrops suggests that the disease's effects may not be limited to an inner ear site-of-lesion (i.e., cochlea and vestibular systems) and could impact the auditory nerve. Understanding impacts on the auditory nerve would be of clinical relevance by potentially shedding light on other peripheral auditory sites of injury, likely important for understanding the wide range of clinical presentations commonly observed in patients with MD. Interestingly, a recent study showed in mice with artificially-induced endolymphatic hydrops that the increase in Ca^{2+} levels within the inner ear caused by endolymhpatic hydrops leads to destruction of peripheral auditory nerve synapses (i.e., cochlear synaptopathy) through excitotoxicity processes (Kim et al., 2018). Thus, contrary to the findings of Ohashi and colleagues (2013), it is theoretically plausible to assume that hypo-function of auditory nerve activity could also be present in MD due to the potential for cochlear synaptopathy from endolymphatic hydrops. Because of the existing discrepancies between hyper- and hypo-function of the auditory nerve with MD symptoms, our goal was to further investigate response properties of the auditory nerve in humans diagnosed with MD.

Given the limited previous literature that suggests potential hyper-function of the auditory nerve in MD (Ohashi et al., 2013), as well as the possibility of the presence of concurrent cochlear synaptopathy due to endolymphatic hydrops (Kim et al., 2018), further investigation into the functional integrity of the auditory nerve is warranted to better understand potential effects of MD on the auditory nerve. To

address this gap in knowledge, the current manuscript describes the results of two experiments aimed at evaluating temporal response properties of the auditory nerve in participants with MD. In our first experiment, we investigated adaptation of the auditory nerve and hypothesized that participants with MD would exhibit less adaptation as measured by the change amplitude of the ECochG CAP response than participants with idiopathic SNHL and a VS. In the second experiment, we investigated adaptation recovery of the auditory nerve and hypothesized that participants with MD would exhibit a faster rate of recovery from adaptation than participants with idiopathic SNHL and a VS.

In attempts to test whether MD alters function of the auditory nerve, we compared a group of participants with MD to a group with a diagnosis of idiopathic SNHL and an additional group of participants with a vestibular schwannoma (VS). VSs are tumors located within the cerebellar pontine angle and the internal auditory canal. With respect to the impact of a VS on the distal portion of the auditory nerve (that which generates the CAP), location of a VS within the internal auditory canal can vary from case to case, making this group of participants somewhat heterogeneous in potential CAP changes caused by the tumor. Koen et al. (2020), using magnetic resonance imaging, found that approximately 19% of VSs encompassed the fundus, an anatomical location immediately adjacent to where SGCs of the auditory nerve reside. This finding suggests that due to the close proximity of the VS relative to the SGCs, peripheral auditory nerve function could potentially be impacted in some instances of VS. Electrophysiological

evidence exists to support peripheral auditory nerve impairment in some cases of VS. For example, Morrison and colleagues (1976) found that the CAP of the ECochG response was abnormally widened in 71.1% of VS cases, reflecting a loss of the P1 component a likely disruption in auditory nerve function. This was later followed-up by Eggermont (1980) who used a combined auditory brainstem response (ABR) and ECochG approach to further study the impact of a VS on auditory nerve function. Eggermont (1980) found that the ABR often displayed a prolongation of the I-III and I-V wave interpeak interval due to slowing of auditory nerve transmission. This finding was found to be accompanied by a disruption (e.g., prolongation) in the CAP morphology of the ECochG response in a subset of patients with a VS, thought to be due to the anatomical location of the tumor relative to the SGCs. Overall, the prior works listed above (both imaging and electrophysiological) suggest that participants with a VS could potentially be used as a human model for auditory neural dysfunction. However, it should be noted that not all participants with a VS exhibit CAP deficits as measured electrophysiologically (Eggermont, 1980), thus this type of a group is likely heterogeneous in the functional integrity of the auditory nerve.

MATERIALS AND METHODS

Participants

Study participants included 13 adults diagnosed with MD (mean age: 53.2 years; standard deviation [SD]: 10.2), 13 adults diagnosed with a VS (mean age: 47.2; SD: 13.7), and 8 adults with idiopathic SNHL (mean age: 61.4; SD: 20.8). All participants were undergoing an inner ear surgical procedure. All participants in the MD group had medical record documentation of meeting classification #2 of The American Academy of Otolaryngology Head and Neck Surgery's (AAO-HNS) 1995 position guidelines for classifications for diagnosing MD: Definite MD as classified as having two or more definitive spontaneous episodes of vertigo lasting at least 20 minutes, documented hearing loss determined by audiometry on at least one occasion, tinnitus or aural fullness in the ear of concern.

Electrophysiological procedures and data collection were carried out from all participants at the time they were undergoing surgical management for their disease [Table 4.1]. This study was approved by the local Biomedical Institutional Review Board (The Ohio State University). All participants provided written consent prior to being enrolled in the study.

ID	Group	Age (yr)	Sex	Surgical Procedure	PTA -1	PTA -2	Adaptation	Recovery
A01	1	57	M	Lab	65	105	X	X
A02	1	58	F	ELS	26	30	X	X
A03	1	48	M	ELS	20	35	X	X
A04	1	57	M	Lab	58	64	X	X
A05	1	50	F	ELS	48	46	X	X
A06	1	42	M	ELS	60	45	X	X
A07	1	61	M	ELS	45	55	X	-
A08	1	30	F	ELS	50	17	X	-
A09	1	66	F	Lab	58	58	X	X
A10	1	47	F	ELS	20	34	X	X
A11	1	65	M	Lab	45	63	X	X
A12	1	51	M	ELS	42	46	X	-
A13	1	62	F	Lab	43	58	X	-
A14	2	35	F	VS	47	56	X	X
A15	2	51	M	VS	120	115	X	-
A16	2	48	F	VS	61	64	X	X
A17	2	67	F	VS	61	80	X	-
A18	2	53	F	VS	38	44	X	-
A19	2	51	F	VS	45	19	X	X
A20	2	39	F	VS	32	44	X	-
A21	2	53	F	VS	18	23	X	-
A22	2	58	F	VS	15	33	X	X
A23	2	34	M	VS	13	18	X	X
A24	2	68	M	VS	47	74	X	X
A25	2	36	M	VS	70	65	X	X
A26	2	21	F	VS	13	14	X	-
A27	3	74	M	CI	53	83	X	-
A28	3	77	F	PCO	40	58	X	X
A29	3	60	M	CI	113	85	X	X
A30	3	28	F	CI	58	70	X	X
A31	3	75	M	PCO	43	78	X	X
A32	3	88	F	CI	67	80	X	X
A33	3	49	F	SCO	7	19	X	X
A34	3	40	M	SCO	18	31	X	X

Table 4.1: Demographic information of study participants. ID: participant identification, Group 1: Ménière's disease, Group 2: vestibular schwannoma, Group 3: sensorineural hearing loss- unknown, Male: M, female: F, endolymphatic sac decompression: ELS, vestibular schwannoma removal: VS, Labyrinthectomy:

lab, posterior canal occlusion: PCO, superior canal occlusion: SCO, Did not test: -, Did test: X, pure tone average method 1: PTA-1 (0.5, 1.0, 2.0 kHz), pure tone average method 2: PTA-2 (2.0, 4.0, 6.0, 8.0 kHz), years: yr.

Procedures

Surgical and Recording Set-Up

ECochG recordings were obtained for all patients intraoperatively at the time of surgical intervention. Intraoperatively, a cortical mastoidectomy was performed followed by a transmastoid facial recess approach for all procedures. A monopolar probe (Kartush raspatory probe, Plainsboro, NJ, or Neurosign 3602-00-TE, Magstim Co., Wales, UK) was positioned at the round window niche. Note, the round window was always closed for the ECochG recordings. The evoked signal was recorded differentially with a common surface electrode (Neuroline 720, Ambu Inc, Ballerup, Denmark) placed on the forehead and a reference electrode placed at the contralateral pre-auricular point. Stimulation and recording of evoked responses were controlled using a Bio-logic Navigator Pro (Natus Medical Inc., San Carlos, CA) evoked potential apparatus. Stimuli were delivered through an insert transducer (ER3b) connected through a sound tube to a foam insert earphone placed in the external auditory canal.

The stimulation approach used alternating (rarefaction and condensation starting phase) acoustic stimuli presented for 250 repetitions per phase. Stimuli for measuring adaptation can be seen in Figure 4.1 and consisted of an initial 100 μs

click followed by a gap of 10 ms and a train of 10 clicks (100 μs in duration) each separated by a 3-ms inter-click-interval for a total stimulus duration of 48 ms, identical to that described by Santarelli and colleagues (Santarelli et al., 2008). Previous studies of the CAP in animals (Eggermont et al., 1973a; Stephens et al., 1974) and humans (Eggermont et al., 1974; Stephens et al., 1974; Yoshie et al., 1971) have demonstrated that a plateau of adaptation is typically reached after a minimum of five clicks of a click train. Thus, this stimulus was chosen, as it was expected to induce sufficient adaptation of the CAP response across groups.

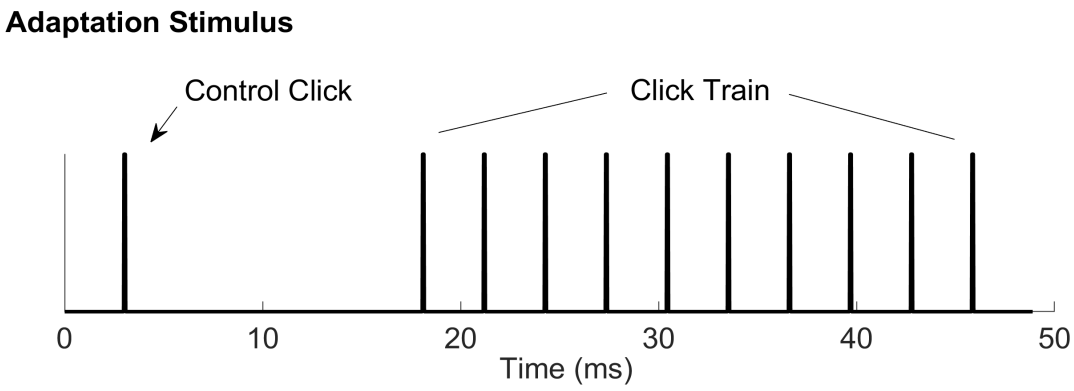

Figure 4.1. Click train stimulus used for the adaptation paradigm.

Three stimuli were used in the recovery testing paradigm. They consisted of a train of seven clicks (“masker”), each 100 μs in duration, with an inter-click-interval of 3 ms for each click followed by an 8th click (“probe”) which was spaced 5, 10, or 15 ms after the final click of the initial click-train masker (Figure 4.2). All clicks used in both the adaptation and the adaptation recovery stimuli were equal in intensity (110 dB SPL). Stimulation levels were calibrated in units of dB peak equivalent sound pressure level (peSPL) using a 2 cc coupler and 1 inch condenser microphone routed to a sound level meter (System 824, Larson Davis, Depew, NY) set to fast mode.

Adaptation Recovery Stimuli

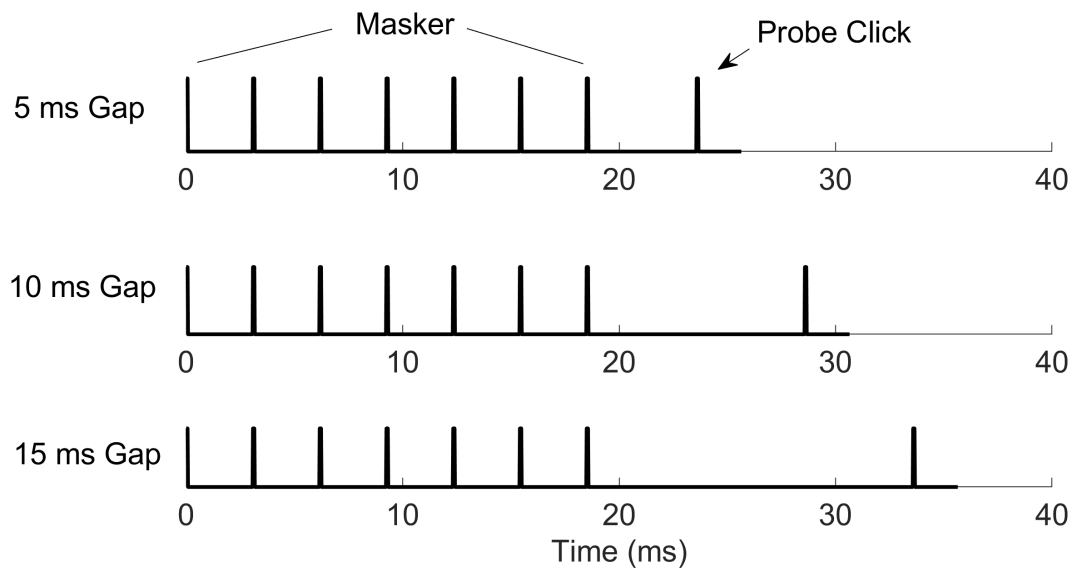

Figure 4.2. A depiction of the three click train stimuli used in the adaptation recovery testing paradigm.

Hearing Sensitivity

All participants underwent a diagnostic audiometric evaluation by a licensed audiologist within six months prior to their surgery, and air conduction pure tone thresholds were obtained via chart review. Hearing sensitivity was calculated using two different pure tone average (PTA) methods: 1) average audiogram threshold at 0.5, 1.0, 2 kHz, and 2) average audiogram threshold at 2.0, 4.0, 6.0, 8.0 kHz. Method 1 was chosen because it is a common audiological metric, and the authors felt it could potentially help capture any differences in hearing loss configuration among the groups that may have been related to the type of etiology, such as the reverse slope audiogram configuration commonly observed in patients with MD (Katsarkas, 1996). Method 2 was chosen to help identify any potential influence of high-frequency sensitivity on adaptation and recovery processes of the auditory nerve, as the frequency response of broadband click stimuli has been shown to maximally excite the 2.0 kHz and 4.0 kHz regions of the basilar membrane and be closely related to audiometric thresholds at these two frequencies in participants with cochlear hearing loss (Gorga et al., 1985).

Data Analysis

Electrophysiological Analysis

Using the average response (average of the ECochG response to condensation and rarefaction phases), the raw CAP amplitude was measured from baseline to peak amplitude (N_1), and the SP amplitude was measured from

baseline to the hump on the leading edge of the CAP (Coats, 1986). Adaptation was calculated as the percent change in CAP amplitude (i.e., CAP attenuation) of the response evoked by the final click of the click train when referenced to the amplitude of the response evoked by the first click of the adaptation stimulus. Additionally, as the SP is a pre-synaptic potential, it is thought to be resistant to adaptation, thus, we also calculated the change in SP-CAP ratio to help exemplify the occurrence of adaptation (Eggermont, 1976).

To measure adaptation recovery, the CAP amplitude evoked by the probe click was referenced to the amplitude of the response evoked by the initial click of the masker. Therefore, recovery was calculated as the percent change in CAP amplitude (i.e., CAP attenuation) between the response evoked by these two clicks of the stimulus for each of the three stimuli (5, 10, 15 ms). Additionally, the SP-CAP ratio change was calculated in similar fashion as the CAP recovery. Note, due to time constraints during surgery, fewer participants (9 MD, 8 VS, and 7 SNHL) had a full ECochG dataset available for assessing adaptation recovery.

Statistical Analysis

Data were graphed and analyzed using MATLAB (MathWorks) and SPSS 27 (IBM Corp., Armonk, New York). Box-and-whisker plots were used to show the distribution of PTA values for each study group. The Kolmogorov-Smirnov test was used to assess PTA and ECochG data for normality. Separate analysis of the variance (ANOVA) procedures were then performed to evaluate differences in preoperative hearing (e.g., PTA) and ECochG adaptation results among groups.

Participant group (MD, VS, SNHL) served as the independent variable, and PTA or percent change of adaptation served as the dependent variable. To analyze the results of the adaptation recovery experiment, linear mixed models (LMMs) with participant group and gap duration as fixed effects and participant as the random effect were used in conjunction with post-hoc Tukey-Kramer pairwise comparisons, when necessary, to measure differences among the groups. Participant group served as the between-subjects factor and stimulus condition (5, 10, 15 ms gap) as the within subjects factor. Pearson product-moment correlation tests were used to assess relationships between PTA and amount of adaptation induced and amount of recovery for each gap duration. All tests were two-tailed, and statistical significance was determined at the 95% confidence level (i.e., $p<0.05$).

RESULTS

Preoperative Hearing

Individual PTA values using both calculation methods for each participant can be found in Table 4.1. The distribution of PTA values by group can be observed in Figure 4.3, where the black bar in each box-and-whisker plot represents the median PTA value. Results of separate one-way ANOVA testing procedures evaluating each PTA method by group indicated no significant differences in preoperative hearing among the groups (Method 1: $F_{(2,32)}= 0.13$, $p=0.88$; Method 2: $F_{(2,31)}= 0.76$, $p= 0.48$), suggesting the groups were sufficient for comparison with respect to their audiometric profiles.

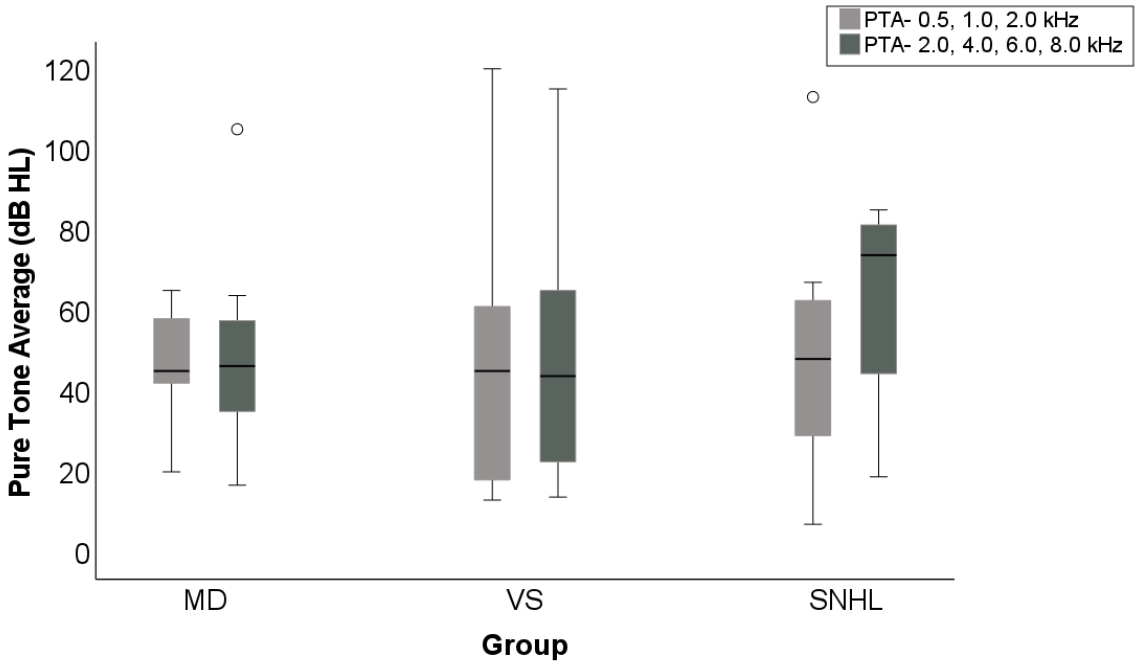

Figure 4.3 Box-and-whisker plots for hearing sensitivity measured via two different pure tone averages (PTA) for each group of participants. Black bars within boxes represent the 50th percentile, boxes represent the 25th and 75th percentile and circles represent outlier (i.e., greater than 1.5 times the interquartile range) PTA values.

Adaptation

Figure 4.4 shows example ECochG responses evoked by the adaptation stimulus from one participant from each group. Average CAP amplitudes for the responses evoked by the initial click (#1) and final click (#11) of the stimulus were 15.1 μV (SD: 11.7) and 10.4 μV (SD: 9.4), 5.1 μV (SD: 4.0) and 3.1 μV (SD: 2.6), and 5.3 μV (SD: 3.6) and 3.6 μV (SD: 3.2) for the MD, VS, and SNHL groups, respectively. The largest CAP amplitudes evoked by the control click were seen in the MD group, while the smallest amplitudes were found in the SNHL group. All groups exhibited a decrease in CAP amplitude with each subsequent click of the click train. As expected, the SP was observed to be most pronounced in the MD group and often exhibited a trend where the SP became larger than the CAP amplitude with each subsequent click of the click train.

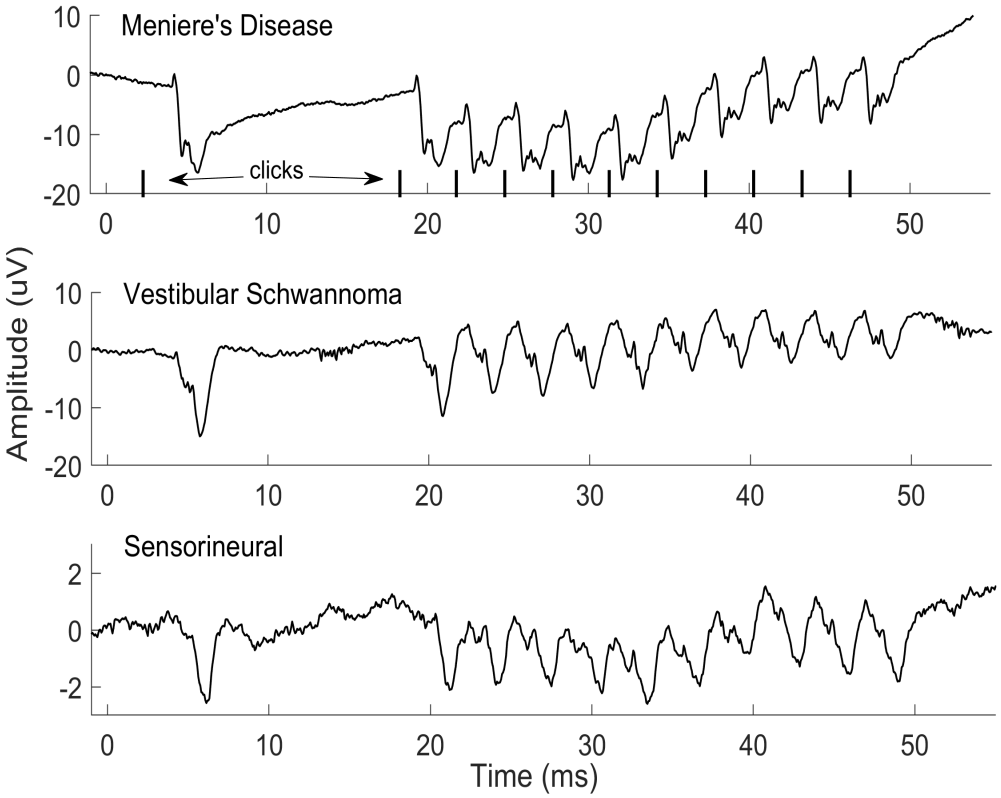

Figure 4.4: Example electrocochleography responses evoked by the adaptation stimulus from a participant of each group (Ménière's disease: A10; vestibular schwannoma: A19; sensorineural: A31). Black lines in the top panel indicate the click position within the stimulus.

The average CAP attenuation by click position for each group is plotted in Figure 4.5 (top panel). It can be observed that the VS group exhibited the largest amount of adaptation, and the MD group exhibited the least. The average attenuation in CAP amplitude at the 11th click was -31.1% (SD: 23.1), -43.5% (SD: 18.2), and -35.6% (SD: 26.3) for the MD, VS, and SNHL groups, respectively. Results of a one-way ANOVA with group as the categorical variable indicated there was not a significant difference in amount of CAP attenuation among the groups ($F_{(2,31)}$ = 1.05, p = 0.36). The change in the SP-CAP ratio was calculated and plotted in the bottom panel of Figure 4.5. Here, it can be seen that, similar to the changes observed in the CAP, the VS group exhibited the greatest increase in the SP-CAP ratio with a mean increase of 70.4% (SD: 43.9), followed by the SNHL group (34.4%, SD: 31.0), and finally the MD group (23.1% change, SD 44.6). When considering change in the SP-CAP ratio, results of a one-way ANOVA were found to be statistically significant ($F_{(2,31)}$= 4.63, p = 0.02). Post-hoc analysis showed that the change for the MD group was statistically smaller than the change observed in the VS group (mean difference: 47.3%, p = 0.02). There was no notable difference found between the MD and the SNHL group (mean difference: 7.71%, p = 1.00) or the VS and the SNHL group (mean difference: 39.6%, p = 0.13).

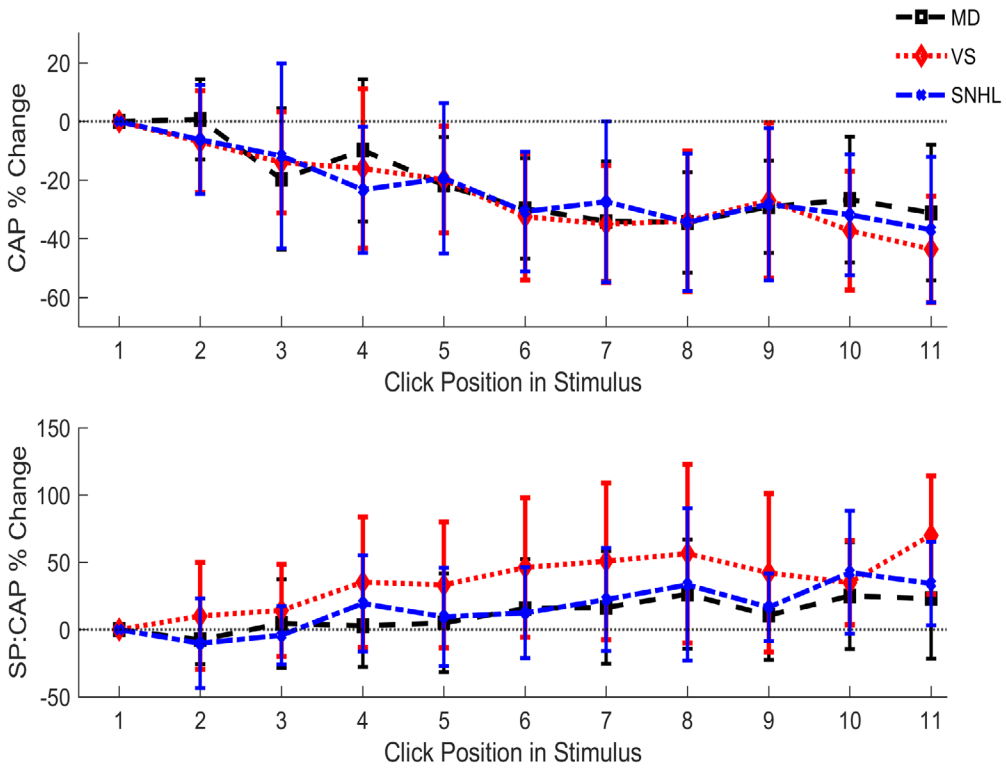

Figure 4.5. The average change in the compound action potential amplitude (CAP) by click position for each group (top panel). The average change in the summation potential (SP) to CAP ratio by click position for each group (bottom panel). Error bars represent 1 standard deviation of the mean.

Adaptation and Hearing Sensitivity Correlations

The percent change in CAP amplitude and the SP-CAP ratio was correlated with each participant's hearing sensitivity (i.e., PTA) to evaluate for any potential influence of residual hearing on the amount of adaptation observed in the ECochG response. Figure 4.6 (panel A) shows a non-significant, but negative, trend in the percent change in CAP amplitude for both methods of calculating PTA (Method 1: $r = -0.20$, $p = 0.09$; Method 2: $r = -0.29$, $p = -0.09$). This suggests that the amount of adaptation was slightly greater for participants with poorer hearing. In contrast, Figure 4.6 (panel B) shows no consistent trend in change in the SP-CAP ratio for either PTA method (Method 1: $r = 0.004$, $p = 0.98$; Method 2: $r = 0.12$, $p = 0.51$).

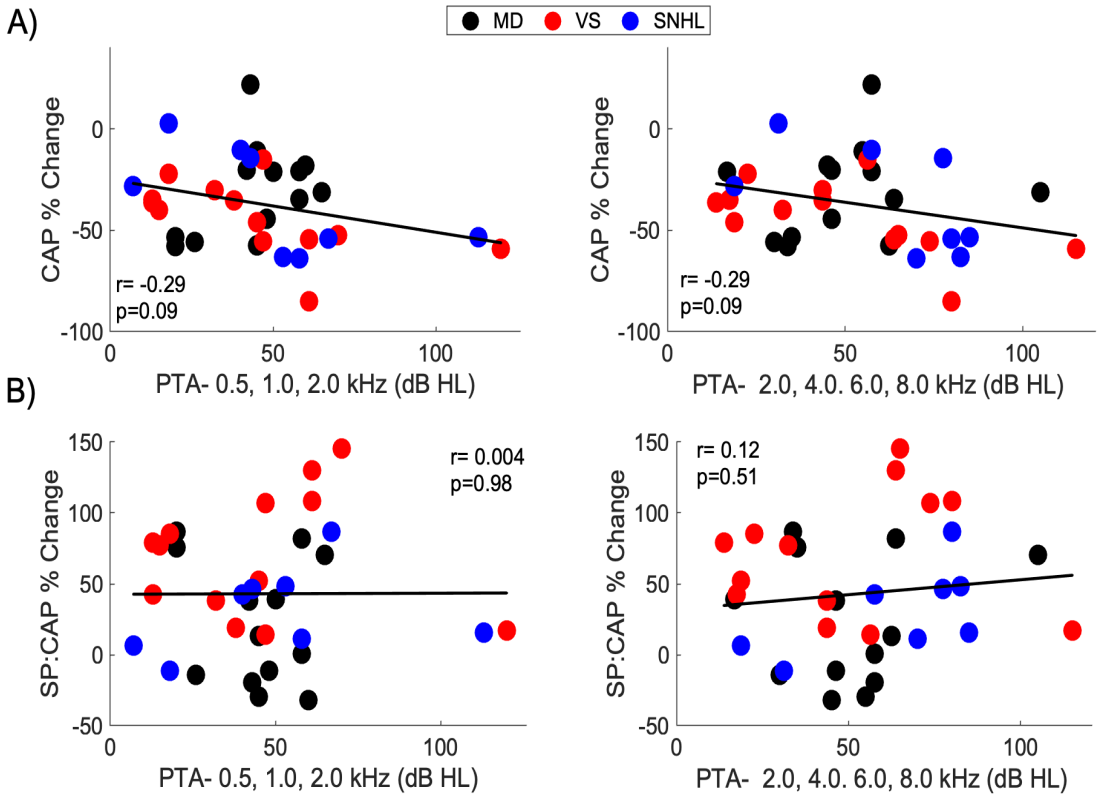

Figure 4.6. A) Pearson product-moment correlations between change in CAP (adaptation stimulus) and each method of calculating PTA (Method 1: 0.5, 1.0, 2.0 kHz; Method 2: 2.0, 4.0, 6.0, 8.0 kHz). B) Pearson product-moment correlations between the change in the SP-CAP ratio (adaptation stimulus) for both PTA methods.

Recovery from Adaptation

Figure 4.7 shows example ECochG results obtained from one participant of each group, where the responses evoked by each of the three forward masking adaptation recovery stimuli are displayed by columns. Figure 4.8 (left column) displays the average CAP attenuation plotted as a function of click position within the stimulus. The 8th click, indicated by the gray background, represents the probe response for each stimulus. Here, it can be observed that all groups typically exhibited the largest decrement in CAP amplitude to the final click of the masker train (7th click). As expected, the amount of recovery, as measured by percent of CAP change from baseline amplitude, was the smallest for the 5 ms gap stimulus and appeared to nearly reach complete recovery by 10 ms. These observations were supported by the results of the LMM, which revealed a significant effect of gap duration ($F_{(2, 43.8)} = 10.4$, $p < 0.01$), but did not reveal an effect of group ($F_{(2, 21.2)} = 0.30$, $p = 0.76$) or their interaction ($F_{(4, 44.1)} = 0.84$, $p = 0.51$). Using pairwise comparisons to evaluate the overall recovery by gap, it was found that the amount of recovery at the 5 ms gap was significantly lower than the values at the 10 ms (mean difference: -15.9, $p < 0.01$) and 15 ms gaps (mean difference: -15.1, $p < 0.01$). There was no difference in the mean recovery between the 10 and the 15 ms gap (mean difference: 0.8, $p = 0.88$), suggesting that all groups had essentially reached recovery equilibrium by 10 ms.

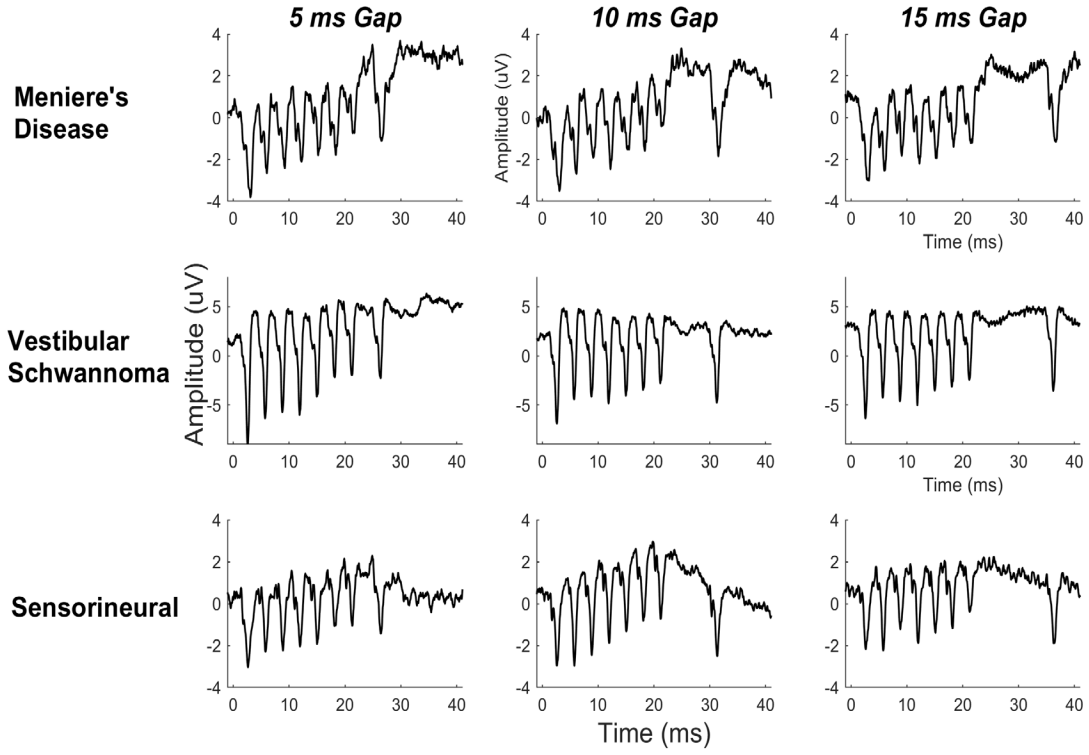

Figure 4.7. Example electrocochleography responses evoked by the adaptation recovery stimuli from a participant of each group (Ménière's disease: A11; vestibular schwannoma: A21; sensorineural: A28). Black lines in the top panel indicate the click position within the stimulus.

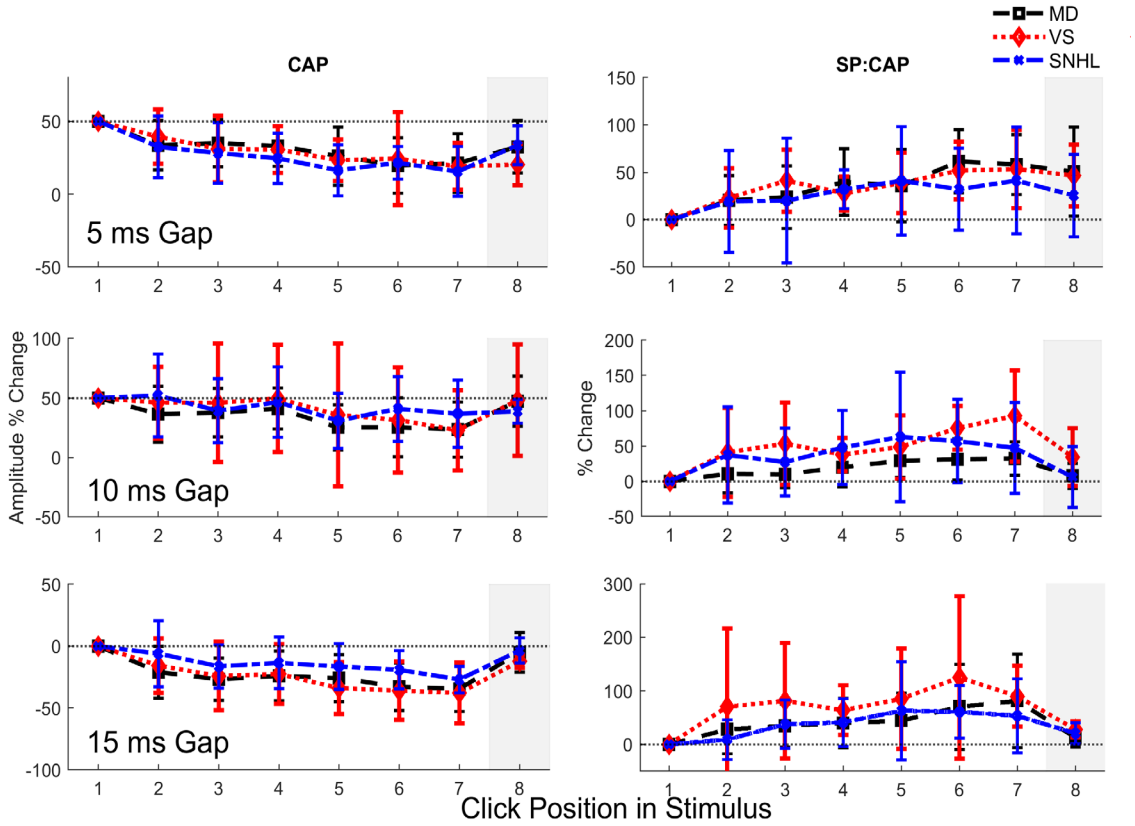

Figure 4.8. The left column of panels display the average change in the compound action potential amplitude (CAP) by click position for each group at three different inter-stimulus-intervals (ISI). The 8th click, indicated by the gray background, represents the probe response for each stimulus. The right column of panels displays the average change in the summation potential (SP) to CAP ratio by click position for each group at three different ISI. Error bars represent 1 standard deviation of the mean.

The change in the SP-CAP ratio can be seen in Figure 4.8 (right panel). Similar to the trend seen in the CAP results, the largest change (i.e., increase) in the SP-CAP ratio was typically observed in response to the final click of the masker for each group. However, on average, the change in the SP-CAP ratio was often found to be much larger for the VS group than the other two groups across each click of the masker. The SP-CAP ratio for the probe response was found to exhibit the largest change from baseline at the 5 ms gap for each group and continued to return to baseline values with increasing gap duration. Interestingly, the change in average the SP-CAP ratio for the VS group was considerably larger at the 10 ms gap compared to that of the MD group, despite both groups exhibiting a similar amount of change at the 5 ms gap. This potentially suggests that the VS group experienced a slower rate of recovery than the MD group. The results of the LMM confirmed a significant effect of gap duration ($F_{(2, 34.5)} = 3.9$, $p = 0.03$) but not group ($F_{(2, 27.8)} = 1.8$, $p = 0.19$) or their interaction ($F_{(4, 34.5)} = 1.03$, $p = 0.40$).

Recovery from Adaptation and Hearing Sensitivity Correlations

The amount of recovery in CAP amplitude for each adaptation recovery stimulus (i.e., 5, 10, 15 ms gaps) was correlated with each participant's PTA using the two methods. No significant correlations between amount of recovery in CAP amplitude and PTA was observed for any stimulus (Figure 4.9 - columns 1 and 2). Note, correlation coefficients and p-values can be found in each panel of Figure 4.9. However, no consistent trends were observed for the change in CAP for any

of the stimuli. Additionally, no significant correlations or consistent trends were found for the SP-CAP ratio change for any stimulus (Figure 4.9 - columns 3 and 4).

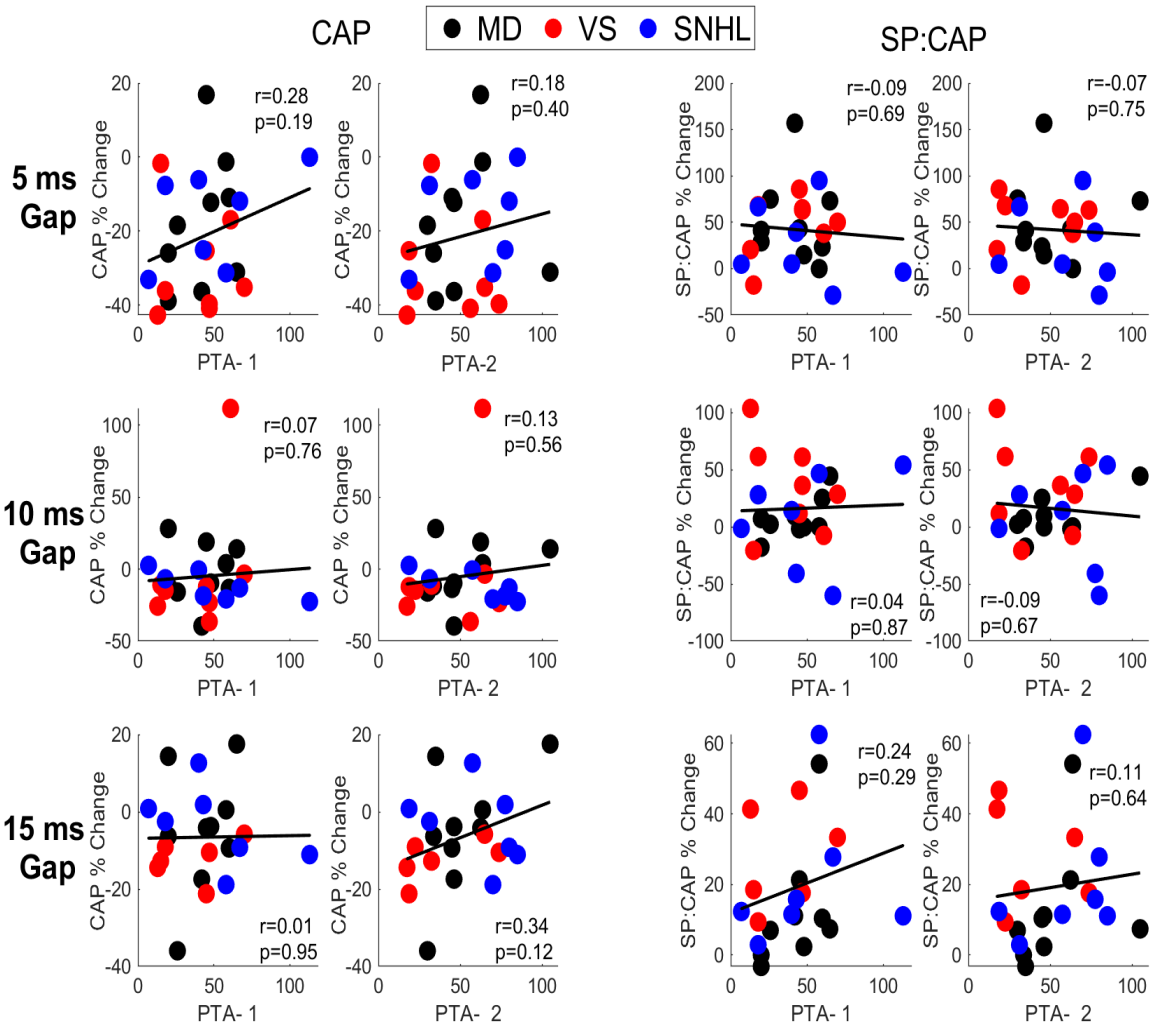

Figure 4.9. Columns 1 and 2) Pearson product-moment correlations between change in CAP amplitude and two methods of calculating PTA (Method 1: 0.5, 1.0, 2.0 kHz; Method 2: 2.0, 4.0, 6.0, 8.0 kHz) for each stimulus (5 ms gap, 10 ms gap, 15 ms gap). Columns 3 and 4) Pearson product-moment correlations between change in the SP-CAP ratio and PTA for each stimulus.

DISCUSSION

The current study utilized round window ECochG to investigate the effects of MD on functional properties of the auditory nerve. In our first experiment, we hypothesized that participants with MD would exhibit less adaptation in the ECochG CAP than participants with idiopathic SNHL or VS. In the second experiment, we hypothesized that participants with MD would exhibit a faster rate of recovery from adaptation than participants with SNHL without the disease. To test these hypotheses, we compared the results from participants with MD to participants with other forms of SNHL. Overall, the results suggest that MD does not result in disruption in physiological properties of the auditory nerve (i.e., adaptation and recovery from adaptation) in ways that are different from what is typically observed in SNHL of unknown origin.

ECochG Adaptation and Recovery Observations

In this study, CAPs of the auditory nerve were evoked by trains of acoustic clicks. The amplitude of the CAP over the duration of each stimulus train consistently declined in amplitude (Figures 4.4 and 4.7) for all three groups for both the adaptation and recovery experiments. In contrast, the SP often remained stable (i.e., similar amplitude) over the course of each stimulus train. Considered a pre-synaptic potential, as it is thought to be primarily generated by sensory hair cells (Dallos et al., 1972), the SP is little affected by adaptation effects (Eggermont & Odenthal, 1974). This appeared to be true for our results, as the SP did not change considerably throughout the click train stimuli. However, it should be noted

that the baseline measurement for each response following a click was occasionally distorted by the CAP response evoked by the prior click. That is, despite a 3-ms inter-click-interval for the CAP responses evoked by the train, there were occurrences when the previous CAP response appeared to influence/distort the location where the baseline measurement was labeled on the ensuing evoked response. This potential distortion could have ultimately impacted the SP and CAP amplitude measurements. In our results, there was a trend in poorer CAP function in the VS than the SNHL group when simply measuring CAP amplitude alone. However, when the CAP is normalized to the SP, the effects of adaptation were more easily observed. Thus, rather than measuring absolute CAP amplitude, normalizing it to the SP amplitude helped reduce the influence of potential artifact from the previous CAP response. This is consistent with previous research in which normalization of the CAP amplitude to the SP aids in controlling for variability in CAP fluctuations (Coats, 1981; Gibson et al., 1983).

The results of adaptation are similar to those found in guinea pigs. In response to short noise burst trains, the amplitude of the guinea pig CAP (i.e., N_1 component) typically reached an equilibrium value (adaptive state) following five stimuli (Eggermont & Spoor, 1973a). Here, it can be seen that most participants reached maximum CAP attenuation at approximately the 6-7th click. This suggests that the 7-click train masker used in the recovery should have been sufficient for inducing maximal adaptation, thus adequately allowing for measuring rate of recovery from an adaptive state.

A few distinct observations were noted by the authors for responses obtained in the adaptation recovery analysis, and these are discussed below. Across all study groups, some participants exhibited a larger amount than others of adaptation to the masker train (i.e., greater reduction in CAP amplitude compared to other participants within each respective group). These participants typically exhibited longer periods to fully recover (i.e., did not reach full recovery until 15 ms). This is somewhat intuitive and is consistent with previous work by Smith (1977), who showed in gerbils that the single unit response of the auditory nerve is not solely dictated by the masker level, but rather the fiber's response to the masker/adaptation stimulus. This suggests that, if the decay in response amplitude caused by the masker does not reach an asymptotic level, then the post-stimulus recovery will be less affected (i.e., quicker recovery). On a group level, the average change in the CAP amplitude often reached an adaptive state by the 6-7th click. Yet, some participants continued to show decrement with later clicks, and thus, it may be of clinical interest to further elucidate these effects. That is, it is possible that those who showed shallower slopes of recovery (worse than SNHL) could have had greater damage at the synapse/auditory nerve. Therefore, they may have experienced greater amounts of adaptation, and this could potentially be related to clinical symptoms. However, further work is needed to support this hypothesis.

Results of the forward masking recovery paradigm suggested that the majority of participants exhibited recovery within 10-15 ms following the click train

masker. These results differ from previous findings where it has been shown that recovery can take up to 1000 ms; however, these authors used long duration tone bursts (400 ms) as maskers (Eggermont & Odenthal, 1974). In contrast, authors who have used shorter masker durations (e.g., 100 ms) have found full recovery of the CAP to occur within approximately 50 ms (Abbas & Gorga, 1981). This suggests that the time of recovery is related to the length of the masker stimulus. Additionally, previous authors have shown that masker duration is directly related to the amount of adaptation exhibited, where shorter duration maskers cause less adaptation (Gorga & Abbas, 1981; Smith, 1977). We did not observe reductions in average group CAP amplitudes that extended beyond the 15-ms recovery window, which could be due to differences in stimuli. Specifically, our click train maskers were much shorter in duration compared to the above-mentioned studies, as our masker train durations were 28 ms for the adaptation stimulus and approximately 19 ms for adaptation recovery.

Observations in the SP-CAP ratio showed a consistent trend across all groups with each click of the click train stimuli. There was an increase in the SP-CAP ratio that regularly reached its largest value at the 6-7th click of the click train. As the average CAP amplitude was consistently found to be the smallest at the 6-7th click, this is an expected finding. It is consistent with the masker train inducing adaptation of the auditory nerve while the SP stayed relatively stable. As the SP predominantly originates from sensory hair cells, which have been shown to lack susceptibility to adaptation effects due to their pre-neural nature, the increase in

the SP-CAP ratio was not surprising. Yet, it reaffirms the assumption that our masker train induced adaptation of the auditory nerve.

Hearing Sensitivity Observations

For both the adaptation and recovery stimulation paradigms, the ECochG results were used in correlation analyses with multiple PTA methods to evaluate any potential associations of residual hearing on the ECochG results. Interestingly, there was a small, non-significant trend of participants with more extensive hearing loss exhibiting greater amounts of adaptation (Figure 4.6). While overall there was minimal association found between hearing sensitivity and ECochG responses, this trend potentially suggests that, in addition to a reduction in cochlear sensitivity that is experienced by listeners with hearing impairment, functional response properties of the auditory nerve (e.g., adaptation) also become degraded with increasing severity of hearing loss.

Experimental Approach Validation

The inclusion of participants with a known tumor disorder helped provide support for validating our experimental approach (i.e., click trains to assess adaptation and adaptation recovery). Tumors in the internal auditory canal (e.g., VS) have previously been shown to result in disruption in the function of the auditory nerve. This can lead to reduced transmission of auditory cues from the cochlea to the central auditory system, resulting in amplitude reduction and latency prolongation in auditory brainstem responses and ECochG CAP responses (Eggermont et al., 1980; Gibson et al., 1976; Riggs et al., 2020). Theoretically, a

VS group would then serve as a logical comparison group to include in measurements that are designed to test auditory nerve function. While a few prior studies have provided early support in using the same stimulus we employed in our adaptation paradigm (Santarelli et al., 2015; Santarelli et al., 2008), our adaptation recovery stimulus was entirely novel. Thus, inclusion of the VS group aided our ability to ensure our ECochG approach was practical. The VS group exhibited reductions in CAP amplitude for the adaptation stimulus that were significantly greater than both the MD and SNHL groups. Additionally, this group showed trends of slower CAP recovery following adaptation than both groups. As a result, these findings are consistent with previous findings of impaired auditory nerve function in participants with VS and provide preliminary support for our experimental approach.

Ménière's Disease and Endolymphatic Hydrops: The Auditory Nerve

A main feature of MD is the accumulation of endolymph within the endolymphatic space, termed endolymphatic hydrops (Gulya et al., 1982). Histologic studies of human temporal bones have noted this morphological entity as a consistent finding in ears diagnosed with MD (Hallpike et al., 1938; Paparella 1984a; Rauch et al., 1989; Salvinelli et al., 1999). Physiologically, the condition is thought to result in elevated calcium (Ca^{2+}) levels within the endolymphatic space that can lead to an alteration in the mechano-electro transduction process of the inner ear (Fettiplace et al., 2006; Ninoyu et al,. 1986; Salt et al., 1994). Ohashi et al. (2013) previously evaluated recovery of the auditory nerve using ECochG and

a two-click stimulus paradigm. These authors reported that many participants with MD exhibited a “hyper” rate of recovery compared to participants with idiopathic SNHL. Ohashi et al. (2013) theorized that the hyper rate of recovery could have resulted from a change in conductance of ions within the inner hair cells. The result would be an excess of Ca^{2+} that may alter the amount of neurotransmitter released into the synaptic cleft when activated due to the change in scala media ionic composition. This theory is indeed plausible given what we know about that ionic alteration to the inner ear in the presence of endolymphatic hydrops. However, while there are differences between our stimuli and those used by Ohashi and colleagues (2013), our results do not support this hypothesis.

While our hypotheses were based on prior literature by Ohashi et al. (2013), it was possible that the MD group could have shown poorer function (i.e., greater amount of adaptation and/ or slower recovery) compared to those of the idiopathic SNHL group based on the potential effects that endolymphatic hydrops can have on the inner hair cell and auditory nerve synapse. Kim et al. (2018) found that endolymphatic hydrops in mice results in cochlear synaptopathy. While we cannot conclude that our approach is sensitive to the condition of cochlear synaptopathy, the current findings do not raise suspicion of compromised neural function outside of what is observed from those with idiopathic SNHL. Thus, future studies are warranted to further test this hypothesis.

Study Limitations

The results of the present study suggest little evidence of impaired neural function in participants with MD that is different from what is observed in idiopathic SNHL, although the current study has limitations. Despite a sample of 34 participants, the overall group sizes were rather small particularly for the adaptation recovery experiment, potentially limiting generalization of the findings.

An additional potential limitation is that the MD group was somewhat heterogeneous in stage of progression of the disease. That is, many of the participants were undergoing an endolymphatic sac decompression procedure, while others were undergoing a labyrinthectomy procedure. The latter procedure results in complete hearing loss and is often only performed when the disease has progressed enough where residual hearing is considered to be of minimal utility. If damage to the auditory nerve is degraded with disease progression, then it is possible that further segregation of participants with MD may be needed to further elucidate its impacts on the auditory nerve.

CONCLUSIONS

Click train stimulation is a feasible approach to studying functional properties of the auditory nerve. Preliminary results suggest that MD does not impair auditory nerve function differently from what is observed in idiopathic SNHL. Furthermore, on average, the current data suggest that the presence of a VS

results in greater amounts of adaptation and a slower rate of recovery of the auditory nerve than what is observed in MD or idiopathic SNHL.

REFERENCES

Abbas, P. J., Gorga, M. P. (1981). AP responses in forward-masking paradigms and their relationship to responses of auditory-nerve fibers. *J Acoust Soc Am, 69*, 492-499.

Coats, A. C. (1981). The summating potential and Ménière's disease. I. Summating potential amplitude in Meniere and non-Meniere ears. *Arch Otolaryngol, 107*, 199-208.

Coats, A. C. (1986). The normal summating potential recorded from external ear canal. *Arch Otolaryngol Head Neck Surg, 112*, 759-768.

Coats, A. C., Dickey, J. R. (1972). Postmasking recovery of human click action potentials and click loudness. *J Acoust Soc Am, 52*, 1607-1612.

Committee on Hearing and Equilibrium guidelines for the diagnosis and evaluation of therapy in Ménière's disease. American Academy of Otolaryngology-Head and Neck Foundation, Inc. (1995). *Otolaryngol Head Neck Surg, 113*, 181-185.

Dallos, P., Schoeny, Z. G., Cheatham, M. A. (1972). Cochlear summating potentials. Descriptive aspects. *Acta Otolaryngol Suppl, 302*, 1-46.

Eggermont, J. J. (1975). Cochlear adaptation: a theoretical description. *Biol Cybern, 19*, 181-189.

Eggermont, J. J. (1976). Electrocochleography. In W. D. Keidel, W. D. Neff (Eds.), *Handbook of Sensory Physiology* (pp. 626-705). New York, NY: Springer-Verlag.

Eggermont, J. J., Don, M., Brackmann, D. E. (1980). Electrocochleography and auditory brainstem electric responses in patients with pontine angle tumors. *Ann Otol Rhinol Laryngol Suppl, 89*, 1-19.

Eggermont, J. J., Odenthal, D. W. (1974). Electrophysiological investigation of the human cochlea. Recruitment, masking and adaptation. *Audiology, 13*, 1-22.

Eggermont, J. J., Spoor, A. (1973a). Cochlear adaptation in guinea pigs. A quantitative description. *Audiology, 12*, 193-220.

Eggermont, J. J., Spoor, A. (1973b). Masking of action potentials in the guinea pig cochlea, its relation to adaptation. *Audiology, 12*, 221-241.

Fettiplace, R., Ricci, A. J. (2006). Mechanoelectrical transduction in auditory hair cells. In R. A. Eatock, R. R. Fay, A. N. Popper (Eds.), *Springer Handbook of Auditory Research* (pp. 154-203). New York, NY: Springer.

Gibson, W. P., Beagley, H. A. (1976). Electrocochleography in the diagnosis of acoustic neuroma. *J Laryngol Otol, 90*, 127-139.

Gibson, W. P., Prasher, D. K., Kilkenny, G. P. (1983). Diagnostic significance of transtympanic electrocochleography in Ménière's disease. *Ann Otol Rhinol Laryngol, 92*, 155-159.

Gorga, M. P., Abbas, P. J. (1981). AP measurements of short-term adaptation in normal and in acoustically traumatized ears. *J Acoust Soc Am, 70*, 1310-1321.

Gorga M. P., Worthington D. W., Reiland J. K., Beauchaine K. A., Goldgar D. E. (1985). Some comparisons between auditory brain stem response thresholds, latencies, and the pure-tone audiogram. *Ear Hear, 2*, 105-12.

Gulya, A. J., Schuknecht, H. F. (1982). Classification of Endolymphatic Hydrops. *American Journal of Otolaryngology, 3*, 319-322.

Hallpike, C. S., Cairns, H. (1938). Observations on the Pathology of Ménière's Syndrome: (Section of Otology). *Proc R Soc Med, 31*, 1317-1336.

Harris, D. M., Dallos, P. (1979). Forward masking of auditory nerve fiber responses. *J Neurophysiol, 42*, 1083-1107.

Katsarkas, A. (1996) Hearing loss and vestibular dysfunction in Ménière's disease. *Acta Oto-Laryngologica, 116*, 185-188

Kiang, N. Y., Watanabe, T., Thomas, E. C., et al. (1965). Discharge patterns of signle fibers in the cat's auditory nerve. *MIT Res, Mon*.

Murnane, O. D., Prieve, B. A., Relkin, E. M. (1998). Recovery of the human compound action potential following prior stimulation. *Hear Res, 124*, 182-189.

Ninoyu, O., Meyer zum Gottesberge, A. M. (1986). Changes in Ca++ activity and DC potential in experimentally induced endolymphatic hydrops. *Arch Otorhinolaryngol, 243*, 106-107.

Ohashi, T., Nishino, H., Arai, Y., et al. (2013). Electrocochleography in Ménière's disease: recovery from adaptation of the auditory action potential. *Acta Otolaryngol, 133*, 564-568.

Ohashi, T., Nishino, H., Arai, Y., et al. (2012). Recovery from adaptation of the action potential in idiopathic sudden sensorineural hearing loss investigated using a paired-click stimulation paradigm. *Acta Otolaryngol, 131*, 1165-1171.

Ohashi, T., Nishino, H., Nishimoto, Y., et al. (2014). The recovery from AP adaptation in sensorineural hearing loss. *Acta Otolaryngol, 134*, 275-279.

Ohashi, T., Ochi, K., Nishino, H., et al. (2005). Recovery of human compound action potential using a paired-click stimulation paradigm. *Hear Res, 203*, 192-200.

Paparella, M. M. (1984a). Pathogenesis of Ménière's disease and Ménière's syndrome. *Acta Otolaryngol Suppl, 406*, 10-25.

Paparella, M. M. (1984b). Pathology of Ménière's disease. *Ann Otol Rhinol Laryngol Suppl, 112*, 31-35.

Rauch, S. D., Merchant, S. N., Thedinger, B. A. (1989). Ménière's syndrome and endolymphatic hydrops. Double-blind temporal bone study. *Ann Otol Rhinol Laryngol, 98*, 873-883.

Relkin, E. M., Doucet, J. R., Sterns, A. (1995). Recovery of the compound action potential following prior stimulation: evidence for a slow component that reflects recovery of low spontaneous-rate auditory neurons. *Hear Res, 83*, 183-189.

Riggs, W. J., Fitzpatrick, D. C., Mattingly, J. K., et al. (2020). Electrocochleography during translabyrinthine approach for vestibular schwannoma removal. *Otol Neurotol, 41*, e369-e377.

Salt, A. N., DeMott, J. (1994). Endolymph calcium increases with time after surgical induction of hydrops in guinea-pigs. *Hear Res, 74*, 115-121.

Salvinelli, F., Greco, F., Trivelli, M., et al. (1999). Ménière's disease. Histopathological changes: a post mortem study on temporal bones. *Eur Rev Med Pharmacol Sci, 3*, 189-193.

Santarelli, R., Rossi, R., Scimemi, P., et al. (2015). OPA1-related auditory neuropathy: site of lesion and outcome of cochlear implantation. *Brain, 138*, 563-576.

Santarelli, R., Starr, A., Michalewski, H. J., et al. (2008). Neural and receptor cochlear potentials obtained by transtympanic electrocochleography in auditory neuropathy. *Clin Neurophysiol, 119*, 1028-1041.

Schuknecht, H. F. (1974). *Pathology opf the ear*. Massachusetts: Harvard University Press.

Smith, R. L. (1977). Short-term adaptation in single auditory nerve fibers: some poststimulatory effects. *J Neurophysiol, 40*, 1098-1111.

Stephens, S. D., Charlet de Sauvage, R., Aran, J. M. (1974). [Adaptation of the electrocochleogram: preliminary report]. *Rev Laryngol Otol Rhinol (Bord), 95*, 129-138.

Tsuji, K., Velazquez-Villasenor, L., Rauch, S. D., et al. (2000). Temporal bone studies of the human peripheral vestibular system. Ménière's disease. *Ann Otol Rhinol Laryngol Suppl, 181*, 26-31.

Westerman, L. A., Smith, R. L. (1984). Rapid and short-term adaptation in auditory nerve responses. *Hear Res, 15*, 249-260.

Yoshie, N., Oashi, T. (1971). Abnormal adaptation of human cochlear nerve action potential responses: clinical observations by non-surgical recording. *Rev Laryngol Otol Rhinol (Bord), 92*, Suppl:673-690.

Young, E., Sachs, M. B. (1973). Recovery from sound exposure in auditory-nerve fibers. *J Acoust Soc Am, 54*, 1535-1543.

CHAPTER 5: MANUSCRIPT 3

Neural Adaptation of the Auditory Nerve and the Effect of Aging

William J. Riggs, Jeffrey Skidmore,

Brittney Carter, Shuman He

Department of Otolaryngology-Head

and Neck Surgery

The Ohio State University Columbus,

43210

ABSTRACT

Objective: This study aimed to investigate effects of advancing age on the temporal encoding property, neural adaptation, of the auditory nerve (AN) to repetitive stimuli in adult CI users.

Design: This was a prospective study with 27 postlingually deafened adult participants. All subjects used a Cochlear® Nucleus™ device with a 24RE [CA], CI512, CI532 of CI632 in the test ear. Participants were split into two groups, younger adults (<65 years; average age: 51.0) and older adults (≥65 years; average age 72.2). Electrical stimuli of interest were 100-ms pulse trains presented at 2 Hz in a monopolar-coupled stimulation mode at four carrier pulse rates: 500, 900, 1800 and 2400 pulses per second (pps). Stimuli were delivered to individual CI electrodes at the maximum comfortable level (i.e., C level) measured at 2400 pps at four electrode locations (3, 9, 15, 21). Amount of neural adaptation at each rate was quantified using the adaptation index (He et al., 2016) defined as the averaged normalized eCAP amplitude measured within three time windows over the course of the pulse train (5, 50, 100 ms).

Results: Adaptation indices were found to be smaller for higher stimulation rates (i.e., greater amount of adaptation) for both older and younger CI users. Additionally, the average adaptation index was smallest when eCAPs were measured at later time windows of the pulse-train compared to earlier time windows. While, on average, older adults exhibited poorer AN responses, results of generalized linear mixed models did not reveal significant differences in the

functionality of the AN between the two age groups in the amount of adaptation that occurred nor the time it took to reach an adaptive level between older and younger adult CI users. Adaptation indices were used in correlation analyses with age and higher pulse rates exhibited trends of greater amounts of adaptation with advancing age, although these trends did not reach significance.

Conclusions: The sensitivity of the AN to steady state pulse trains of clinically relevant pulse rates was not found to be significantly different between older and younger adult CI users, although trends of poorer function in older adults did exist, especially at higher pulse rates. The amount of adaptation that occurred was significantly impacted by stimulation rate, where faster rates resulted in greater amount of adaptation for both CI age groups, while the rate at which adaptation occurred was found to be highly variable for both groups. Further work is warranted to elucidate effects of aging on functional properties of the AN.

INTRODUCTION

It is well known that the auditory system undergoes changes due to the aging process, termed presbycusis, whereby auditory thresholds become elevated and the ability for a listener to process speech in adverse listening conditions declines with advancing age (Dubno et al., 1984; Gordon-Salant, 2005; Gordon-Salant et al., 1993). Clinically, word recognition abilities in older adults are often worse than would be predicted by their audiometric profile (Dubno et al., 1984; Frisina et al., 1997). Results from longitudinal studies have suggested that hearing sensitivity begins to decline above age 30 for males and age 50 for females (Pearson et al., 1995) and that the degree of hearing loss is often greater in males (Cruickshanks et al., 1998; Moscicki et al., 1985).

The causes of presbycusis remain unclear, however, evaluation of the peripheral auditory system through human temporal bone studies have confirmed several anatomical changes that take place. Cochlear findings have included degeneration of the stria vascularis (strial presbycusis), loss of inner and outer hair cells (sensory presbycusis), and stiffening of the basilar membrane (mechanical presbycusis) (Kurata et al., 2016; Schuknecht, 1955; Schuknecht et al., 1993). The auditory nerve (AN) has also been found to be significantly impacted by the aging process (neural presbycusis). Findings of the AN have included a reduction in spiral ganglion neurons and peripheral axons with variability in the loss of outer and inner hair cells with advancing age (Schuknecht & Gacek, 1993; Viana et al., 2015; Wu et al., 2019). The findings of neuronal degeneration despite variation in

hair cell injury across the cochlea has also been consistently found in aging animals studies as well (Keithley et al., 1982; Keithley et al., 1989; Tarnowski et al., 1991). Furthermore, in addition to neuronal loss, loss of synaptic structures such as presynaptic ribbons and postsynaptic receptors begin to occur in the aging ear often long before changes in sensory cells (Sergeyenko et al., 2013; Stamataki et al., 2006). Finally, Schmiedt et al., (1996) showed that advancing age in gerbils results in a decline in the spontaneous firing rate of AN fibers, suggesting a decrease in excitability of remaining never fibers with advancing age. Hence, it is clear that, in addition to cochlear effects, the AN is also a primary target of the aging process.

A growing treatment for adults with hearing loss, in particular those 60 years and older with severe-to-profound sensorineural hearing loss (SNHL), is CIs (Lin et al., 2012). CIs bypass the sensory cells of the inner ear and directly stimulate the AN using electrical currents. Although Cis are considered a successful treatment for older adults (Lin et al., 2012), limitations in auditory performance (i.e., speech recognition/perception) are known to occur following implantation. Previous authors have reported poorer speech perception outcomes in older adults than their younger counterparts (Beyea et al., 2016; Friedland et al., 2010; Roberts et al., 2013), suggesting functional changes due to advancing age. Specific functional changes in a higher-level brain process, phonological sensitivity, has also been shown to decline with advancing age (Moberly et al., 2017; Moberly et al., 2016). This decline is likely one contributing source for poorer speech

perception outcomes in older adults. In contrast, peripheral factors in CI users, such as AN sensitivity to amplitude modulated electrical pulses (Riggs et al., 2021) and the rate of recovery from pulse train stimulation (Mussoi et al., 2019), have been shown to decline with advancing age, suggesting functional changes in the AN due to the aging process. As speech perception outcomes following CI are known to be variable, especially in older adults, and the AN degenerates with advancing age, it is entirely possible that one contributing reason for variable CI outcomes could be due to functional changes of the AN with advancing age.

Given the observed performance variability and known functional changes in auditory processing in older CI users, further investigations into underlying alterations due to the aging process are of clinical relevance. The current investigation focuses on using electrically-evoked compound action potentials (eCAPs) obtained through the CI to assess the effect of aging on peripheral AN sensitivity. In particular, we focused on non-stationary temporal effects of the AN, neural adaptation, in adult CI users. Neural adaptation to electrical stimulation is defined as the decrement in the amplitude of the AN fiber group response (i.e., eCAP) following previous stimulations (Litvak et al., 2001). This response property can be studied through a CI using repetitive electrical pulses grouped into trains. Thus, eCAPs evoked by pulse-train stimuli provide information about temporal effects of prior neural activity on response properties of the AN (Cartee et al., 2000; Matsuoka et al., 2000; Wilson et al., 1997). Conversely, the eCAP to a single biphasic pulse is independent of the history of prior neural activity (Clay et al.,

2007) and mainly reflects the inherent excitability of the electro-neural interface. In this scenario, the eCAP response is thought to be void of adaptation effects due to the lack of prior stimulation, and thus exhibits maximal amplitude when stimulated with a single pulse (Jeng et al., 2009).

Adaptation may be an important physiological property of neurons. It has been suggested as having implications for AN encoding of speech signals. Peaks in AN fiber discharge rate due to adaptation have been shown to be essential for encoding spectro-temporal regions of speech signals that contain rich phonetic cues and enhancing spectral contrast between successive speech segments (Delgutte, 1997). This suggests that adaptation at the AN level would also likely be important for CI users, as CIs directly stimulate the AN. Single pulse stimulation of the AN has been shown to produce highly synchronous responses of AN fibers (Miller et al., 1999; van den Honert et al., 1984), but the AN fibers become less synchronous with repetitive stimulation due to susceptibility to adaptation effects of neurons (Zhang et al., 2007). In CI users, understanding how older users process repetitive stimuli could be impactful for informing clinicians about CI mapping parameters. Slower stimulation rates may be more beneficial for this population, as higher rates may be more likely to limit their ability to encode all temporal features of speech due to adaptation effects.

The objective of this study was to investigate the effects advanced age has on adaptation properties of the AN by using single-pulse and pulse-train stimulation in adult CI users. We argue that combining single-pulse and pulse-train

stimulation is a scientifically rigorous and productive approach to evaluating the functional status of the AN. Our overall hypotheses was that older adults would, on average, exhibit a greater amount of adaptation, as measured by the adaptation index, and reach an adaptive level at a quicker rate than younger CI users.

MATERIALS AND METHODS

Participants

Study participants included 27 post-lingually deafened adults who had previously been implanted with a Cochlear® Nucleus™ device (Cochlear Ltd., Macquarie, NSW, Australia) in the test ear. Participants A003, A008, A011, A019, A034 and A049 were bilateral users. Thus, only one ear was included, and the ear to be included was pseudo-randomly selected. Participants were parsed into two groups: 1) younger adults, those who were less than 65 years of age (n: 14, mean: 51.0 years, standard deviation [SD]: 13.1), and 2) older adults, those who were age 65 and older (n: 13, mean: 72.2 years, SD: 6.8). All participants were required to have at least five months of CI experience with their device and were compensated for their participation in the study. Detailed demographic information of these participants is listed in Table 5.1. The study was approved by the Ohio State University Biomedical Institutional Review Board (2017H0131). Written, informed consents were obtained from study participants prior to participation.

ID	Sex	Ear tested	Etiology	AAI (yrs)	AAT (yrs)	Group	Internal electrode array	Electrode tested
A003	M	L	SHL	58.9	61.8	Y	CI512	e4, e6, e9, e12, e15, e18, e21
A004	F	L	Unknown	61.3	66.1	Y	CI422	e12, e15, e18, e21
A006	M	L	Ménière's	60.7	69.0	O	CI512	e3, e9, e12, e15, e18, e21
A007	M	R	Unknown	43.3	52.7	Y	24RE (CA)	e3, e9, e15, e21
A008	F	L	Hereditary	54.4	67.6	O	24RE (CA)	e3, e9, e15, e21
A009	F	L	Trauma	31.5	38.0	Y	24RE (CA)	e3, e6, e9, e12, e15, e18, e21
A011	M	R	Noise	77.5	80.7	O	24RE (CA)	e3, e9, e15, e21
A014	M	R	Measles	52.5	61.5	Y	CI512	e9, e15
A019	F	R	Rubella	44.7	54.7	Y	24RE (CA)	e3, e9, e15, e21
A020	M	R	Trauma	60.3	62.8	Y	CI522	e4, e6, e8, e12, e15, e18, e21
A021	F	R	Unknown	23.6	24.8	Y	24RE (CA)	e3, e6, e9, e12, e15, e18, e21
A024	M	R	Hereditary	25.6	36.8	Y	24RE (CA)	e3, e9, e15, e21
A025	M	L	Unknown	74.9	83.2	O	24RE (CA)	e10,e15, e21
A029	F	R	Hereditary	48.5	59.6	Y	24RE (CA)	e3, e12, e15, e21
A030	F	R	Unknown	64.9	65.6	O	CI532	e3, e9, e15, e21
A032	M	L	Unknown	59.4	60.0	Y	CI532	e3, e9, e15, e21
A034	M	L	Trauma	70.2	70.8	O	CI532	e3, e9, e15, e21
A037	F	R	Unknown	15.2	28.7	Y	CI532	e15, e18, e20
A040	M	R	Unknown	58.9	59.6	Y	CI532	e15, e20
A041	F	R	Hereditary	73.3	79.8	O	24RE (CA)	e5, e9, e15, e21
A045	F	L	Autoimmune	67.5	79.4	O	24RE (CA)	e4, e15, e16, e21
A048	F	L	Hereditary	57.3	59.7	Y	CI532	e9, e14, e21
A049	M	R	SHL	51.3	52.9	Y	CI532	e9, e15
A050	M	R	Noise	75.1	76.7	O	CI522	e4, e9, e15, e20
A051	M	R	SHL	55.8	62.4	Y	24RE (CA)	e3, e9, e15, e21
A052	M	L	VS	65.2	67.6	O	CI532	e3, e9, e15, e21
A054	M	L	Noise	69.2	69.7	O	CI622	e15, e18, e21

Table 5.1. Demographic information of study participants. ID: participant identification, M: male, F: female, L: left, R: right, SHL: sudden hearing loss, VS: vestibular schwannoma, AAI: age at implantation, AAT: age at testing, eCAP: the electrically evoked compound action potential, 24RE (CA): Freedom Contour Advance electrode array.

Testing Electrodes

For the Cochlear® Nucleus™ device, the electrode is numbered in a base-to-apex direction, with electrode 1 placed near the base and electrode 22 placed at the most apical location of the electrode array. For each patient, a minimum of four electrodes (typically electrodes 3, 12, 15, and 21) across the electrode array were routinely tested in this study, although three participants (A014, A040, A049) only had two electrodes tested due to various technical reasons (high impedances, low behavioral threshold stimulation levels, etc.). An adjacent electrode when possible was substituted when results of impedance measures suggested either open- or short-circuit. The rationale for testing multiple electrodes across the electrode array was that this approach could capture potential variation in the functional status of AN fibers at different locations within the cochlea due to aging effects. Electrodes tested in individual study participants are listed in Table 5.1.

Procedures and Stimuli

Testing was carried out in a sound-treated booth with participants seated in a recliner. The Advanced Neural Response Telemetry (NRT) function implemented in Custom Sound EP (v. 5.1) commercial software (Cochlear Ltd, Macquarie, NSW, Australia) was used to deliver stimuli and record electrophysiological responses of the AN. Two types of stimuli were utilized for this experiment: 1) a single biphasic cathodic-leading electrical pulse presented at 15 Hz, and 2) 100-ms pulse trains presented at 2 Hz in a monopolar-coupled

stimulation mode at four carrier pulse rates: 500, 900, 1800 and 2400 pulses per second (pps). The number of masker pulses in each train ranged from 1-29, 106-120, and 225-239 masker pulses for 2400 pps and declined with decreasing rate. That is, due to the difference in pulse rates, slower pulse rate stimuli had fewer masker pulses than higher pulse rates over the 100 ms duration. Fifty sweeps per trial were used for all eCAP recordings. Stimuli were delivered to individual CI electrodes via an N6 sound processor interfaced with a programming pod.

Stimuli were presented to individual CI electrodes in the NRT software using the "Stimulation Only" feature by a licensed audiologist. Prior to each experimental session, each participant's maximum comfortable level (i.e., C level) was assessed at each test electrode using a visual loudness rating scale [1-10], where 1 is "barely audible" and 10 is "very uncomfortable". To avoid any participant discomfort due to differences in stimulation rates (e.g., 2400, 1800 etc.) we found each participant's C level using the 100-ms unmodulated train presented at 2400 pps, as this rate was typically found to be perceptually loudest to the participant.

eCAP Measurements & Analysis

The eCAP was analyzed using custom routines in Matlab (R2019, Mathworks). eCAP peaks attributed to the traditionally labeled negative N_1 and positive P_2 peaks (Abbas et al., 1999) were manually identified by two experienced researchers (WJR, SH). eCAP amplitude was calculated as the difference between the N_1 and P_2 peaks in μV. The eCAP response evoked by a single pulse

stimulation was measured using a two-pulse forward masking paradigm. Two consecutive pulses were presented with a short inter-pulse interval (Brown et al., 1990). Briefly, this technique uses the initial pulse as the masker, which is expected to contain both eCAP activity and electrical artifact, and the second response is expected to contain predominately artifact as the nerve is thought to be in refractory and unable to respond. Using a subtraction technique, the neural response to the probe stimulus can then be derived (see Brown et al., 1990 for in-depth review).

For pulse trains, since the NRT software does not allow for measuring eCAP amplitudes to individual pulses of the train, we used pulse trains that varied in the number of pulses (see *Procedures and Stimuli* for details on pulse trains) over three approximately 5-ms time windows around 5, 50 and 100 ms) and then measured the eCAP evoked by the last pulse of the train. To achieve an artifact-free waveform, we used a modified forward masking technique. This technique has been reported in detail in He et al. (2017).

To quantify the amount of adaptation, we implemented the adaptation index (He et al., 2016). This approach calculates the averaged normalized amplitudes of eCAPs recorded within each time window, whereby smaller indices indicate greater amount of neural adaptation. Our interest was also to capture the rate of adaptation exhibited by the AN. For this approach, we used mathematical modeling to estimate the time constant (i.e., tau) of a decaying exponential

function. Tau represents the time (ms) it takes for the eCAP amplitude to decay to 37% of the single pulse eCAP amplitude. Its function is described by the following equation:

$$A = \exp(-\frac{t}{tau})$$

where *A* refers to the eCAP amplitude normalized to the single pulse amplitude, *t* is time (ms), and *tau* is the time constant in ms.

Statistical Analysis

SPSS v27 (IBM Corp.) was used to carry out all statistical analyses presented below. Dependent variables included the adaptation index and rate of adaptation (tau). Three separate generalized linear mixed models (GLMMs) were used to assess between-group and within-group differences on the adaptation index and adaptation time constant. The GLMM was selected due to its ability to robustly handle missing data and allowing for comparison of differently distributed datasets (Neuhaus et al., 2011). In the first GLMM, we tested the effect of pulse rate on adaptation index by group, where pulse rate and group were set as the fixed effects and study participant as the random effect. In the second GLMM, we assessed group differences in the amount of adaptation by pulse train duration (i.e., time window) where group, rate, and time window served as the fixed effects, and study participant served as the random effect. Finally, in the third GLMM, we assessed group differences in the rate of adaptation (tau), where fixed effects

consisted of group and rate, while study participant served as the random effect. When necessary, post-hoc analyses were carried out using Bonferroni correction. Pearson product-moment correlation tests were used to assess relationships between participant age as a continuous variable and the adaptation index and rate of adaptation for each stimulation rate. All tests were two-tailed, and statistical significance was determined using an alpha of 0.05 (i.e., 95% confidence level).

RESULTS

eCAP Response Observations

Figure 5.1 shows example eCAP responses for two participants (A034- older adult and A009- younger adult) obtained at 2400 pps. A consistent, but not unexpected, observation across participants was that the maximal eCAP amplitude was found following the initial single pulse, while responses across the pulse train were often drastically reduced in amplitude, typically reaching an asymptotic level around the 50 ms time window. Additionally, an alternating pattern was observed in eCAP amplitude, most prominent for the earlier time windows of the pulse train.

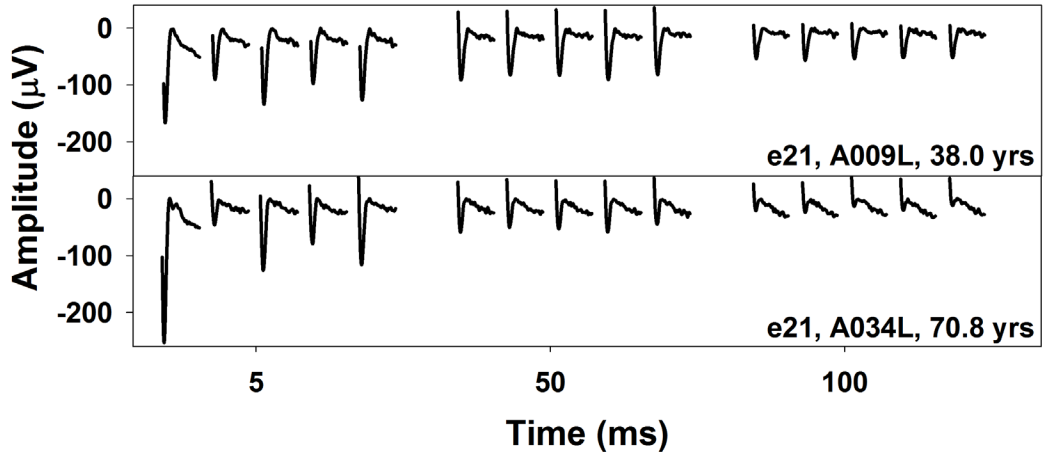

Figure 5.1 Examples of electrically evoked compound action potentials (eCAPs) obtained from one participant in the young group and one participant in the older group obtained using a 2400 pps stimulation rate

Effect of Pulse Rate on Adaptation Index

Figure 5.2 shows the means and standard deviations of the average adaptation index results across electrodes (averaged across all time windows) as a function of rate. Here, it can be seen that the amount of adaptation was smallest (i.e., higher adaptation index values) at lower stimulation rates and increased with increasing stimulation rate for both study groups. On average, the younger adults exhibited larger adaptation indices (suggesting less adaptation occurring) at each stimulation rate compared to the older group. The results of the GLMM revealed a significant effect of rate ($F_{(7,355)} = 246.80$, $p < 0.01$) but not for group ($F_{(1,25)} = 2.84$, $p = 0.09$) nor their interaction ($F_{(3,355)} = 0.12$, $p = 0.95$). The results of pairwise comparisons revealed that the adaptation index was statistically different for all test rate comparisons (see Table 2.2 for results).

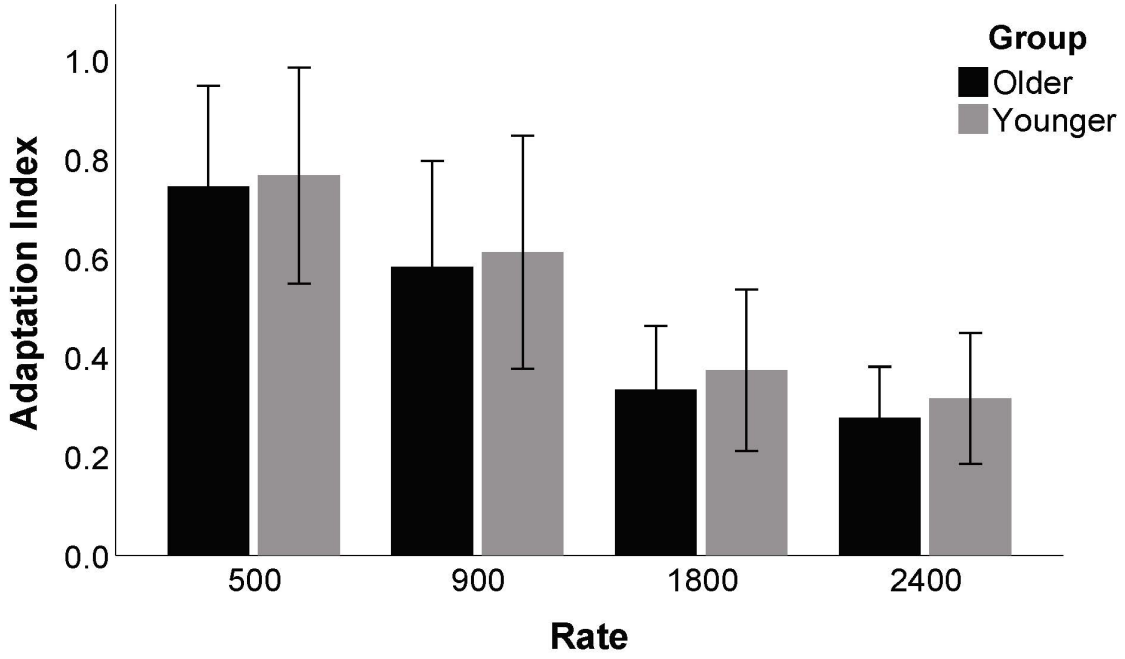

Figure 5.2. Average and standard deviations of the adaptation index values averaged together across all electrode locations by group. Here it can be seen that index values decrease with increasing pulse rate, suggesting greater adaptation taking place. No significant differences we noted between groups, however there was significant effect of pulse rate whereby the average index was different for each pulse rate.

Rate	Rate	Contrast	t	p	95% Lower Bound	95% Upper Bound
500	900	0.16	14.65	<0.01	0.13	0.19
500	1800	0.40	37.09	<0.01	0.37	0.43
500	2400	0.46	42.33	<0.01	0.43	0.49
900	1800	0.24	22.44	<0.01	0.22	0.27
900	2400	0.30	27.69	<0.01	0.28	0.32
1800	2400	0.06	5.25	<0.01	0.04	0.08

Table 5.2. Results of pairwise comparison for adaptation index values each measured at different stimulation rates.

Effect of Pulse Train Duration (i.e., Time) on Adaptation Index

Figure 5.3 plots the means and standard deviations of the adaptation index for each group by rate obtained at each recording window (5, 50, 100 ms). Similar to the results seen above for both groups, the adaptation index for 500 pps was the largest (i.e., smallest effect) and decreased with increasing pulse rate. However, when considering time window, it can be observed that the adaptation index decreased with increasing time window similarly between groups for all pulse rates, suggesting longer stimulation periods induced greater amounts of adaptation. Results of the GLMM showed that there was a significant effect of rate ($F_{(3,275)} = 1700.10$, $p < 0.01$), time window ($F_{(2, 275)} = 414.60$, $p < 0.01$), as well as their interaction ($F_{(6,275)} = 4.50$, $p < 0.01$). There was no significant effect of group ($F_{(177)} = 1.38$, $p = 0.24$), or the interaction of rate by group ($F_{(3,275)} = 0.83$, $p = 0.48$), group by time window ($F_{(2,275)} = 1.77$, $p = 0.17$), nor the interaction of time, group, and rate ($F_{(6, 275)} = 0.03$, $p > 0.99$). Overall, the results suggest that, when considering adaptation by pulse train duration in addition to rate, the amount of adaptation differed with time. This amount differed for each rate across time windows. Interestingly, there was no effect of age group.

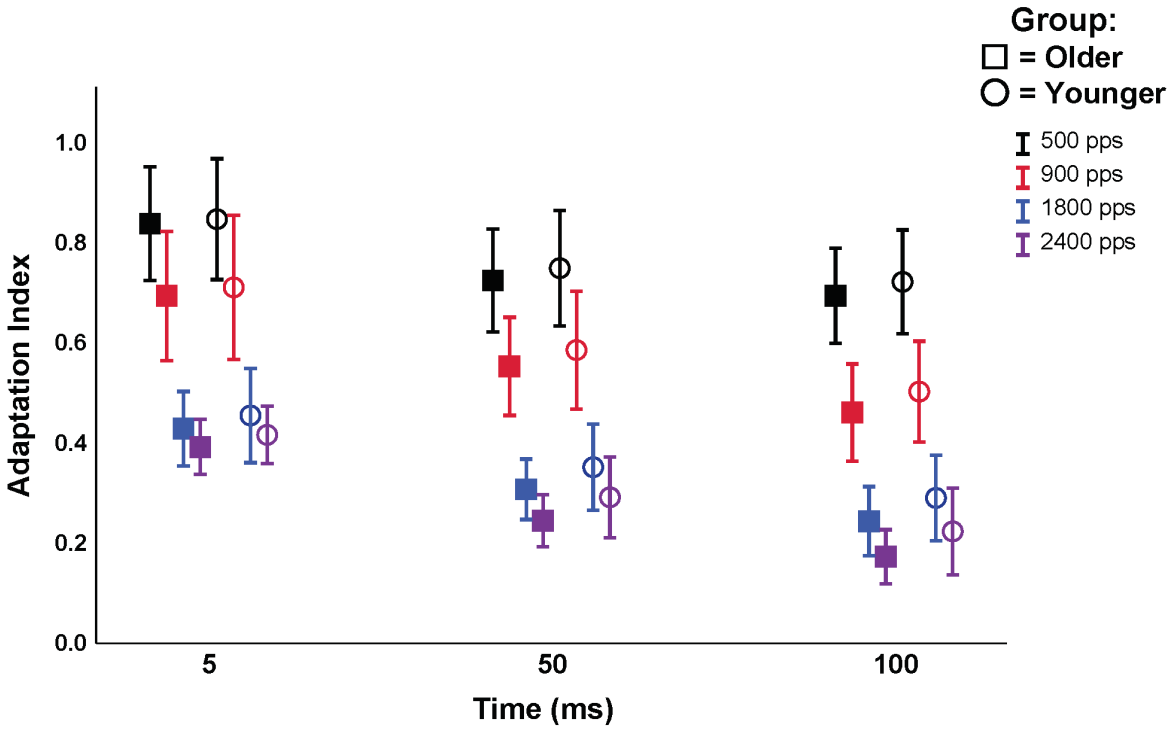

Figure 5.3. Average and standard deviation of adaptation index averaged together across all electrode locations for each time window and rate for each group (filled boxes represent the older group; circles represent the younger group). Here it can be observed that the adaptation index values decline when measured at the later time points of the stimulus train (e.g., 100 ms) for all pulse rates. Similarly, the adaptation index declines with increasing rate. The decline in adaptation index value by time window and rate were similar for both age groups.

Adaptation Index and Age Correlations

The adaptation index was used in correlation analysis with participant age for each stimulation rate (Figure 5.4). No significant correlations were found for any stimulation rate, although a small negative trend was observed for 1800 and 2400 pps (see each panel of Figure 5.4 for correlation coefficients and their associated p-value). A noticeable observation for each correlation is that the two youngest participants (A021 and A037) appear to exhibit adaptation indices similar to, or smaller than, many of the participants age 75 and older, and consistently lower than most participants less than age 75.

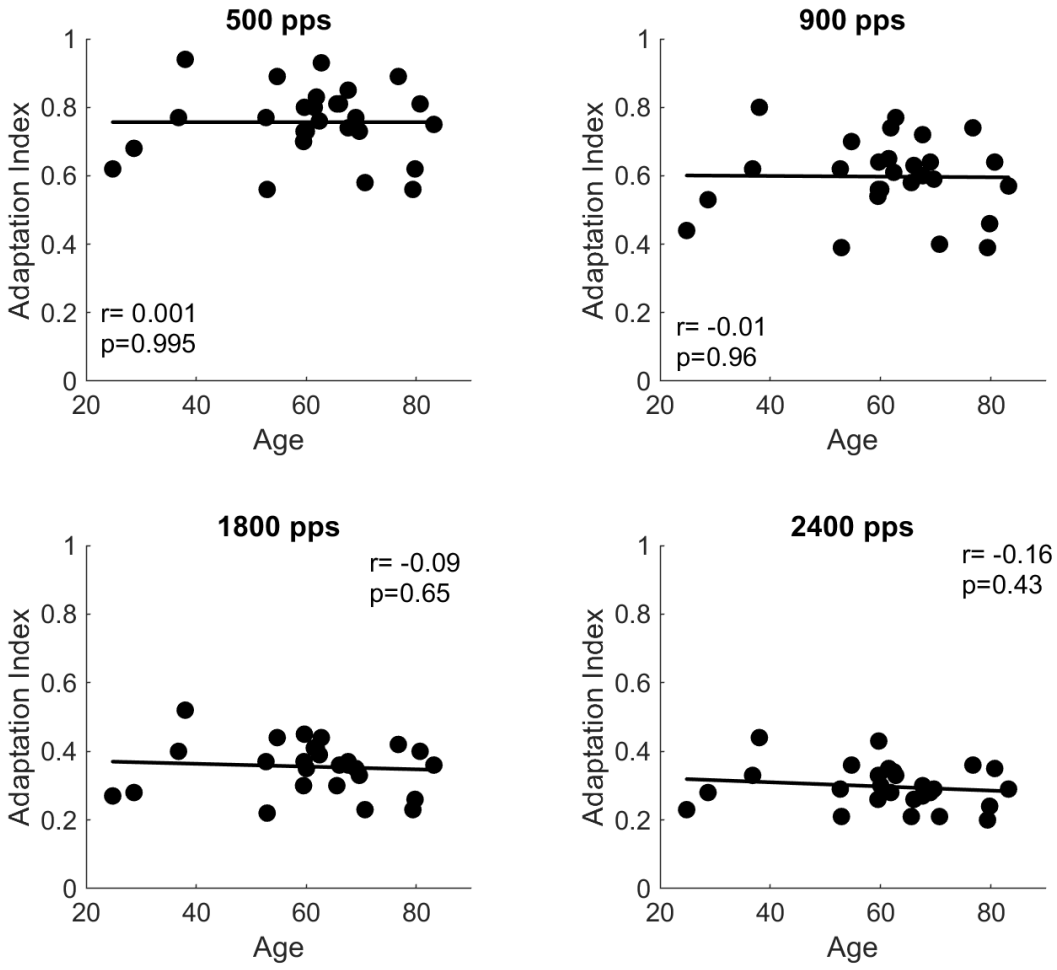

Figure 5.4. Results of Pearson product-moment correlations between age and adaptation indices for each stimulation rate.

Adaptation Time Constant

Figure 5.5 displays the means and standard deviations for the times of adaptation (tau) by rate for each group. These data show considerable variation, especially at the lower stimulation rates (500, 900 pps) for both groups. At higher stimulation rates, it can be observed that the younger group on average exhibited longer time constants (i.e., required longer stimulation before reaching an asymptotic level of adaptation - 37% of the single pulse amplitude). The average rates of decay for the older and younger groups, respectively, were 915 and 887 ms at 500 pps, 782 and 265 ms at 900 pps, 27 and 64 ms at 1800 pps, and 13 and 108 ms at 2400 pps. Results of the GLMM showed a significant effect of rate ($F_{(3,75)} = 17.02$, $p < 0.01$), but no significant effect of group ($F_{(1,25)} = 0.37$, $p = 0.55$) nor the interaction of group and rate ($F_{(3,75)} = 2.0$, $p = 0.12$).

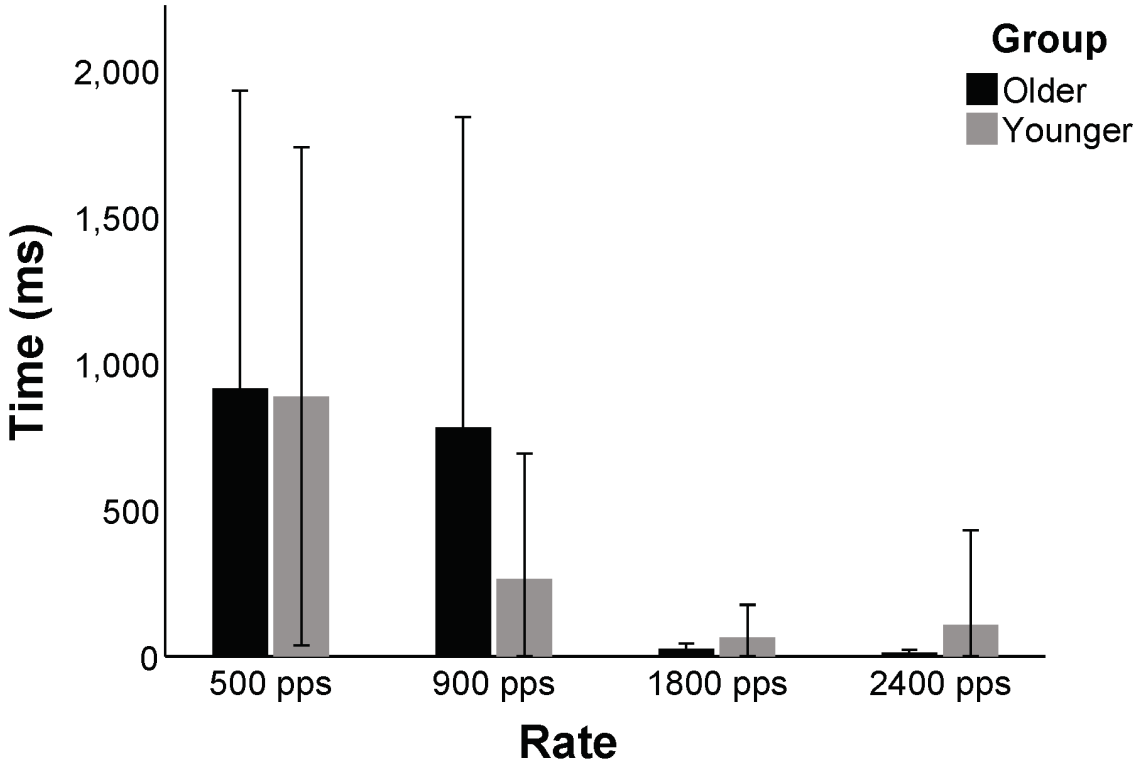

Figure 5.5. Bars represent the averages and standard deviations of the adaptation time constant averaged together across all electrode locations by rate for each group. It can be observed that the average time to reach an adapted state (i.e., 37% of the single pulse eCAP amplitude). There was an overall significant effect of pulse rate but no group effect.

Adaptation Rate and Age Correlations

The time it took to reach an adapted level was used in correlation analysis with participant age for each stimulation rate (Figure 5.6). No significant correlations were observed for any rate (see each panel of Figure 5.6 for correlation coefficients and their associated p-value). The correlations for 500 pps and 900 pps show positive trends whereby older adults took longer to reach an adaptive level (i.e., slower rate of adaptation) than younger adults. However, this trend reverses at 1800 pps and 2400 pps. Overall, there was considerable variability in the rate of adaptation for the lower pulse rates (i.e., 500 pps and 900 pps) and low variability at the two highest pulse rates.

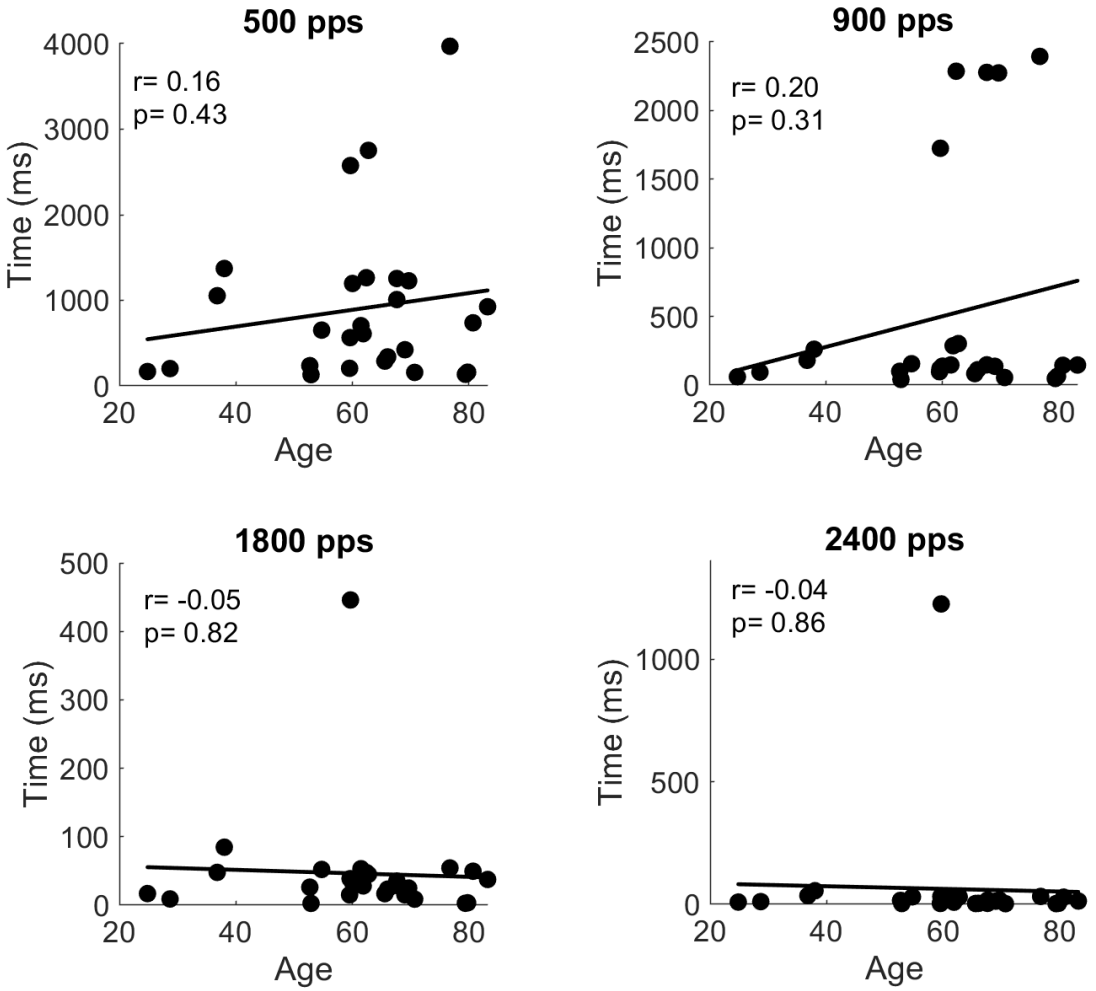

Figure 5.6 Results of Pearson product-moment correlations between participant age and rate at which adaptation occurred for each stimulation rate.

DISCUSSION

The current study investigated the effects of aging on adaptation of the electrically-stimulated AN in adult CI users using pulse train stimulation. We hypothesized that the AN response would exhibit greater amounts of adaptation with advancing age at testing, as we expected a degradation in functional properties of the AN due to age. Additionally, we hypothesized that the time it takes to reach an adaptive state to repetitive electrical stimuli would be shorter in older adults than younger adults, also reflective of declining function in AN properties. Overall, the results fail to support our hypotheses, as no age group differences were found in regard to the amount of adaptation or to the speed at which the AN reaches an adaptive level.

AN Responses to Pulse Train Stimulation

The stimuli utilized in the current study were unmodulated pulse trains presented at four carrier rates. A consistent finding observed was that the eCAPs evaluated later in the pulse train were of the smallest amplitude. This was an expected finding across both age groups, as longer duration stimuli are expected to be more challenging to the AN. Similar to previous reports evaluating neural adaptation effects (Hay-McCutcheon et al., 2005; He et al., 2016; Hughes et al., 2012; Wilson et al., 1997), we also observed an alternating zig-zag response pattern in eCAP amplitude predominately at the earlier time window (i.e., 5 ms) of the pulse train. This pattern is thought to reflect desynchronized response firing of the AN due to refractory properties, whereby subpopulations of nerve fibers are

responding with ongoing pulses of the pulse train. The whole nerve response is expected to occur following the initial pulse of the train (Wilson et al., 1997). This pattern is also expected be observed more often in responses evoked earlier in the stimulus rather than later, due to reaching asymptotic levels of adaptation as stimulus duration lengthens (He et al., 2016). This finding was consistently observed in the eCAP responses of both age groups.

The adaptation index was previous described by He et al., (2016) who evaluated AN function via a CI in children with auditory neuropathy spectrum disorder and those without (i.e., SNHL). Similar to their findings, the greatest amount of adaptation was consistently found in eCAPs evoked by a 2400 pps pulse rate, and the lowest amount induced was found at 500 pps across stimulation sites of the electrode array. These authors, however, found that time window (e.g., 5, 50, 100 ms) of where the adaptation index was calculated was an important factor in identifying group differences. Specifically, eCAPs evoked by the last pulses of the pulse train (e.g., 100 ms) exhibited group differences, whereas indices obtained at earlier time windows were similar between groups. This reinforced the notions that the length of the pulse train is important and that longer duration pulse trains tax the AN, whereby functional differences can be identified. While our results showed a similar trend, the adaptation index found at the longest time window did not reach statistical significance for detecting differences between older and younger adult CI users.

Aging and Neural Adaptation

The stimulation rate of the pulse train was regularly found to significantly impact the eCAP response for both groups. This is consistent with previous reports evaluating temporal responses of the AN, which have shown that higher rates maximally stress the AN (He et al., 2016; Hughes et al., 2012; Litvak et al., 2001; Wilson et al., 1997). The amount of adaptation exhibited by AN fibers when stimulated with unmodulated pulse trains increases with increasing rate. As previous aging studies have confirmed, older listeners often have reduced speech perception capabilities compared to younger listeners in challenging listening environments (e.g., background noise) (Dubno et al., 1984). They also exhibit a reduction in the number of remaining spiral ganglion neurons across the cochlea (Wu et al., 2019). We expected the functionality of the remaining spiral ganglion neurons to exhibit differences between the two age groups, especially at the most challenging stimulation rates. It should be noted that, despite failing to find a significant effect of stimulation rate, the adaptation index means for the older group at all stimulation rates were always lower than the younger group. This was even more pronounced at the higher stimulation rates. This trend could suggest that further investigations potentially with a larger sample size may yield more supportive evidence of an age effect at higher stimulation rates.

We were also interested in determining if the rate (i.e., speed) at which an asymptotic level of adaptation was reached was also affected by age. We theorized that longer time periods prior to reaching adaptation steady state might

reflect a related functional property of the AN that is different from simply the overall amount of adaptation that occurred. That is, if an asymptotic level of adaptation was reached immediately following the initial pulse of the pulse train, this could potentially reflect poor neural membrane integrity. However, the current results do not suggest a significant difference between the two age groups when considering the rate of adaptation. Furthermore, there was substantial inter- and intra-participant variability observed in the time constant values for both groups across all stimulation rates, potentially suggesting it is an insensitive measurement for assessing overall AN function. This lack of utility in measurement of adaptation time constants is in line with previous work by Hay-McCutcheon and colleagues (2005). These authors reported a rapid decline in their eCAP amplitudes, but stated that slope measurements were not useful for their analysis when evaluated with behavioral measures of temporal integration. Therefore, they chose not to present these findings. Overall, further modeling techniques other than an exponential decay approach used in the current study might be necessary to more accurately capture rate of adaptation of the AN.

Etiology of Hearing Loss and Advancing Age

It is important to note that studying aging effects on auditory function can be complicated by the etiology of a participant's hearing loss. As can be observed in Table 5.1, participants in the current study had a wide range of suspected causes of hearing loss (e.g., genetic, autoimmune, sudden etc.). This presents a unique challenge in purely studying the effects of advancing age on auditory

function, as it can be difficult to exactly identify each participant's true cause of hearing loss. Additionally, the differences in etiology can result in different sites-of-lesion (e.g., sensory cells vs. spiral ganglion cells). For example, in CI users, Shearer and colleagues (2017) found that etiological diagnosis of deafness using clinical presentation in conjunction with genetic testing can strongly predict CI performance, as this approach significantly helps to account for differences in site of lesion. This has been supported by other findings in CI users in whom outcome performance has been shown to be strongly related to site of lesion in various genetic-linked causes of hearing loss (Shearer & Hansen, 2019; Lee et al., 2020). Thus, it is reasonable to assume that the underlying pathology in hearing loss from participant to participant could mask detection of true age-related changes in auditory function measured via eCAPs.

Furthermore, it is possible that etiologies that cause hearing loss in pediatric and young adult populations may be somewhat different from etiologies that cause hearing loss in middle-to-older aged adults as a result of the aging process. The results for the two youngest adults (Figures 5.4 and 5.6) provide potential support for this theory. Specifically, their adaptation indices were often similar to those values observed in the oldest participants, which were consistently lower than those adults between the ages of 38-65 years. These data could highlight the potential confounding factor of etiology when studying the effects of advancing age on auditory function. It should be noted that the inclusion of these two participants

may have limited/masked some of the observed trends in our data, however, we did not have a scientifically valid reason for excluding them from analyses.

Study Limitations

Although the current data failed to strongly suggest a decline in AN sensitivity with advancing age, our participants had a wide variety of underlying etiologies regarding their hearing loss. We attempted to minimize this confound by averaging the eCAP responses from multiple electrodes across the array, however, the effect of etiology cannot be entirely ruled out and could have affected our ability to accurately assess the effect of age. Additionally, while we arbitrarily chose the age cutoff of 65 years, as this helped provide a similar number of participants in the two groups. It is likely that a greater number of participants whose ages span the two age range categories would provide a more robust assessment of the effects of aging on the functional properties of the AN, as many of our participants fell within the age bracket of 50-75 years old.

CONCLUSIONS

The sensitivity of the AN to steady state pulse trains of clinically-relevant pulse rates was not found to be significantly different between older and younger adult CI users, although trends of greater amounts of adaptation were observed in older adults at higher stimulation rates. The amount of adaptation that occurred was significantly impacted by stimulation rate, where faster rates resulted in

greater amount of adaption for both CI age groups, while the rate at which adaptation occurred was found to be highly variable for both groups. Further work is warranted to elucidate effects of aging on functional properties of the AN.

Source of Funding: This work was supported by the R01 grant from NIDCD/NIGMS (1R01DC016038).

REFERENCES

Abbas, P. J., Brown, C. J., Shallop, J. K., et al. (1999). Summary of results using the nucleus CI24M implant to record the electrically evoked compound action potential. *Ear Hear, 20*, 45-59.

Beyea, J. A., McMullen, K. P., Harris, M. S., et al. (2016). Cochlear Implants in Adults: Effects of Age and Duration of Deafness on Speech Recognition. *Otol Neurotol, 37*, 1238-1245.

Brown, C. J., Abbas, P. J., Gantz, B. (1990). Electrically evoked whole-nerve action potentials: data from human cochlear implant users. *J Acoust Soc Am, 88*, 1385-1391.

Cartee, L. A., van den Honert, C., Finley, C. C., et al. (2000). Evaluation of a model of the cochlear neural membrane. I. Physiological measurement of membrane characteristics in response to intrameatal electrical stimulation. *Hear Res, 146*, 143-152.

Clay, K. M., Brown, C. J. (2007). Adaptation of the electrically evoked compound action potential (ECAP) recorded from nucleus CI24 cochlear implant users. *Ear Hear, 28*, 850-861.

Cruickshanks, K. J., Wiley, T. L., Tweed, T. S., et al. (1998). Prevalence of hearing loss in older adults in Beaver Dam, Wisconsin. The Epidemiology of Hearing Loss Study. *Am J Epidemiol, 148*, 879-886.

Delgutte, B. (1997). Auditory neural processing of speech. In W. Hardcastle, J. Laver (Eds.), *The handbook of phonetic science* (pp. 507-538). Oxford: Blackwell.

Dubno, J. R., Dirks, D. D., Morgan, D. E. (1984). Effects of age and mild hearing loss on speech recognition in noise. *J Acoust Soc Am, 76*, 87-96.

Friedland, D. R., Runge-Samuelson, C., Baig, H., et al. (2010). Case-control analysis of cochlear implant performance in elderly patients. *Arch Otolaryngol Head Neck Surg, 136*, 432-438.

Frisina, D. R., Frisina, R. D. (1997). Speech recognition in noise and presbycusis: relations to possible neural mechanisms. *Hear Res, 106*, 95-104.

Gordon-Salant, S. (2005). Hearing loss and aging: new research findings and clinical implications. *J Rehabil Res Dev, 42*, 9-24.

Gordon-Salant, S., Fitzgibbons, P. J. (1993). Temporal factors and speech recognition performance in young and elderly listeners. *J Speech Hear Res, 36*, 1276-1285.

Hay-McCutcheon, M. J., Brown, C. J., Abbas, P. J. (2005). An analysis of the impact of auditory-nerve adaptation on behavioral measures of temporal integration in cochlear implant recipients. *J Acoust Soc Am, 118*, 2444-2457.

He, S., Abbas, P. J., Doyle, D. V., et al. (2016). Temporal Response Properties of the Auditory Nerve in Implanted Children with Auditory Neuropathy Spectrum Disorder and Implanted Children with Sensorineural Hearing Loss. *Ear Hear, 37*, 397-411.

He, S., Teagle, H. F. B., Buchman, C. A. (2017). The Electrically Evoked Compound Action Potential: From Laboratory to Clinic. *Front Neurosci, 11*, 339.

Hughes, M. L., Castioni, E. E., Goehring, J. L., et al. (2012). Temporal response properties of the auditory nerve: data from human cochlear-implant recipients. *Hear Res, 285*, 46-57.

Jeng, F. C., Abbas, P. J., Hu, N., et al. (2009). Effects of temporal properties on compound action potentials in response to amplitude-modulated electric pulse trains in guinea pigs. *Hear Res, 247*, 47-59.

Keithley, E. M., Feldman, M. L. (1982). Hair cell counts in an age-graded series of rat cochleas. *Hear Res, 8*, 249-262.

Keithley, E. M., Ryan, A. F., Woolf, N. K. (1989). Spiral ganglion cell density in young and old gerbils. *Hear Res, 38*, 125-133.

Kurata, N., Schachern, P. A., Paparella, M. M., et al. (2016). Histopathologic Evaluation of Vascular Findings in the Cochlea in Patients With Presbycusis. *JAMA Otolaryngol Head Neck Surg, 142*, 173-178.

Lee, S.Y., Shim, Y.J., Han, J.H., et al. (2020). The molecular etiology of deafness and auditory performance in the postlingually deafened cochlear implantees. *Sci Rep, 10*: 5768

Lin, F. R., Chien, W. W., Li, L., et al. (2012). Cochlear implantation in older adults. *Medicine (Baltimore), 91*, 229-241.

Litvak, L., Delgutte, B., Eddington, D. (2001). Auditory nerve fiber responses to electric stimulation: modulated and unmodulated pulse trains. *J Acoust Soc Am, 110*, 368-379.

Matsuoka, A. J., Abbas, P. J., Rubinstein, J. T., et al. (2000). The neuronal response to electrical constant-amplitude pulse train stimulation: evoked compound action potential recordings. *Hear Res, 149*, 115-128.

Miller, C. A., Abbas, P. J., Robinson, B. K., et al. (1999). Electrically evoked single-fiber action potentials from cat: responses to monopolar, monophasic stimulation. *Hear Res, 130*, 197-218.

Moberly, A. C., Harris, M. S., Boyce, L., et al. (2017). Speech Recognition in Adults With Cochlear Implants: The Effects of Working Memory, Phonological Sensitivity, and Aging. *J Speech Lang Hear Res, 60*, 1046-1061.

Moberly, A. C., Lowenstein, J. H., Nittrouer, S. (2016). Word Recognition Variability With Cochlear Implants: "Perceptual Attention" Versus "Auditory Sensitivity". *Ear Hear, 37*, 14-26.

Moscicki, E. K., Elkins, E. F., Baum, H. M., et al. (1985). Hearing loss in the elderly: an epidemiologic study of the Framingham Heart Study Cohort. *Ear Hear, 6*, 184-190.

Mussoi, B. S. S., Brown, C. J. (2019). Age-Related Changes in Temporal Resolution Revisited: Electrophysiological and Behavioral Findings From Cochlear Implant Users. *Ear Hear, 40*, 1328-1344.

Neuhaus, J., McCulloch, C. (2011). Generalized linear models. *Wiley Interdisciplinary Reviews-Computational Statistics, 3*, 407-413.

Pearson, J. D., Morrell, C. H., Gordon-Salant, S., et al. (1995). Gender differences in a longitudinal study of age-associated hearing loss. *J Acoust Soc Am, 97*, 1196-1205.

Riggs, W. J., Vaughan, C., Skidmore, J., et al. (2021). The sensitivity of the electrically-stimulated auditory nerve to amplitude modulation cues declines with advancing age. *Ear Hear*, In press.

Roberts, D. S., Lin, H. W., Herrmann, B. S., et al. (2013). Differential cochlear implant outcomes in older adults. *Laryngoscope, 123*, 1952-1956.

Schmiedt, R. A., Mills, J. H., & Boettcher, F. A. (1996). Age-reated loss of activity of auditory-nerve fibers. *J Neurophysiol, 76*, 2799-2803.

Schuknecht, H. F. (1955). Presbycusis. *Laryngoscope, 65*, 402-419.

Schuknecht, H. F., Gacek, M. R. (1993). Cochlear pathology in presbycusis. *Ann Otol Rhinol Laryngol, 102*, 1-16.

Sergeyenko, Y., Lall, K., Liberman, M. C., et al. (2013). Age-related cochlear synaptopathy: an early-onset contributor to auditory functional decline. *J Neurosci, 33*, 13686-13694.

Shearer, A. E., Eppsteiner, R. W., Frees, K., et al. (2017). Genetic variants in the peripheral auditory system significantly affect adult cochlear implant performance. *Hear Res, 348*, 138-142.

Shearer, A. E., & Hansen, M. R. (2019). Auditory synaptopathy, auditory neuropathy, and cochlear implantation. *Laryngoscope Investig Otolaryngol, 4,* 429-440.

Stamataki, S., Francis, H. W., Lehar, M., et al. (2006). Synaptic alterations at inner hair cells precede spiral ganglion cell loss in aging C57BL/6J mice. *Hear Res, 221*, 104-118.

Tarnowski, B. I., Schmiedt, R. A., Hellstrom, L. I., et al. (1991). Age-related changes in cochleas of mongolian gerbils. *Hear Res, 54*, 123-134.

van den Honert, C., Stypulkowski, P. H. (1984). Physiological properties of the electrically stimulated auditory nerve. II. Single fiber recordings. *Hear Res, 14*, 225-243.

Viana, L. M., O'Malley, J. T., Burgess, B. J., et al. (2015). Cochlear neuropathy in human presbycusis: Confocal analysis of hidden hearing loss in post-mortem tissue. *Hear Res, 327*, 78-88.

Wilson, B. S., Finley, C. C., Lawson, D. T., et al. (1997). Temporal representations with cochlear implants. *Am J Otol, 18*, S30-34.

Wu, P. Z., Liberman, L. D., Bennett, K., et al. (2019). Primary neural degeneration in the human cochlea: Evidence for hidden hearing loss in the aging ear. *Neuroscience, 407*, 8-20.

Zhang, F., Miller, C. A., Robinson, B. K., et al. (2007). Changes across time in spike rate and spike amplitude of auditory nerve fibers stimulated by electric pulse trains. *J Assoc Res Otolaryngol, 8*, 356-372.

CHAPTER 6: GENERAL SUMMARY AND DISCUSSION

The three manuscripts presented here examined and discussed the utility of auditory evoked potentials for evaluating peripheral auditory function in humans. The overall objective of these research investigations was to gain further understanding of how the peripheral auditory system processes acoustic and electrical information in hearing-impaired listeners.

Chapter 3 established a framework for evaluating temporal and spectral response characteristics of speech-like ECochG stimuli in normal and hearing-impaired listeners. Real-world stimuli have become increasing utilized in the objective assessment of auditory processing by the central auditory system. However, peripheral encoding of this information has been somewhat ignored, primarily due to due difficulty in obtaining near-field recording sites to obtain ear-specific information. The current work overcame this hurdle by using an intraoperative approach that allowed access to the round window of the cochlea. The major findings included defining ECochG response morphology, including waveform peak identification and peak amplitude and latency characteristics. Spectral information encoded by the auditory nerve was also identified. There were no discernable differences in peak amplitudes, latencies, or spectral content encoded by the auditory nerve between listeners with normal/mild SNHL and listeners with moderate/moderately severe SNHL. Finally, it was found that the amount of spectral content encoded by the sensory hair cells, as measured by the

difference waveform of the ECochG response, was directly correlated with a listener's WRS, underscoring the importance of spectral encoding by the hair cells of the cochlea.

The investigations in Chapter 4 evaluated the function of the auditory nerve in patients diagnosed with Ménière's Disease (MD). MD is a debilitating disorder that is known to result in extensive damage to the cochlea and vestibular portions of the inner ear. The major findings of this investigation were that adaptation of the auditory nerve in MD participants does is not operate differently from participants with idiopathic hearing loss. This is accompanied by a similarity in the rate at which the auditory nerve recovers from an adapted state following repetitive stimulation. These findings suggest that the pathophysiology, while known to result in alterations and deteriorations of the inner ear, do not appear to impair functioning of the auditory nerve differently from what is observed in traditional SNHL.

Chapter 5 evaluated the effect of advancing age on temporal responsiveness of the auditory nerve when stimulated electrically. In contrast to ECochG, this study utilized electrical stimulation through a CI electrode array to activate the auditory nerve. As multiple studies have suggested that the auditory system is negatively impacted by advancing age, evaluating functional properties of the auditory nerve to electrical stimulation is of clinical relevance. Speech perception outcomes in CI users are negatively impacted by advancing age (Beyea et al., 2016; Friedland et al., 2010; Roberts et al., 2013). Understanding the functional deficits underlying this association may yield important information for

clinicians and CI mapping strategies. The investigation did not reveal significant differences between younger and older adults on measures of adaptation, although this could have been confounded by the variation in etiology of hearing loss across participants. However, it is important to note that noticeable trends were observed in eCAP amplitudes that suggested age does cause declines in auditory nerve responsiveness to electrical stimulation, especially at faster stimulation rates.

Future Directions

The peripheral auditory system serves as the bottleneck for up-stream centers of the auditory system to process and make sense of incoming sound. As such, understanding auditory encoding by the sensory hair cells and auditory nerve is critical in helping to delineate processing at higher levels. Future work would benefit from combining peripheral auditory evoked potentials with behavioral measures and evoked potentials of the central auditory nervous system. In this fashion, temporal and spectral encoding cues can be identified in the peripheral auditory system and tracked along the ascending auditory pathway. This approach not only allows for improving our understanding of the physiological processing of sound but how alterations in encoding at the periphery disrupt or influence upstream centers both physiologically and behaviorally.

Additionally, the current work has provided a foundation to investigate basic encoding properties of the auditory nerve. Understanding response properties of acoustic and electrical stimulation can aid in improving diagnostic accuracy of site-

of-lesion testing. Future work would benefit from combining acoustic and electrical stimulation paradigms to help identify specific regions of the auditory system that are impaired in SNHL. Understanding more specific sites of impairment can help improve our understanding of variability often observed in different treatment outcomes.

BIBLIOGRAPHY

Abbas, P. J., Brown, C. J., Shallop, J. K., et al. (1999). Summary of results using the nucleus CI24M implant to record the electrically evoked compound action potential. *Ear Hear, 20*, 45-59.

Abbas, P. J., Gorga, M. P. (1981). AP responses in forward-masking paradigms and their relationship to responses of auditory-nerve fibers. *J Acoust Soc Am, 69*, 492-499.

Adunka, O., Roush, P., Grose, J., et al. (2006). Monitoring of cochlear function during cochlear implantation. *Laryngoscope, 116*, 1017-1020.

Akhoun, I., Gallego, S., Moulin, A., et al. (2008). The temporal relationship between speech auditory brainstem responses and the acoustic pattern of the phoneme /ba/ in normal-hearing adults. *Clin Neurophysiol, 119*, 922-933.

Anderson, S., Parbery-Clark, A., White-Schwoch, T., et al. (2013). Auditory brainstem response to complex sounds predicts self-reported speech-in-noise performance. *J Speech Lang Hear Res, 56*, 31-43.

Berlin, C. I., Morlet, T., Hood, L. J. (2003). Auditory neuropathy/dyssynchrony: its diagnosis and management. *Pediatr Clin North Am, 50*, 331-340, vii-viii.

Beyea, J. A., McMullen, K. P., Harris, M. S., et al. (2016). Cochlear implants in adults: effects of age and duration of deafness on speech recognition. *Otol Neurotol, 37*, 1238-1245.

Bidelman, G. M. (2018). Subcortical sources dominate the neuroelectric auditory frequency-following response to speech. *Neuroimage, 175*, 56-69.

Brown, C. J., Abbas, P. J. (1990). Electrically evoked whole-nerve action potentials: parametric data from the cat. *J Acoust Soc Am, 88*, 2205-2210.

Brown, C. J., Abbas, P. J., Gantz, B. (1990). Electrically evoked whole-nerve action potentials: data from human cochlear implant users. *J Acoust Soc Am, 88*, 1385-1391.

Brown, C. J., Abbas, P. J., Gantz, B. J. (1998). Preliminary experience with neural response telemetry in the nucleus CI24M cochlear implant. *Am J Otol, 19*, 320-327.

Brown, C. J., Hughes, M. L., Luk, B., et al. (2000). The relationship between EAP and EABR thresholds and levels used to program the nucleus 24 speech processor: data from adults. *Ear Hear, 21*, 151-163.

Campbell, L., Kaicer, A., Briggs, R., et al. (2015). Cochlear response telemetry: intracochlear electrocochleography via cochlear implant neural response telemetry pilot study results. *Otol Neurotol, 36*, 399-405.

Canfarotta, M. W., O'Connell, B. P., Giardina, C. K., et al. (2020). Relationship between electrocochleography, angular insertion depth, and cochlear implant speech perception outcomes. *Ear Hear, Publish Ahead of Print*.

Cartee, L. A., van den Honert, C., Finley, C. C., et al. (2000). Evaluation of a model of the cochlear neural membrane. I. Physiological measurement of membrane characteristics in response to intrameatal electrical stimulation. *Hear Res, 146*, 143-152.

Choudhury, B., Fitzpatrick, D. C., Buchman, C. A., et al. (2012). Intraoperative round window recordings to acoustic stimuli from cochlear implant patients. *Otol Neurotol, 33*, 1507-1515.

Clark, J. G. (1981). Uses and abuses of hearing loss classification. *ASHA, 23*, 493-500.

Clay, K. M., Brown, C. J. (2007). Adaptation of the electrically evoked compound action potential (ECAP) recorded from nucleus CI24 cochlear implant users. *Ear Hear, 28*, 850-861.

Coats, A. C. (1981). The summating potential and Ménière's disease. I. Summating potential amplitude in Meniere and non-Meniere ears. *Arch Otolaryngol, 107*, 199-208.

Coats, A. C. (1986). The normal summating potential recorded from external ear canal. *Arch Otolaryngol Head Neck Surg, 112*, 759-768.

Coats, A. C., Dickey, J. R. (1972). Postmasking recovery of human click action potentials and click loudness. *J Acoust Soc Am, 52*, 1607-1612.

Committee on Hearing and Equilibrium guidelines for the diagnosis and evaluation of therapy in Ménière's disease. American Academy of Otolaryngology-Head and Neck Foundation, Inc. (1995). *Otolaryngol Head Neck Surg, 113*, 181-185.

Cruickshanks, K. J., Wiley, T. L., Tweed, T. S., et al. (1998). Prevalence of hearing loss in older adults in Beaver Dam, Wisconsin. The Epidemiology of Hearing Loss Study. *Am J Epidemiol, 148*, 879-886.

Cunningham, J., Nicol, T., Zecker, S. G., et al. (2001). Neurobiologic responses to speech in noise in children with learning problems: deficits and strategies for improvement. *Clin Neurophysiol, 112*, 758-767.

Dallos, P., Schoeny, Z. G., Cheatham, M. A. (1972). Cochlear summating potentials. Descriptive aspects. *Acta Otolaryngol Suppl, 302*, 1-46.

Delgutte, B. (1980). Representation of speech-like sounds in the discharge patterns of auditory-nerve fibers. *J Acoust Soc Am, 68*, 843-857.

Delgutte, B. (1997). Auditory neural processing of speech. In W. Hardcastle, J. Laver (Eds.), *The handbook of phonetic science* (pp. 507-538). Oxford: Blackwell.

Don, M., Kwong, B., Tanaka, C. (2005). A diagnostic test for Ménière's Disease and Cochlear Hydrops: impaired high-pass noise masking of auditory brainstem responses. *Otol Neurotol, 26*, 711-722.

Dubno, J. R., Dirks, D. D., Morgan, D. E. (1984). Effects of age and mild hearing loss on speech recognition in noise. *J Acoust Soc Am, 76*, 87-96.

Durrant, J. D., Wang, J., Ding, D. L., et al. (1998). Are inner or outer hair cells the source of summating potentials recorded from the round window? *J Acoust Soc Am, 104*, 370-377.

Eggermont, J. J. (1975). Cochlear adaptation: a theoretical description. *Biol Cybern, 19*, 181-189.

Eggermont, J. J. (1976). Electrocochleography. In W. D. Keidel, W. D. Neff (Eds.), *Handbook of Sensory Physiology* (pp. 626-705). New York, NY: Springer-Verlag.

Eggermont, J. J. (2017). Ups and Downs in 75 Years of Electrocochleography. *Front Syst Neurosci, 11*, 2.

Eggermont, J. J., Don, M., Brackmann, D. E. (1980). Electrocochleography and auditory brainstem electric responses in patients with pontine angle tumors. *Ann Otol Rhinol Laryngol Suppl, 89*, 1-19.

Eggermont, J. J., Odenthal, D. W. (1974). Electrophysiological investigation of the human cochlea. Recruitment, masking and adaptation. *Audiology, 13*, 1-22.

Eggermont, J. J., Spoor, A. (1973a). Cochlear adaptation in guinea pigs. A quantitative description. *Audiology, 12*, 193-220.

Eggermont, J. J., Spoor, A. (1973b). Masking of action potentials in the guinea pig cochlea, its relation to adaptation. *Audiology, 12*, 221-241.

Fettiplace, R., Ricci, A. J. (2006). Mechanoelectrical transduction in auditory hair cells. In R. A. Eatock, R. R. Fay, A. N. Popper (Eds.), *Springer Handbook of Auditory Research* (pp. 154-203). New York, NY: Springer.

Fitzpatrick, D. C., Campbell, A. T., Choudhury, B., et al. (2014). Round window electrocochleography just before cochlear implantation: relationship to word recognition outcomes in adults. *Otol Neurotol, 35*, 64-71.

Fontenot, T. E., Giardina, C. K., Dillon, M., et al. (2019). Residual cochlear function in adults and children receiving cochlear implants: correlations with speech perception outcomes. *Ear Hear, 40*, 577-591.

Franck, K. H., Norton, S. J. (2001). Estimation of psychophysical levels using the electrically evoked compound action potential measured with the neural response telemetry capabilities of Cochlear Corporation's CI24M device. *Ear Hear, 22*, 289-299.

Friedland, D. R., Runge-Samuelson, C., Baig, H., et al. (2010). Case-control analysis of cochlear implant performance in elderly patients. *Arch Otolaryngol Head Neck Surg, 136*, 432-438.

Frisina, D. R., Frisina, R. D. (1997). Speech recognition in noise and presbycusis: relations to possible neural mechanisms. *Hear Res, 106*, 95-104.

Gibson, W. P. (1991). The use of electrocochleography in the diagnosis of Ménière's disease. *Acta Otolaryngol Suppl, 485*, 46-52.

Gibson, W. P., Beagley, H. A. (1976). Electrocochleography in the diagnosis of acoustic neuroma. *J Laryngol Otol, 90*, 127-139.

Gibson, W. P., Prasher, D. K., Kilkenny, G. P. (1983). Diagnostic significance of transtympanic electrocochleography in Ménière's disease. *Ann Otol Rhinol Laryngol, 92*, 155-159.

Goldstein, M. H., Kiang, N. Y. S. (1958). Synchrony of neural activity in electric responses evoked by transient acoustic stimuli. *J. Acoust. Soc. Am., 30*, 107–114.

Gordon, K. A., Ebinger, K. A., Gilden, J. E., et al. (2002). Neural response telemetry in 12- to 24-month-old children. *Ann Otol Rhinol Laryngol Suppl, 189*, 42-48.

Gordon, K. A., Papsin, B. C., Harrison, R. V. (2004). Toward a battery of behavioral and objective measures to achieve optimal cochlear implant stimulation levels in children. *Ear Hear, 25*, 447-463.

Gordon-Salant, S. (2005). Hearing loss and aging: new research findings and clinical implications. *J Rehabil Res Dev, 42*, 9-24.

Gordon-Salant, S., Fitzgibbons, P. J. (1993). Temporal factors and speech recognition performance in young and elderly listeners. *J Speech Hear Res, 36*, 1276-1285.

Gorga, M. P., Abbas, P. J. (1981). AP measurements of short-term adaptation in normal and in acoustically traumatized ears. *J Acoust Soc Am, 70*, 1310-1321.

Gorga M. P., Worthington D. W., Reiland J. K., Beauchaine K. A., Goldgar D. E. (1985). Some comparisons between auditory brain stem response thresholds, latencies, and the pure-tone audiogram. *Ear Hear, 2*, 105-12.

Gulya, A. J., Schuknecht, H. F. (1982). Classification of Endolymphatic Hydrops. *American Journal of Otolaryngology, 3*, 319-322.

Hall, J. W., 3rd, Rupp, K. A. (1997). Auditory brainstem response: recent developments in recording and analysis. *Adv Otorhinolaryngol, 53*, 21-45.

Hallpike, C. S., Cairns, H. (1938). Observations on the Pathology of Ménière's Syndrome: (Section of Otology). *Proc R Soc Med, 31*, 1317-1336.

Harris, D. M., Dallos, P. (1979). Forward masking of auditory nerve fiber responses. *J Neurophysiol, 42*, 1083-1107.

Harris, M. S., Riggs, W. J., Giardina, C. K., et al. (2017). Patterns seen during electrode insertion using intracochlear electrocochleography obtained directly through a cochlear implant. *Otol Neurotol, 38*, 1415-1420.

Harris, M. S., Riggs, W. J., Koka, K., et al. (2017). Real-Time intracochlear electrocochleography obtained directly through a cochlear implant. *Otol Neurotol, 38*, e107-e113.

Haumann, S., Imsiecke, M., Bauernfeind, G., et al. (2019). Monitoring of the inner ear function during and after cochlear implant insertion using electrocochleography. *Trends in Hearing, 23*.

Hay-McCutcheon, M. J., Brown, C. J., Abbas, P. J. (2005). An analysis of the impact of auditory-nerve adaptation on behavioral measures of temporal integration in cochlear implant recipients. *J Acoust Soc Am, 118*, 2444-2457.

He, S., Abbas, P. J., Doyle, D. V., et al. (2016). Temporal response properties of the auditory nerve in implanted children with auditory neuropathy spectrum disorder and implanted children with sensorineural hearing loss. *Ear Hear, 37*, 397-411.

He, S., Chao, X., Wang, R., et al. (2020). Recommendations for measuring the electrically evoked compound action potential in children with cochlear nerve deficiency. *Ear Hear, 41*, 465-475.

He, S., Shahsavarani, B. S., McFayden, T. C., et al. (2018). Responsiveness of the electrically stimulated cochlear nerve in children with cochlear nerve deficiency. *Ear Hear, 39*, 238-250.

He, S., Teagle, H. F. B., Buchman, C. A. (2017). The Electrically evoked compound action potential: from laboratory to clinic. *Front Neurosci, 11*, 339.

Hudspeth, A. J. (1982). Extracellular current flow and the site of transduction by vertebrate hair cells. *J Neurosci, 2*, 1-10.

Hughes, M. L., Brown, C. J., Abbas, P. J., et al. (2000). Comparison of EAP thresholds with MAP levels in the nucleus 24 cochlear implant: data from children. *Ear Hear, 21*, 164-174.

Hughes, M. L., Castioni, E. E., Goehring, J. L., et al. (2012). Temporal response properties of the auditory nerve: data from human cochlear-implant recipients. *Hear Res, 285*, 46-57.

Humes, L. E. (1983) . Spectral and temporal resolution by the hearing impaired. In: Studebaker GA, Bess FH, eds. *Monographs in Contemporary Audiology: The Vanderbilt Hearing Aid Report* . Upper Darby: 16-31.

Jeng, F. C., Abbas, P. J., Hu, N., et al. (2009). Effects of temporal properties on compound action potentials in response to amplitude-modulated electric pulse trains in guinea pigs. *Hear Res, 247*, 47-59.

Jewett, D. L., Romano, M. N., Williston, J. S. (1970). Human auditory evoked potentials: possible brain stem components detected on the scalp. *Science, 167*, 1517-1518.

Johnson, K. L., Nicol, T., Zecker, S. G., et al. (2008). Brainstem encoding of voiced consonant--vowel stop syllables. *Clin Neurophysiol, 119*, 2623-2635.

Katsarkas, A. (1996) Hearing loss and vestibular dysfunction in Ménière's disease. *Acta Oto-Laryngologica, 116*, 185-188

Keithley, E. M., Feldman, M. L. (1982). Hair cell counts in an age-graded series of rat cochleas. *Hear Res, 8*, 249-262.

Keithley, E. M., Ryan, A. F., Woolf, N. K. (1989). Spiral ganglion cell density in young and old gerbils. *Hear Res, 38*, 125-133.

Kiang, N. Y. (1980). Processing of speech by the auditory nervous system. *J Acoust Soc Am, 68*, 830-835.

Kiang, N. Y., Eddington, D. K., Delgutte, B. (1979). Fundamental considerations in designing auditory implants. *Acta Otolaryngol, 87*, 204-218.

Kiang, N. Y., Watanabe, T., Thomas, E. C., et al. (1965). Discharge patterns of signle fibers in the cat's auditory nerve. *MIT Res, Mon*.

Klein, W., Plomp, R., Pols, L. C. (1970). Vowel spectra, vowel spaces, and vowel identification. *J Acoust Soc Am, 48*, 999-1009.

Koka, K., Saoji, A. A., Litvak, L. M. (2017). Electrocochleography in cochlear implant recipients with residual hearing: comparison with audiometric thresholds. *Ear Hear, 38*, e161-e167.

Kraus, N., Thompson, E. C., Krizman, J., et al. (2016). Auditory biological marker of concussion in children. *Sci Rep, 6*, 39009.

Kraus, N., White-Schwoch, T. (2015). Unraveling the biology of auditory learning: a cognitive-sensorimotor-reward framework. *Trends Cogn Sci, 19*, 642-654.

Kujawa, S. G., Liberman, M. C. (2009). Adding insult to injury: cochlear nerve degeneration after "temporary" noise-induced hearing loss. *J Neurosci* 29:14077–14085

Kurata, N., Schachern, P. A., Paparella, M. M., et al. (2016). Histopathologic evaluation of vascular findings in the cochlea in patients with presbycusis. *JAMA Otolaryngol Head Neck Surg, 142*, 173-178.

Lee, S.Y., Shim, Y.J., Han, J.H., et al. (2020). The molecular etiology of deafness and auditory performance in the postlingually deafened cochlear implantees. *Sci Rep, 10*: 5768

Lin, F. R., Chien, W. W., Li, L., et al. (2012). Cochlear implantation in older adults. *Medicine (Baltimore), 91*, 229-241.

Litvak, L., Delgutte, B., Eddington, D. (2001). Auditory nerve fiber responses to electric stimulation: modulated and unmodulated pulse trains. *J Acoust Soc Am, 110*, 368-379.

Luo, J., Xu, L., Chao, X., et al. (2020). The Effects of GJB2 or SLC26A4 gene mutations on neural response of the electrically stimulated auditory nerve in children. *Ear Hear, 41*, 194-207.

Matsuoka, A. J., Abbas, P. J., Rubinstein, J. T., et al. (2000). The neuronal response to electrical constant-amplitude pulse train stimulation: evoked compound action potential recordings. *Hear Res, 149*, 115-128.

McMahon, C. M., Patuzzi, R. B., Gibson, W. P., et al. (2008). Frequency-specific electrocochleography indicates that presynaptic and postsynaptic mechanisms of auditory neuropathy exist. *Ear Hear, 29*, 314-325.

Merchant, S. N., Adams, J. C., Nadol Jr., J. B. (2005). Pathophysiology of Ménière's syn- drome: are symptoms caused by endolymphatic hydrops. *Otol. Neurotol*, 26, 74–81.

Miller, C. A., Abbas, P. J., Robinson, B. K., et al. (1999). Electrically evoked single-fiber action potentials from cat: responses to monopolar, monophasic stimulation. *Hear Res, 130*, 197-218.

Moberly, A. C., Harris, M. S., Boyce, L., et al. (2017). Speech recognition in adults with cochlear implants: the effects of working memory, phonological sensitivity, and aging. *J Speech Lang Hear Res, 60*, 1046-1061.

Moberly, A. C., Lowenstein, J. H., Nittrouer, S. (2016). Word recognition variability with cochlear implants: "perceptual attention" versus "auditory sensitivity". *Ear Hear, 37*, 14-26.

Moller, A. R. (2000). *Hearing: Its Physiology and Pathophysiology*. New York: Academic Press.

Monsell, E., Balkany, T. A., Gates, G. A., et al. (1995). Committee on Hearing and Equilibrium guidelines for the diagnosis and evaluation of therapy in Ménière's disease. American Academy of Otolaryngology-Head and Neck Foundation, Inc. *Otolaryngol Head Neck Surg, 113*, 181-185.

Moscicki, E. K., Elkins, E. F., Baum, H. M., et al. (1985). Hearing loss in the elderly: an epidemiologic study of the Framingham Heart Study Cohort. *Ear Hear, 6*, 184-190.

Murnane, O. D., Prieve, B. A., Relkin, E. M. (1998). Recovery of the human compound action potential following prior stimulation. *Hear Res, 124*, 182-189.

Musiek, F. E. (2007). Structure and function of the auditory nerve. In F. E. Musiek, J. A. Baran (Eds.), *The Auditory System*. Boston, MA: Pearson.

Mussoi, B. S., Brown, C. J. (2020). The effect of aging on the electrically evoked compound action potential. *Otol Neurotol, 41*, e804-e811.

Mussoi, B. S. S., Brown, C. J. (2019). Age-Related changes in temporal resolution revisited: electrophysiological and behavioral findings from cochlear implant users. *Ear Hear, 40*, 1328-1344.

Neuhaus, J., McCulloch, C. (2011). Generalized linear models. *Wiley Interdisciplinary Reviews-Computational Statistics, 3*, 407-413.

Ninoyu, O., Meyer zum Gottesberge, A. M. (1986). Changes in Ca++ activity and DC potential in experimentally induced endolymphatic hydrops. *Arch Otorhinolaryngol, 243*, 106-107.

Nuttall, H. E., Moore, D. R., Barry, J. G., et al. (2015). The influence of cochlear spectral processing on the timing and amplitude of the speech-evoked auditory brain stem response. *J Neurophysiol, 113*, 3683-3691.

O'Connell, B. P., Holder, J. T., Dwyer, R. T., et al. (2017). Intra- and postoperative electrocochleography may be predictive of final electrode position and postoperative hearing preservation. *Front Neurosci, 11*, 291.

Ohashi, T., Nishino, H., Arai, Y., et al. (2013). Electrocochleography in Ménière's disease: recovery from adaptation of the auditory action potential. *Acta Otolaryngol, 133*, 564-568.

Ohashi, T., Nishino, H., Arai, Y., et al. (2012). Recovery from adaptation of the action potential in idiopathic sudden sensorineural hearing loss investigated using a paired-click stimulation paradigm. *Acta Otolaryngol, 131*, 1165-1171.

Ohashi, T., Nishino, H., Nishimoto, Y., et al. (2014). The recovery from AP adaptation in sensorineural hearing loss. *Acta Otolaryngol, 134*, 275-279.

Ohashi, T., Ochi, K., Nishino, H., et al. (2005). Recovery of human compound action potential using a paired-click stimulation paradigm. *Hear Res, 203*, 192-200.

Paparella, M. M. (1984a). Pathogenesis of Ménière's disease and Ménière's syndrome. *Acta Otolaryngol Suppl, 406*, 10-25.

Paparella, M. M. (1984b). Pathology of Ménière's disease. *Ann Otol Rhinol Laryngol Suppl, 112*, 31-35.

Pearson, J. D., Morrell, C. H., Gordon-Salant, S., et al. (1995). Gender differences in a longitudinal study of age-associated hearing loss. *J Acoust Soc Am, 97*, 1196-1205.

Peterson, G. E., Barney, H. L. (1952). Control methods used in a study of the vowels. *Journal of the Acoustical Society of America, 24*, 175-184.

Picton, T. W., Woods, D. L., Baribeau-Braun, J., et al. (1976). Evoked potential audiometry. *J Otolaryngol, 6*, 90-119.

Potts, L. G., Skinner, M. W., Gotter, B. D., et al. (2007). Relation between neural response telemetry thresholds, T- and C-levels, and loudness judgments in 12 adult nucleus 24 cochlear implant recipients. *Ear and Hearing, 28*, 495-511.

Rauch, S. D., Merchant, S. N., Thedinger, B. A. (1989). Ménière's syndrome and endolymphatic hydrops. Double-blind temporal bone study. *Ann Otol Rhinol Laryngol, 98*, 873-883.

Relkin, E. M., Doucet, J. R., Sterns, A. (1995). Recovery of the compound action potential following prior stimulation: evidence for a slow component that reflects recovery of low spontaneous-rate auditory neurons. *Hear Res, 83*, 183-189.

Riggs, W. J., Fitzpatrick, D. C., Mattingly, J. K., et al. (2020). Electrocochleography during translabyrinthine approach for vestibular schwannoma removal. *Otol Neurotol, 41*, e369-e377.

Riggs, W. J., Hiss, M. M., Skidmore, J., et al. (2020). Utilizing electrocochleography as a microphone for fully implantable cochlear implants. *Sci Rep, 10*, 3714.

Riggs, W. J., Vaughan, C., Skidmore, J., et al. (2021). The sensitivity of the electrically-stimulated auditory nerve to amplitude modulation cues declines with advancing age. *Ear Hear*, (In press).

Roberts, D. S., Lin, H. W., Herrmann, B. S., et al. (2013). Differential cochlear implant outcomes in older adults. *Laryngoscope, 123*, 1952-1956.

Russo, N., Nicol, T., Musacchia, G., et al. (2004). Brainstem responses to speech syllables. *Clin Neurophysiol, 115*, 2021-2030.

Salt, A. N., DeMott, J. (1994). Endolymph calcium increases with time after surgical induction of hydrops in guinea-pigs. *Hear Res, 74*, 115-121.

Salvi, R. J., Eddins, A. C., Wang, J. (2007). Cochlear Physiology II: Mostly Electrophysiology. In F. E. Musiek, J. A. Baran (Eds.), *The Auditory System*. Boston, MA: Pearson.

Salvinelli, F., Greco, F., Trivelli, M., et al. (1999). Ménière's disease. histopathological changes: a post mortem study on temporal bones. *Eur Rev Med Pharmacol Sci, 3*, 189-193.

Santarelli, R., Rossi, R., Scimemi, P., et al. (2015). OPA1-related auditory neuropathy: site of lesion and outcome of cochlear implantation. *Brain, 138*, 563-576.

Santarelli, R., Starr, A., Michalewski, H. J., et al. (2008). Neural and receptor cochlear potentials obtained by transtympanic electrocochleography in auditory neuropathy. *Clin Neurophysiol, 119*, 1028-1041.

Saoji, A. A., Patel, N. S., Carlson, M. L., et al. (2019). Multi-frequency Electrocochleography measurements can be used to monitor and optimize electrode placement during cochlear implant surgery. *Otol Neurotol, 40*, 1287-1291.

Schaette, R., McAlpine D. (2011). Tinnitus with a normal audiogram: physiological evidence for hidden hearing loss and computational model. *J Neurosci, 31*, (38):13452-7.

Schmiedt, R. A., Mills, J. H., & Boettcher, F. A. (1996). Age-reated loss of activity of auditory-nerve fibers. *J Neurophysiol, 76*, 2799-2803.

Schuknecht, H. F. (1955). Presbycusis. *Laryngoscope, 65*, 402-419.

Schuknecht, H. F. (1974). *Pathology of the ear*. Massachusetts: Harvard University Press.

Schuknecht, H. F., Gacek, M. R. (1993). Cochlear pathology in presbycusis. *Ann Otol Rhinol Laryngol, 102*, 1-16.

Sergeyenko, Y., Lall, K., Liberman, M. C., et al. (2013). Age-related cochlear synaptopathy: an early-onset contributor to auditory functional decline. *J Neurosci, 33*, 13686-13694.

Shearer, A. E., Eppsteiner, R.W., Frees, K., et al. (2017). Genetic variants in the peripheral auditory system significantly affect adult cochlear implant performance. *Hear Res, 348*, 138-142.

Shearer, A. E., & Hansen, M. R. (2019). Auditory synaptopathy, auditory neuropathy, and cochlear implantation. *Laryngoscope Investig Otolaryngol, 4,* 429-440.

Skoe, E., Kraus, N. (2010). Auditory brain stem response to complex sounds: a tutorial. *Ear Hear, 31*, 302-324.

Skoe, E., Krizman, J., Anderson, S., et al. (2015). Stability and plasticity of auditory brainstem function across the lifespan. *Cereb Cortex, 25*, 1415-1426.

Smith, R. L. (1977). Short-term adaptation in single auditory nerve fibers: some poststimulatory effects. *J Neurophysiol, 40*, 1098-1111.

Song, J. H., Skoe, E., Banai, K., & Kraus, N. (2011). Perception of speech in noise: neural correlates. *J Cogn Neurosci, 23*, (9), 2268–2279.

Stamataki, S., Francis, H. W., Lehar, M., et al. (2006). Synaptic alterations at inner hair cells precede spiral ganglion cell loss in aging C57BL/6J mice. *Hear Res, 221*, 104-118.

Stapells, D. R., Oates, P. (1997). Estimation of the pure-tone audiogram by the auditory brainstem response: a review. *Audiol Neurootol, 2*, 257-280.

Starr, A., Picton, T. W., Sininger, Y., et al. (1996). Auditory neuropathy. *Brain, 119 (Pt 3)*, 741-753.

Stephens, S. D., Charlet de Sauvage, R., Aran, J. M. (1974). Adaptation of the electrocochleogram: preliminary report. *Rev Laryngol Otol Rhinol (Bord), 95*, 129-138.

Tarnowski, B. I., Schmiedt, R. A., Hellstrom, L. I., et al. (1991). Age-related changes in cochleas of mongolian gerbils. *Hear Res, 54*, 123-134.

Tejani, V. D., Abbas, P. J., Brown, C. J. (2017). Relationship between peripheral and psychophysical measures of amplitude modulation detection in cochlear implant users. *Ear Hear, 38*, e268-e284.

Thai-Van, H., Truy, E., Charasse, B., et al. (2004). Modeling the relationship between psychophysical perception and electrically evoked compound action potential threshold in young cochlear implant recipients: clinical implications for implant fitting. *Clin Neurophysiol, 115*, 2811-2824.

Tsuji, K., Velazquez-Villasenor, L., Rauch, S. D., et al. (2000). Temporal bone studies of the human peripheral vestibular system. Ménière's disease. *Ann Otol Rhinol Laryngol Suppl, 181*, 26-31.

van den Honert, C., Stypulkowski, P. H. (1984). Physiological properties of the electrically stimulated auditory nerve. II. Single fiber recordings. *Hear Res, 14*, 225-243.

Viana, L. M., O'Malley, J. T., Burgess, B. J., et al. (2015). Cochlear neuropathy in human presbycusis: Confocal analysis of hidden hearing loss in post-mortem tissue. *Hear Res, 327*, 78-88.

Wang, Z., Bovik, A. C. (2002). A universal image quality index. *Ieee Signal Processing Letters, 9*, 81-84.

Wang, Z., Bovik, A. C., Sheikh, H. R., et al. (2004). Image quality assessment: From error visibility to structural similarity. *Ieee Transactions on Image Processing, 13*, 600-612.

Westerman, L. A., Smith, R. L. (1984). Rapid and short-term adaptation in auditory nerve responses. *Hear Res, 15*, 249-260.

Wever, E. G., Bray, C. (1930). Action currents in the auditory nerve in response to acoustic stimulation. *Proc. Nat. Acad. Sci., U.S. A., 16*, 344-350.

Whitfield, I. C., Ross, H. F. (1965). Cochlear-microphonic and summating potentials and the outputs of individual hair-cell generators. *J Acoust Soc Am, 38*, 126-131.

Wilson, B. S., Finley, C. C., Lawson, D. T., et al. (1997). Temporal representations with cochlear implants. *Am J Otol, 18*, S30-34.

Wu, P. Z., Liberman, L. D., Bennett, K., et al. (2019). Primary neural degeneration in the human cochlea: evidence for hidden hearing loss in the aging ear. *Neuroscience, 407*, 8-20.

Yoshie, N., Oashi, T. (1971). Abnormal adaptation of human cochlear nerve action potential responses: clinical observations by non-surgical recording. *Rev Laryngol Otol Rhinol (Bord), 92*, Suppl:673-690.

Young, E., Sachs, M. B. (1973). Recovery from sound exposure in auditory-nerve fibers. *J Acoust Soc Am, 54*, 1535-1543.

Zhang, F., Miller, C. A., Robinson, B. K., et al. (2007). Changes across time in spike rate and spike amplitude of auditory nerve fibers stimulated by electric pulse trains. *J Assoc Res Otolaryngol, 8*, 356-372.